FACULTEIT
BIO-INGENIEURSWETENSCHAPPEN

Unravelling drought regulation of the wheat cultivar Hartog during grain filling

Sarah Verbeke
Student number: 01104179

Promoter: Prof. Dr. ir. Kathy Steppe
Copromoter: Prof. Dr. ir. Geert Haesaert
Tutor: Prof. Dr. ir. Kathy Steppe

Master's Dissertation submitted to Ghent University in partial fulfilment of the requirements
for the degree of Master in Bioscience Engineering: Cell and Gene Biotechnology

Academic year: 2016-2017

UNIVERSITEIT
GENT

Copyright

The author and the promotors grant permission to make this thesis available for consultation and to copy parts of it for personal use. Any other use is subject to the copyright laws, more specifically regarding the obligation to explicitly specify the source when using results from this thesis.

De auteur en de promotoren geven de toelating deze scriptie voor consultatie beschikbaar te stellen en delen ervan te kopiëren voor persoonlijk gebruik. Elk ander gebruik valt onder de beperkingen van het auteursrecht, in het bijzonder met betrekking tot de verplichting uitdrukkelijk de bron te vermelden bij het aanhalen van resultaten uit deze scriptie.

June 9, 2017

The promoters,

Prof. Dr. ir. Kathy Steppe   Prof. Dr. ir. Geert Haesaert

The author,

Sarah Verbeke

Preface

This master thesis has been a learning process and a journey through unknown territory for me. As a master student in biotechnology, I had seen molecular methods and techniques to research plants, but lacked knowledge in their physiological processes. This thesis has given me the opportunity to combine these disciplines, but more importantly to discover the power of modelling, something I was long interested in learning. I have experienced the frustrations and struggles that come along with modelling, but these made the 'eureka' moments afterwards even more intense.

The goal I set out to achieve during my thesis was to incorporate genetic information within a plant model. Unfortunately, this goal was a bit too ambitious. I underestimated the time it would take to immerse myself in the subject and to become really acquainted with the methodologies in this type of research. By then, the experiments were already planned and I became aware that I would have to use the data otherwise. This is the reason why the focus of the literature study does not exactly match my experiments and analyses. Nevertheless, I think I set the base with my thesis and I hope this research will be continued in the future.

The development and completion of this master thesis would not have been possible without the help and input of some amazing people.

I would like to thank my tutor and promotor, Kathy Steppe. Over a year ago, she gave me the opportunity to start a master thesis in a subject I was contemplating for over two years: combining plant genetics and modelling. Up until then, I didn't even know if it was possible. During my thesis, Kathy gave me the freedom to choose any direction I was interested in, while constantly giving me guidance and feedback. With her inexhaustible source of enthusiasm and positivism, it was impossible to ever doubt the research I was doing or my capability of conducting it.

I would also like to thank my copromotor, Geert Haesaert, for giving me feedback on my thesis report.

Next, I would like to give a special thanks to Szanne Degraeve. She helped me through all the practical aspects of my thesis: from planning the experiments and growing the wheat plants, to showing me how to take samples and reading my thesis. Even when I messed up and accidentally almost killed the wheat plants for my experiment, she managed to find other plants.

I would also like to thank the following people: Dirk De Pauw, for all his help concerning PhytoSim, answering all my questions and solving all my problems. Philip Deman, for all the help with the sensors, calibrations and practical questions I had. Ilse Delaere for giving me the opportunity to use the lab of the Department of Crop protection and to store my samples. Ive De Smet and Brigitte Van De Cotte, for all their help concerning the protein extraction and proteomic analysis. Jonas von der Crone, for his clear explanations of the sensors and how

Contents

List of abbreviations

ABA	abscisic acid
ABF	ABRE-Binding Factors
ABRE	ABA-Responsive Element
ARF	Auxin Response Factors
ASI	anthesis-silking-interval
CBF	Cold Binding Factor
DOY	Day of Year
DREB	DRE-Binding transcription factor
DRE/C	Dehydration Responsive Element C repeat
G×E	genotype by environment interaction
GSP	genotype-specific parameter
LAI	leaf area index
LC	liquid chromatography
LER	leaf elongation rate
LMM	linear mixed model
MAS	marker-assisted selection
MS	mass spectrometry
OA	osmotic adjustment
PBSM	process-based simulation models
QTL	quantitative trait loci
SA	sensitivity analysis
SNP	single nucleotide polymorphism
SPAC	soil-plant-atmosphere continuum
PAR	photosynthetically active radiation
PM	Penman-Monteith
VPD	vapour pressure deficit
VWC	volumetric water content
WSC	water-soluble carbohydrates
WUE	water use efficiency

Abstract

Ecophysiological models for crop growth are widely used to simulate crop yield and grain quality under a range of environmental and crop management conditions. These models incorporate many basic principles of plant ecophysiology, but they often do not yet accommodate for the increasing knowledge in plant genetics and genomics. There is still an important knowledge gap between genotype and phenotype due to the complex regulation of physiological properties like drought. This regulation is also heavily influenced by environmental factors like vapour pressure deficit and temperature.

By combining the results of a proteomic analysis with the ecophysiological model, the proteins that are differentially expressed can be linked to different variables that are hard to measure, but easy to simulate. In this study, the models of Penman-Monteith, Cropsyst and HydGro were combined to simulate the water balance in a wheat plant. More precisely, transpiration, water uptake, storage and transport during well watered and water deficit conditions were compared. To do this, several parameters were measured both in the environment and of the plant itself, like air temperature, humidity, soil moisture and stem sap flow. The physiological changes when the plant adapts to drought stress are discussed and linked to the changes in protein content. Moreover, a drought index is constructed that differentiates between drought caused by a high atmospheric demand and drought caused by a soil water deficit.

In this research, we prove that the process of grain filling has to be incorporated in the HydGro model to accurately simulate drought in wheat. We also show that the increase and decrease in stem diameter as a response to water transport in wheat differs from trees.

Samenvatting

Ecofysiologische modellen voor de groei van gewassen worden vaak gebruikt om de opbrengst en graankwaliteit te simuleren onder verschillende omgevings- en management condities. Deze modellen zijn gebaseerd op verschillende basis principes van de planten ecofysiologie, maar zij houden vaak nog geen rekening met de toenemende kennis in de plantengenetica. Er is nog altijd een kennishiaat tussen het genotype en fenotype van de plant door de complexe regulatie van fysiologische responsen zoals droogte. Deze regulatie is bovendien sterk beïnvloed door omgevingsfactoren zoals de vapour pressure deficit en de temperatuur.

Door het combineren van een proteoomanalyse met een ecofysiologisch model kunnen de proteïnen die differentieel tot expressie werden gebracht, gelinkt worden aan verschillende variabelen die misschien moeilijk te meten zijn, maar gemakkelijk te simuleren. In dit onderzoek werden de modellen van Penman-Monteith, Cropsyst en HydGro gecombineerd om de water balans in een tarwe plant te simuleren. Meer bepaald transpiratie, wateropname, -opslag en -transport in goed bewaterde en in droogte condities werden vergeleken. Hiervoor werden verschillende parameters gemeten zowel in de omgeving als in de plant zelf, zoals luchttemperatuur, luchtvochtigheid, bodem watergehalte en sapstroom in de stengel. De fysiologische veranderingen wanneer de plant zich aanpast aan droogte worden besproken en gelinkt aan de veranderingen in proteïne inhoud. Bovendien werd een droogte index opgesteld dat een onderscheid maakt tussen droogte door een droge lucht en droogte door watertekort.

In dit onderzoek wordt aangetoond dat het proces van korrelvulling moet opgenomen worden in het HydGro model om droogte correct the kunnen simuleren in tarwe. Bovendien wordt gedemonstreerd dat het zwellen en krimpen van de stengeldiameter als gevolg van watertransport in tarwe verschilt van bomen.

Chapter 1

Introduction

Ecophysiological models for crop growth are widely used to simulate crop yield and grain quality under a range of environmental and crop management conditions. These models incorporate many basic principles of plant ecophysiology, but often they do not yet accommodate for the increasing knowledge in plant genetics and genomics. Incorporating genetic information could improve our understanding in the control of physiological processes and increase the simulation accuracy by incorporation of an additional process (White, 2006). Furthermore, by simulating the effect of a combination of genes, one could design new ideotypes, specifically adapted for future climates or new areas.

Cereals constitute the basic staple foods of humankind and it is a cheap source of protein. Due to the constant increase in population, there is an everlasting increase in demand, and pressure on resources will increase even further. Meanwhile, quality, plant health, food safety and respect for the environment are becoming increasingly important to the consumers, making plant production systems evolve regularly (Génard *et al.*, 2016). Scientists and breeding companies need to ensure yield stability, while at the same time increase productivity. Crop cultivation will need to extend to less favourable soils. Moreover, in the face of climate change, breeders not only need to develop varieties for the current environments, but also need to think forward and adapt the current varieties to even more extreme conditions (Xu & Buck-Sorlin, 2016).

Wheat is one of the most important crops worldwide. In important wheat growing areas in the world, high temperatures often arise at the end of the growing season. This can lead to drought stress during the grain filling period (Araus *et al.*, 2008), also known as 'terminal drought' (Reynolds *et al.*, 2005). It is a major reason for yield losses since it results in a poor grain set (Farooq *et al.*, 2014).
In the face of global warming, regions where drought prevails will only increase both in frequency and in duration. Heat waves are also very likely to occur more often and last longer, this in combination with more intense and extreme precipitation events (IPCC, 2014). A thorough understanding of the molecular and physiological mechanisms of drought adaptation can lead to more resistant, high yielding crops in these environments. At the moment, most of the knowledge is based on the model plant *Arabidopsis thaliana*.
There is an urgent need to better understand the molecular basis of drought regulation in crops like wheat. Since wheat is a hexaploid, genetic research is cumbersome and slowly evolving. Integrating differential expression of genes within growth models can accelerate the

learning process and quickly point out key regulating genes.

In this research the wheat cultivar Hartog was used to study drought and its regulation during grain filling. Soil moisture and sap flow were measured to indicate drought in the plants. Since the atmosphere is a major determinant in the water demand of the plant, several athmospheric parameters were also measured. The wheat plants were monitored in a well watered condition as a control and in a water deficient condition to study drought. But more importantly, an ecophysiological model was built based on the already existing models of Penman-Monteith (Allen *et al.*, 1998), Cropsyst (Stöckle & Nelson, 2003) and HydGro (Steppe *et al.*, 2006). Measurements of air temperature, net radiation and humidity serve as an input to calculate potential and actual transpiration of the wheat plant, while sap flow measurements are the input to determine a whole array of physiological variables, the most important being the sap flow to the storage compartments and the waterpotentials of the xylem and storage compartments. These are all calculated for the stem, the leaves and the ear separately.
With the simulations of the potential transpiration and the sap flow measurements, a first draft of a drought index was created that is able to distinguish drought caused by a high atmospheric demand from drought due to soil water deficit.
In a second part of this research, proteins were extracted and analysed with liquid chromatography and mass spectrometry at different time points during the drought stress. The change in proteins and their concentration was then linked to different physiological parameters in the plant, both measured and simulated. The goal was to see if proteins that are important to the drought response of the plant could be identified and linked to physiological parameters, both measured and simulated.

This research is a first attempt to combine genetic information with ecophysiological modelling and to prove the additive benefits of bringing these two research fields together. Incorporating the genetic regulation within the model was not yet achieved since the experimental design did not allow for this, but it is a logical next step in future research. However, by building and using an ecophysiological model, we were able to show a methodology to link hard-to-measure parameters in the plant to the expression of stress-induced proteins, something that indicates the benefit of using models in genetic research.

Chapter 2

Literature study

2.1 Wheat growth

Wheat (*Triticum aestivum* L.) can be classified as winter or spring wheat. The former needs vernalization, while the latter has limited vernalization requirements for normal development and can be planted after winter (Simmons *et al.*, 1995).

Wheat growth can be described in 9 to 11 stages, depending on the source. A popular system for describing these stages is the decimal code, also called the Zadoks system, in which the first digit refers to the principal stage. The second digit subdivides the principle stages into sub-stages. This staging system is however not completely chronological, making it unsuitable for modelling. Instead the Feekes-Large system is used, which is based on growing degree days. It is less detailed, but makes it possible to determine the growth stage based on the thermal time accumulation (Simmons *et al.*, 1995; Zheng *et al.*, 2014).

Growth starts at the germination of the sown kernel (Figure 2.1). The coleoptile is formed and when it emerges from the soil at the emergence stage, it stops growth. At the same time, the first true leaf pushes through (Simmons *et al.*, 1995).

During the juvenile stage, more nodes, leaves and tillers are formed. Tillers arise at the point of attachment of the coleoptile and the lower leaves on the main shoot. On average, a wheat plant will produce up to eight or nine leaves and three tillers, but this number differs for different varieties and field conditions.

Floral initiation starts when the head, or the ear, is formed inside the flag leaf (the last leaf). It is still microscopically small at this time, but the floral structures and kernels are initiated. When the formation is complete, the top internodes of the main stem begin elongating ('jointing' stage), starting from the fourth internode. The last stem segment, the peduncle, carrying the ear elongates the most. At the time it reaches its final length, the individual florets prepare to be fertilized. The ear is still enclosed by the flag leaf, which shows now a swelling, typical for the 'boot' stage.

Finally, the ear is pushed out in the 'heading' stage. A few days later, flowering and (mostly self-) pollination begins in the middle of the ear and progresses up and down (Simmons *et al.*, 1995; Zheng *et al.*, 2014).

The 'grain filling' stage consists of three phases. First, the number of endosperm cells increases without much weight gain. This stage is guided by hormones and negatively influenced by temperature and drought stress (Hess *et al.*, 2002; Ho, 1988). Second, the kernels begin

accumulating starch an proteins rapidly until their maximum dry weight. And finally, they lose much of their water content, making the kernels brown and hard. High temperatures decreases the grain weight and shortens the grain filling period (Dias & Lidon, 2009). Maturity of the plant is reached when the head and peduncle lose their green colour (Simmons *et al.*, 1995; Zheng *et al.*, 2014).
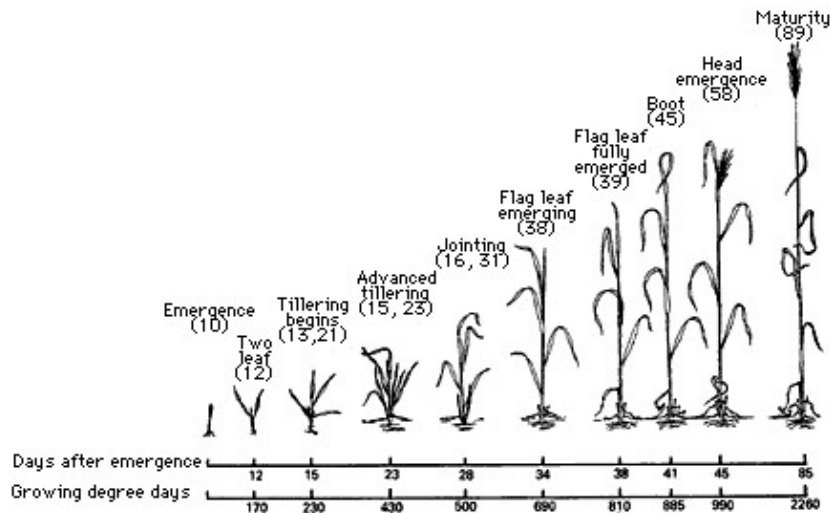
Figure 2.1: Different growth stages of in this case barley, but the same principle applies to wheat (Simmons *et al.*, 2013).

2.2   Drought resistance

2.2.1   Morphological and physiological drought adaptation

Of all the environmental abiotic stresses (drought, cold, high salinity, etc.), drought or water deficit is the most severe limiting factor of plant growth and crop production (Seki *et al.*, 2001). Drought is the condition in which the amount of available water in the environment does not meet the requirement of the plant due to high transpiration rates (Tuberosa, 2012). Light interception by the leaves and stomatal opening causes plant transpiration. In case of water deficit, this transpiration can lead to drought stress.
Drought resistance is then the capacity of the plant to maintain biomass accumulation under a given soil water deficit (Luquet *et al.*, 2016).

The availability of water in the soil-plant-atmosphere continuum (SPAC) is expressed in terms of water potential. Water is transported from high to low water potentials. All water potential values in the SPAC are negative with the atmosphere having the lowest value. This means that water flows from the soil through the plant and evaporates by the leaves into the atmosphere through suction forces exerted by the atmosphere. This force is called the vapour pressure deficit (VPD). The flow rate of water between two organs depends on the water potential difference ($\Delta\psi$) and the hydraulic resistance (R; Elfving *et al.*, 1972; De Swaef *et al.*, 2012).

Drought resistance is often linked to water use efficiency (WUE). WUE has several different definitions when used for different purposes (Tambussi *et al.*, 2007). Overall, it expresses the amount of dry matter produced per unit of invested water.

WUE is a major determinant in grain yield under drought stress (Passioura, 1977). Normally, a better (higher) WUE means the plant uses the scarce water supply more efficiently which leads to a higher biomass. Yet in cereals, it can be negatively correlated with grain yield when water is plentiful (Blum, 2005, 2006, 2009). In some cases, a lower WUE (more wasteful with water) means that the plant is able to extract more water from the soil whilst maintaining a higher stomatal conductance. Photosynthesis is therefore higher which results in a higher yield (Merah, 2001; Blum, 2006, 2009; Tuberosa, 2012). When soil moisture is limited however, these plants will not support biomass accumulation for long (Tambussi *et al.*, 2007; Barnabas *et al.*, 2008).

This shows that WUE cannot be equated to drought tolerance, since it is the ratio of two agronomic entities (yield and crop water use) that are not necessarily linked. Instead, it can merely be used as an indication for drought tolerance (Blum, 2005; Tuberosa, 2012).

Plant mechanisms to overcome water deficiencies do not necessarily coincide with an increased ability of cells to survive tissue dehydration (Cushman & Bohert, 2000). Instead, drought resistance is expressed in terms of tolerance and avoidance traits (Levitt, 1972; Luquet *et al.*, 2016).

Drought avoidance

Blum (2005) defines drought avoidance as the conservation of a high plant water status or cellular hydration under the effect of drought. Drought can be avoided by an enhanced capture of soil moisture and limited crop water loss (Blum, 2005). This is achieved both in the long and short term.

In the long run, early vigour is important to optimize WUE. It establishes a fast ground cover, deep rooting system and reduces early loss of water due to evaporation. This way, more stored water will be available to the plant in later developmental stages (Slafer *et al.*, 2005; Richards, 2006). Excessive early growth can however cause an early depletion of soil moisture, so there is always a trade-off (Tuberosa, 2012). An improved early vigour has however already led to better yielding wheat varieties (Asseng *et al.*, 2003).

The root size and architecture is important to access the water stored in the soil when water is limited or when competition between neighbouring plants limits the accessibility (Sharp *et al.*, 1988; King *et al.*, 2009; Tuberosa, 2012).

Flowering time is the most critical factor for a plant to adapt to environments differing in water availability and distribution (Richards, 2006). It allows the plant to start the grain filling stage when water availability is starting to reduce. For annual crops in temperate regions like wheat, the genetic basis is quite complex, as the flowering time is not only influenced by water availability but also by temperature and day length (Distelfeld *et al.*, 2009; Salvi *et al.*, 2011). Other small adaptations of the plant are an increased epicuticular wax layer to increase the crop albedo (Holmes & Keiller, 2002) and hence decrease the transpiration. Albedo is the reflection of the radiative energy by the canopy (Blum, 2005). So by increasing the albedo, less energy is intercepted by the plant, leading to a reduced transpiration.

Plants can avoid drought stress in an immediate way by affecting plant water demand, light interception, photosynthetic conversion, transpiration efficiency and the control of various gas exchanges (Luquet *et al.*, 2016). The stomata close, leaf growth is ceased and early senescence is started (Tardieu, 2003). These adaptations reduce water loss by transpiration. However, also photosynthesis and growth is reduced (Reymond *et al.*, 2003), since the diffusion of CO_2 is also diminished. In other words, during the regulation of the stomata, there is a trade-off between the photosynthetic gain and water loss (Cowan & Farquhar, 2012; Katul *et al.*, 2010; Manzoni *et al.*, 2011; Medlyn *et al.*, 2011; Prentice *et al.*, 2014; Sperry *et al.*, 2016).
While the older leaves are selectively killed, stomatal conductance and photosynthesis is retained as long as possible in the younger leaves by osmotic adjustment (OA; Blum, 2005). OA is the metabolic process in response to drought stress resulting in a net increase in intercellular solutes (Morgan, 1984; Zhang *et al.*, 1999; Serraj & Sinclair, 2002). This ensues water import and thus cell turgor maintenance. In wheat, OA has been shown to sustain yield under drought (Ali *et al.*, 1999; Blum *et al.*, 1999; Fan *et al.*, 2008; Izanloo *et al.*, 2008). Yet genotypes with a high capacity to adjust osmotically are likely to show reduced growth rates, due to the high metabolic cost of these osmolytes (Munns, 1988; Serraj & Sinclair, 2002; Palta *et al.*, 2007).

Overall, the reduction in growth under drought stress can have two origins, sink limitation and source limitation, and depends on the level of drought stress (Luquet *et al.*, 2016). Under moderate drought stress, plants will store their internal reserves. ABA (abscisic acid, see Section 2.2.2) stimulates enzymes for sucrose-to-starch conversion (Yang *et al.*, 2004). Starch is not osmotically active, so the cell water demand will decrease, making the sinks less water and nutrient demanding (sink limitation).
At higher water deficiencies, bio-accumulation is hindered due to the reduced photosynthesis. Growth ceases simply because of the lack of nutrients and water (source limitation; Luquet *et al.*, 2008, 2016; Pantin *et al.*, 2011). At this moment, ABA suppresses the rate of cell division in endosperm for example to prevent further damage (Myers *et al.*, 1990).

Since yield is the main goal in crop development, it is the aim of most research groups to develop plants that are not simply tolerant to water deficit, but optimize the trade-off between water use and biomass accumulation (Tardieu, 2003). This would not necessarily require a greater photosynthetic potential, but could also result from a better storage management (improved sink limited growth; Luquet *et al.*, 2016).
For example, plants displaying the limited-transpiration trait show a higher yield in almost all environments (Sadok & Sinclair, 2010; Sinclair *et al.*, 2016). This trait constrains the plant transpiration under high atmospheric VPD conditions, conserving early-season soil water for the seed filling stage (Sinclair *et al.*, 2016).

Drought tolerance

When the previous adaptations do not prevent severe dehydration, the plant defence starts and processes classified under drought tolerance mechanisms are invoked. This way, the plant is able to maintain (partial) functionality in the dehydrated state (Blum, 2005). The purpose of the drought tolerance mechanisms is survival of the plant, rather than maintaining growth.

Extreme cases of drought tolerance (also termed dehydration or desiccation tolerance) are

known in resurrection plants (Blum, 2005). They are able to enter a dormant state that ensures their survival when no, or little, water is present. Other examples in which drought tolerance effectively protects and saves the plant in the long term are rare. At the base of this scarcity is the selection (both natural and by man) of avoidance traits over tolerance traits as the main strategy for dealing with drought (Blum, 2005).

The few known tolerance mechanisms comprise remobilization of stem water-soluble carbohydrates (WSC) and accumulation of molecular protectants (Tuberosa, 2012).
To nullify the negative effects of post-anthesis drought on grain filling, WSC can be remobilized from the leaves and stem to the grains (Blum, 1998; Rebetzke *et al.*, 2008). Thus even when photosynthesis has arrested due to stress, effective grain filling still occurs (Blum, 2005).

2.2.2   Molecular control and genetic pathways

Hormones are important regulators in the adaptation of plants to their environment, including stress. Changes in auxin and ABA (abscisic acid) have been shown in drought experiments. As mentioned before, the plant will regulate its growth when confronted with water deficit. Auxin is an important phytohormone that regulates plant development during drought (Ludwig-Müller, 2011; Sharma *et al.*, 2015). Auxin Response Factors (ARFs) are upregulated in the flag leaves of stress tolerant wheat genotypes (Liu *et al.*, 2016, 2017). These bind to conserved elements within the promoters of auxin-responsive genes (Hagen & Guilfoyle, 2002; Guilfoyle & Hagen, 2007).

For a long time, ABA has been known to be the main signal in immediate stress responses (Seki *et al.*, 2002; Rabbani *et al.*, 2003; Christmann *et al.*, 2006; Adie *et al.*, 2007; Christmann *et al.*, 2007; Ton *et al.*, 2009). Its levels increase during stress and decrease again when the stress is relieved (Zeevaart, 1980). Moreover, this response is rather quick, as already 4 to 5 hours after the stress, maximum ABA levels are reached (Zeevaart, 1980).
How a reduction in soil water potential is translated into physiologically active ABA levels is still largely unknown (Raghavendra *et al.*, 2010). A hydraulic signal is induced primarily in vascular tissues by drought, but also other stresses like cold and high salinity can start this signal. It is then transported rapidly through the vascular tissue to the leaf cells and grain tissues where it induces ABA synthesis (Christmann *et al.*, 2007). The ABA targets are mainly ion channels and transcription factors, activating the ABA-responsive genes. A common result of ABA signalling are the changes in transcription patterns of the responsive genes that will be thus up or down regulated. Not only genes for drought tolerance, like guard cell responses, root growth and osmoregulation, but also genes for seed development are affected (Sharp *et al.*, 1988; Zhu, 2002; Sirichandra *et al.*, 2009).

For example, when drought is perceived by the plant, ABA mediates stomatal closure. Several ion and proton channels are activated in the guard cells. This depolarizes the guard cell plasma membrane (Levchenko *et al.*, 2005; Siegel *et al.*, 2009; Sirichandra *et al.*, 2009). Water is transported out of the cells and turgor pressure weakens, enabling stomatal closure (Figure 2.2a).

In case of transcriptional regulation, transcription factors are phosporylated by protein kinases and thus activated (Johnson *et al.*, 2002; Zhu *et al.*, 2007). Two different ABA-dependent

pathways exist here (Yamaguchi-Shinozaki & Shinozaki, 1993; Riera *et al.*, 2005). In the first pathway, the promoters of the drought-inducible genes contain an ABA-Responsive Element (ABRE; Shinozaki & Yamaguchi-Shinozaki, 2000, see also Figure 2.2b). These motifs are target binding sites for the b-zip transcription factors (ABFs or ABRE-Binding Factors; Choi *et al.*, 2005; Finkelstein *et al.*, 2005). Binding of the transcription factor will activate the gene. In the second pathway, ABA induces an AP2-type and MYC/MYB transcription factors (Yamaguchi-Shinozaki & Shinozaki, 2006, see also Figure 2.3). The corresponding drought-responsive genes have MYC/MYB recognition sequences (Urao *et al.*, 1993; Abe *et al.*, 1997, 2003).
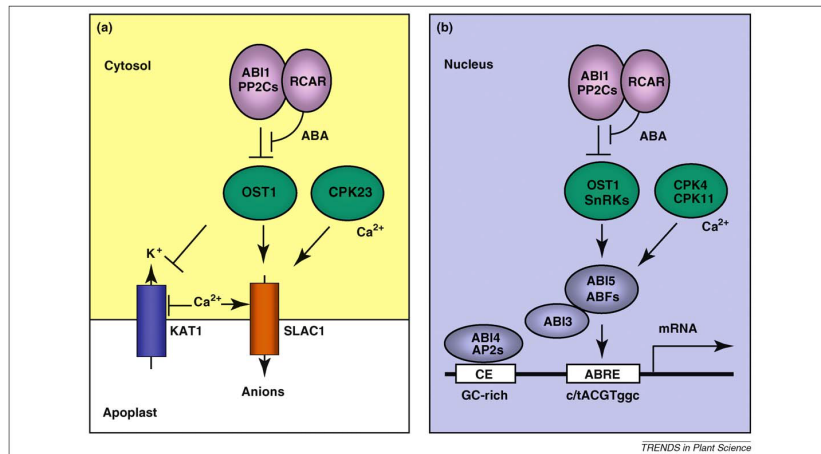
Figure 2.2: ABA-signaling pathways. (a) regulation of ion channels in stomatal closure. (b) activation of drought-responsive genes (Raghavendra *et al.*, 2010).

However, also an ABA-independent response pathway has been identified (Yamaguchi-Shinozaki & Shinozaki, 2005, see also Figure 2.3). There, the DREB (DRE-Binding) transcription factors recognize the DRE/C core motif (Dehydration Responsive Element C repeat; Riera *et al.*, 2005). What induces these transcription factors is not yet known.

Riera *et al.* (2005) conclude that the ABA-based signalling pathway is the predominant factor in primary or rapid responses to drought. This was proven by Finkelstein *et al.* (2002) and confirmed by Riera *et al.* (2005), were all mutants affected in their drought tolerance had an altered sensitivity towards ABA. This was either due to an affected ABA biosynthesis or due to an altered perception. These mutants were the base for identifying key regulatory genes (Riera *et al.*, 2005).

By changing its gene expression, a plant under water deficit will repress cell growth and photosynthesis while activating respiration. They will also bring about the accumulation of osmolytes and stress tolerance proteins, as already mentioned in Section 2.2.1.

The different induced genes will not be summarized or explained in this work. In short, the drought-inducible genes of *Arabidopsis* and rice can be classified into two groups (Rabbani *et al.*, 2003; Shinozaki *et al.*, 2003). The first group are the regulatory proteins. These are the transcription factors and protein kinases, some of which have already been discussed. They arrange further regulation of signal transduction. The second group includes the functional proteins e.g. enzymes for osmolyte biosynthesis, water channel proteins and many more (see
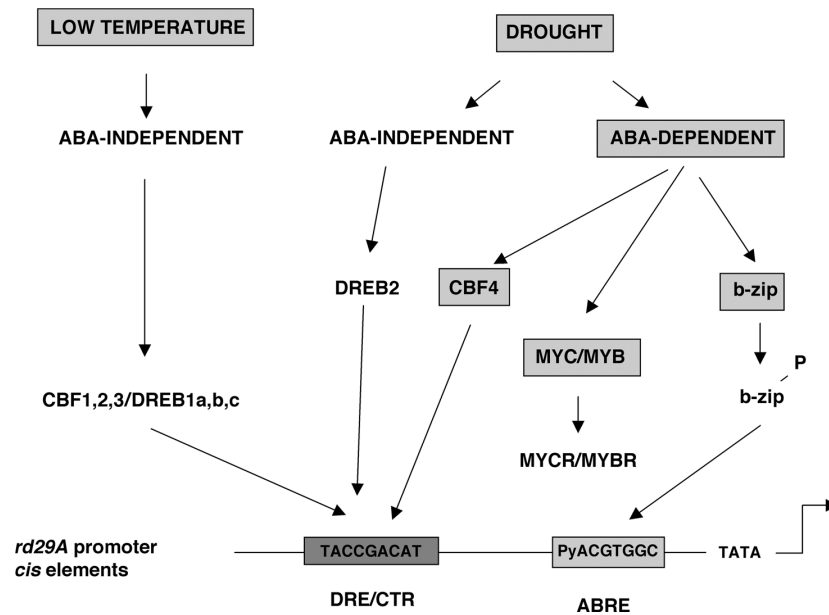
Figure 2.3: Crosstalk among several ABA-independent and ABA-dependent stress responsive pathways (Riera *et al.*, 2005).

Figure 2.4).

Often, the genes induced as a response to drought are also responsive to high salinity and cold (Seki *et al.*, 2002), suggesting cross-talk between the different signalling pathways.
Further downstream of the signalling pathway, a striking similarity leading to cross-talk is the shared core motif (DRE/C) in both promoters of dehydration-responsive and cold-responsive elements (Yamaguchi-Shinozaki & Shinozaki, 1994; Haake *et al.*, 2002). So transcription factors like DREB or CBF (Cold Binding Factor), can either be activated by drought ór cold but can induce the expression of both response elements (Figure 2.3). Crosstalk is also possible with biotic stresses (Cheng *et al.*, 2013).

2.3 Crop models

Crop models have been in use for decades to simulate and predict physiological processes and genetic traits (Duncan *et al.*, 1978; Landivar *et al.*, 1983a,b; Elwell *et al.*, 1987) and to understand crop responses to environmental and management changes.
Mechanistic crop simulation models describe photosynthesis, respiration, translocation and partitioning (Boote *et al.*, 1998). Integration of these processes returns biomass accumulation and yield over time (Boote *et al.*, 2016). Ecophysiological models include environmental variables like temperature, relative humidity, water and soil nitrogen availability (Boote *et al.*, 2016). These environmental inputs influence the processes within the crop, e.g. timing of flowering, onset of reproductive growth, rate of leaf node appearance, leaf area expansion, height increase,... But these traits are also shaped by the genetic make-up of the plant species or even the plant cultivar (see also G×E interaction in Section 2.4). The different values of
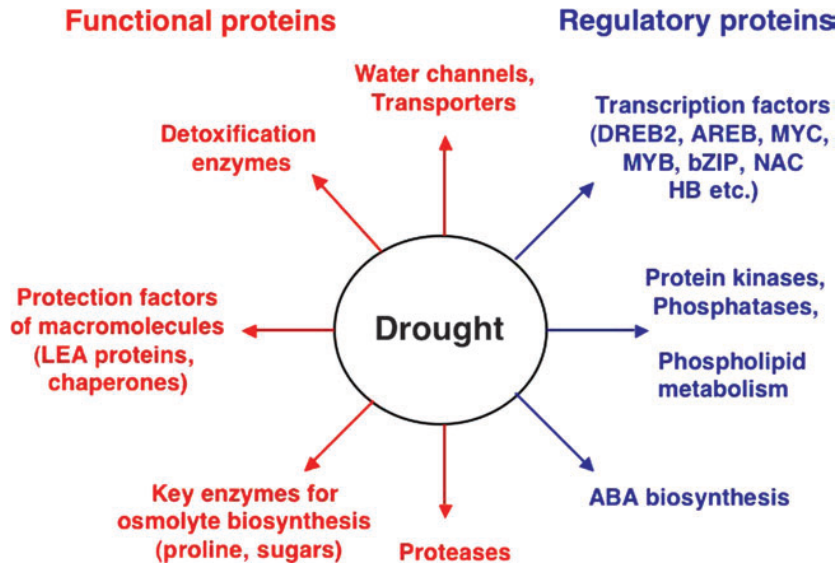
Figure 2.4: Function of drought-inducible genes in stress tolerance and response (Shinozaki & Yamaguchi-Shinozaki, 2007).

the model parameters are considered to represent genetic diversity. They are therefore called cultivar-specific parameters. One set of parameters represents one genotype (Tardieu, 2003).

2.4 Modelling genotype by environment interaction

A genotype cultivated under different environmental conditions, yields different phenotypes. This is called phenotypic plasticity and is visualized by reaction norms (DeWitt & Scheiner, 2004). The reaction norms of different genotypes can be parallel, but can also be non-parallel. This indicates the existence of genotype by environment (G×E) interaction (Finlay & Wilkinson, 1963; van Eeuwijk *et al.*, 2005). An extreme (and most important) form of G×E interaction is cross-over interaction, where the ranking of the genotypes varies with the environmental conditions (Baker, 1988; Crossa *et al.*, 2004; Bustos-Korts *et al.*, 2016).
The existence of G×E interaction means that when a genotype is known (phenotypic evaluations of that genotype in other environments) and when an environment is known (evaluations of other genotypes in that environment), it does not mean one can necessarily predict its phenotype in that environment (Bustos-Korts *et al.*, 2016).

In plant breeding, the assessment of this G×E interaction is one of the major foci and is very hard and time consuming to detect with the classical methods. Until recently, this was primarily done with statistical models, but crop models are becoming amply accurate to account for environmental and management effects (Boote *et al.*, 2016). Bustos-Korts *et al.* (2016) explain how the phenotype y_{ij} can be predicted by means of a linear mixed model (LMM), either via the fixed part of the model, or the random part (underlined):

$$y_{ij} = \mu_j + x_i \alpha_j + \beta_i z_j + \underline{GE}_{ij} + \underline{e}_{ij} \tag{2.1}$$

where y_{ij} is the phenotype of genotype i in environment j. For prediction via the fixed part, one needs molecular markers (x_i) and environmental covariables (z_j). Instead of molecular markers, pedigree information can also be used (Crossa *et al.*, 2010). The slopes, α_j and β_i, are estimated via a regression analysis. This requires enormous amounts of phenotypical data. For prediction via the random part, one needs correlations among genotypes and environments.

Of course, crop growth models would simplify these methods: the output is modelled by interaction between physiological parameters and environmental information (Chapman *et al.*, 2002; Hammer *et al.*, 2002, 2006, 2010; Chapman, 2008). Boote *et al.* (2016) propose in addition that by using crop models, dynamic phenotypes can be predicted in new environments, where statistical models are limited to the same environment.

2.5 Modelling genes

The goal of modelling genes is to predict phenotypic performance as a function of genes, transcripts, proteins and even metabolites (Boote *et al.*, 2016). White & Hoogenboom (2003) identified six levels of genetic detail that can be included in plant growth and development models (Table 2.1). Most crop models like APSIM (Zheng *et al.*, 2014), CROPGRO (Boote *et al.*, 1998), BEANGRO (Hoogenboom *et al.*, 1994) and Cropsyst (Stöckle *et al.*, 2003) correspond to level 3. They discriminate between cultivars through cultivar-specific parameters like maximum grain size or maximum expected transpiration. These parameters are also called 'genetic coefficients' (White & Hoogenboom, 1996), 'model-input traits' (Yin *et al.*, 2000) or 'genotype-specific parameters' (GSP; Boote *et al.*, 2016). They are usually determined empirically through calibrations using phenotypic data (White, 2006; Boote *et al.*, 2016).

By substituting the cultivar-specific parameters with the effects of certain alleles, one can upgrade a model from level 3 to level 4. Most current models are on level 3. Level 4 is being developed in several research groups (Baldazzi *et al.*, 2016). Level 4 gives the benefit that the parameters can be estimated using genetic data obtained through a simple marker or other genetic analysis. If all genetic coefficients could be described like this, calibration would become redundant.

Table 2.1: Different levels of genetic detail in crop models (White & Hoogenboom, 2003).

(1)	Generic model with no reference to species.
(2)	Species-specific model with no reference to genotypes.
(3)	Genetic differences represented by cultivar-specific parameters.
(4)	Genetic differences represented by specific alleles, with gene action/gene effects represented through linear effects on model parameters.
(5)	Genetic differences represented by genotypes, with gene action explicitly simulated based on knowledge of regulation of gene expression and effects of gene products.
(6)	Genetic differences represented by genotypes, with gene action simulated at the level of interactions of regulators, gene-products, and other metabolites.

Different approaches for implementing information from conventional genetics and genomics are possible. The two most common approaches are gene-based modelling and QTL-based modelling. They are classified as classical approaches, where the model parameters are specified as a function of gene or QTL effects respectively using simple empirical relations (Baldazzi *et al.*, 2016). These are further discussed in Sections 2.6.1 and 2.6.2. They result in a level 4 of the classification according to White & Hoogenboom (2003).

New approaches, in which complete regulatory networks are integrated, are starting to develop under the name of crop systems biology (see Section 2.7). They respond to level 5 and 6 of the classification.

2.6 Classical approaches

2.6.1 Gene-based modelling

In gene-based modelling the linear equations, replacing the cultivar-specific parameters, represent additive and epistatic gene effects. An important example is the GeneGro model developed by Hoogenboom *et al.* (2004), which uses the effect of merely seven genes in common bean (*Phaseolus vulgaris*) to replace all 30 cultivar-specific parameters in the BEANGRO model (Hoogenboom *et al.*, 1994). The independent variables reflected gene loci and were assigned a value of 1 for homozygous dominant loci and 0 for recessive loci. An example of a linear equation would be (for the photoperiod sensitivity slope, $PPSEN$):

$$PPSEN = 0.004 + 0.0154 \times Ppd + 0.036 \times Hr - 0.0104 \times Ppd \times Hr \qquad (2.2)$$

with Ppd and Hr the expression values (0 or 1) of the genes for 'basic photoperiod response' and 'enhanced effect of Ppd' respectively (Hoogenboom *et al.*, 2004). GeneGro simulated growth and development as well as BEANGRO, but has the advantage that no field calibration data is necessary (Hoogenboom *et al.*, 2004). Moreover, validation experiments with 17 new cultivars in new environments revealed that GeneGro could successfully simulate performances of new genotypes in new environments. G×E interaction was partially explained (White, 2006; see also Section 2.4).

More recently, this approach has also been included into the soybean simulation model CROPGRO-soybean (Messina *et al.*, 2006). Six loci were used to characterize the effect on growth and development. Zheng *et al.* (2013) demonstrated that the flowering time of spring wheat genotypes could be modelled using different allelic combinations of only two genes, *VRN1* and *Ppd-D1*. Bogard *et al.* (2014) did the same for winter wheat while using major genes and SNPs (single nucleotide polymorphisms) derived from association mapping.

Even though modelling of genes directly gives a much larger opportunity of interpreting the regulation mechanism on a molecular level, not many examples like this exist in literature, due to the lack of known regulating genes. Only a few, if any, important genes are known for the trait and cultivar of interest. This is still not enough to use as input parameters in an ecophysiological model, which is why modelling of QTLs is more common.

2.6.2 QTL-based modelling

QTLs, or Quantitative Trait Loci, are loci on the genome that show a strong correlation to a certain quantitative trait in a population of segregating progenies generated from a biparental cross (Edmeades *et al.*, 2004). The loci are identified using expressions of molecular markers and various statistical procedures to detect an association between the quantitative traits and those markers (Kearsey & Farquhar, 1998). Although a QTL is defined as a specific genetic position on the chromosome, a lot of ambiguity concerning this position exist due to uncertainties in mapping and statistical procedures. So it might be more accurate to view a QTL not as a point locus, but as a region defined by a confidence interval. A typical QTL region could therefore contain up to a few hundred genes (Edmeades *et al.*, 2004). If a QTL matches a classical locus, gene-based and QTL-based approaches overlap (White, 2006).

QTLs are often used in strictly statistical models. These models can predict the phenotype of a plant with any combination of alleles present in the model, without extra experiments. However, because a QTL model has no explicit environmental inputs, it can only be used in the same climatic scenario as that in which the QTLs were detected (Boote *et al.*, 2016). When studying stress responses, the QTLs of the trait are compared in a control and stressed treatment (e.g. Teulat *et al.*, 1998; Sanguineti *et al.*, 1999; Hirel *et al.*, 2001). This method has however the disadvantage of resulting in non-stable QTLs, because it is impossible to exactly reproduce environmental conditions in terms of temperature, soil water status and VPD. This means there will always be differences in the climatic scenarios between experiments, so that one cannot determine if a QTL-effect is due to the difference in alleles or in environment. This drawback can be overcome by incorporating an ecophysiological model, provided that the QTL analysis is performed on the parameters of the ecophysiological model (Reymond *et al.*, 2003; Tardieu, 2003).

The main advantage in using QTLs instead of genes, is that no major genes have to be identified, which are still often missing and remains difficult. That is why examples in literature on the integration of QTL information in growth models are so numerous.
For example, for barley (*Hordeum vulgare* L.), first growth and development and later also phenology, were successfully modelled using QTLs (Yin *et al.*, 2000; Struik *et al.*, 2005). Nakagawa *et al.* (2005) used a similar approach for the flowering response of rice (*Oriza sativa* L.). The response to temperature and water deficit was elucidated for maize (*Zea mays* L.) by Reymond *et al.* (2003), using an ecophysiological model for leaf expansion (see also paragraph 2.8). Germination and early growth of *Medicago truncatula* was modelled in response to temperature and water potential by Brunel *et al.* (2009). Laperche *et al.* (2006) simulated nitrogen adaptation in winter wheat and Quilot *et al.* (2005) peach fruit quality. Amelong *et al.* (2015) predicted maize kernel number and Reuning *et al.* (2015) *Arabidopsis* stomatal conductance. All models were based on the QTLs they found in a segregating population to co-localize with their trait of interest.

Yet also difficulties arise that are inherent to all QTL analyses (Kearsey & Farquhar, 1998; Edmeades *et al.*, 2004). First, possible epistatic effects are often not considered. This occurs when the alleles of one locus influence the expression of those on another locus. Second, validation and evaluation of G×E interaction remains a demanding task, even with the integration into ecophysiological models. Third, false positives among the candidate genetic markers proves to be difficult to detect. And finally, one preferably needs large population sizes

($>$250 individuals or lines) to reliably detect QTLs (Charmet, 2000; Hackett, 2002; Bernardo, 2004; Schon *et al.*, 2004). Phenotyping these large populations would require a large amount of work and effort. High-throughput phenotyping methods are promising, but remain costly and are not yet able to phenotype most traits (Xu & Buck-Sorlin, 2016).

Moreover, populations of biparental crosses are usually necessary to detect QTLs, although this can be overcome if one has a large population with variation on the quantitative trait (Gebhardt *et al.*, 2004).

2.6.3   Quantitative proteomics to represent the genetic input

In recent years, the genetic analysis of quantitative traits through QTLs has seen rapid advances due to the development of many molecular genetic techniques. The use of markers based on SNPs is widely adopted in the molecular breeding of crops due their abundance in the genome and the possibility of high-throughput analysis (Mammadov *et al.*, 2012).

As Hammer *et al.* (2004) suggest however, by quantifying the proteins present in the plant, we are not focussing on the complex gene networks, but rather on their final outcome. The proteins are the performers of the information flow of genes in the plant, they are the end result. The challenge here lies in the limited, and maybe less accurate, methodologies available. There have been a few proteomic studies on drought in wheat (Hajheidari *et al.*, 2007; Caruso *et al.*, 2009; Peng *et al.*, 2009; Kamal *et al.*, 2010; Bazargani *et al.*, 2011). Most of them however, use 2D gel-based methods. Only in recent years, mass spectrometry has become more important (Ford *et al.*, 2011).

The use of proteomics to study drought resistance in plants is not new, however the inclusion of proteomic results in plant models have not yet been reported in literature. Using proteins as the genetic input in ecophysiological models has its benefits. No prior knowledge of the plants genome is necessary, nor of its regulating genes. No primers must be developed, no DNA samples purified in bacterial cultures, no genes isolated and sequenced.

This reduces the time from sampling to genetic (or in this case proteomic) data from several months to a single day. Moreover, the gene product itself is measured, not the genes, giving more specific information on the physiological processes and consequences of the drought stress on a cellular level. Genes are always present, but it is the gene product that results in the final phenotype.

2.7   Plant biology and crop systems biology

The previous approaches all explain relatively simple traits with well-defined influences of some dominant environmental factor, e.g. vapour pressure deficit (Yin *et al.*, 2016). Moreover, they do not implement any knowledge on the molecular regulatory networks. With an increasing number of methods developed for genetic analysis and high-throughput techniques, it is becoming possible to model genetic responses in specific processes or to even model complete networks of genes, proteins and other molecules (corresponding to level 5 and 6 respectively in Table 2.1). They are often called multi-scale models, since the processes on the molecular level are upscaled to the plant, or even crop level.

Level 5 (plant biology) is still rarely encountered and is restricted to model species (e.g. *Arabidopsis thaliana* in Welch *et al.*, 2003, 2016; Beemster *et al.*, 2006; Kuchen *et al.*, 2012). For other species, not enough genes are known concerning the physiological processes that are modelled (Baldazzi *et al.*, 2016).

Plant systems biology (level 6) differs from plant biology (level 5) in that it has a 'systems approach'. This means that a system is defined as a network of interacting elements receiving certain inputs and producing certain outputs. It moves from the genome level upwards, starting from bio-informatics to modelling single organelles, cells or specific processes (White, 2006).

A decade ago, level 6 was only achieved in case of unicellular organisms (Tomita *et al.*, 1999). Only recently, an example has emerged in the model plant *Arabidopsis thaliana* (Band *et al.*, 2012). The authors explained the dynamics of cell elongation in the roots by simulating the movement of the gibberellin hormone and a complex signalling network for the distribution of DELLA proteins. However, these examples are rare, and interactions with the environment have not yet been taken into account (Baldazzi *et al.*, 2016).

In multi-scale models, one can choose to analyse gene regulatory networks or metabolic networks (Metabolic Pathway Analysis; Baldazzi *et al.*, 2016). In the former, a gene can be represented as a binary switch (Boolean model) that can be either on (value 1) or off (value 0). Depending on the state of certain genes in the model, other genes can be switched on or off. These transitions are expressed as logical rules. An extension of the Boolean formalism are the logical models. Gene states or transcription factor levels are represented as p discrete values (0, 1, 2, ..., p). Gene activation/ inactivation is now level-dependent. In piece-wise linear models, a time-continuous description of the gene regulation is modelled (see also Snoussi, 1989; Wittmann *et al.*, 2009).

Metabolic Pathway Analysis takes into account the stoichiometry of the metabolites and the thermodynamics of biochemical interactions to describe all possible steady-state behaviours of the system (Schilling *et al.*, 2000; Schuster *et al.*, 2000; Papin *et al.*, 2003; Baldazzi *et al.*, 2016). Plants are, however, subject to environmental fluctuations so that a steady-state assumption might not be accurate. A kinetic model of the system, in which metabolite concentrations change over time according to, for example, a Michaelis-Menten kinetic, is more appropriate. To determine the appropriate rate law however requires a lot of experience and is extremely expensive, so only small metabolic networks are described (Baldazzi *et al.*, 2016).

Eventually, the goal is to model entire plants or ecosystems, although a lot of problems and difficulties still arise. Often, there is a lack of knowledge and characterization of specific genes or loci controlling the traits, including epistatic interactions and pleiotropic effects (different phenotypic characteristics influenced by a single gene; Baldazzi *et al.*, 2016). The complexity increases by several orders of magnitude when upscaling to whole organisms (Hammer *et al.*, 2004). Baldazzi *et al.* (2016) state that the complexity of the genetic control accounted for in models is usually the inverse of the complexity of the modelled system. This means that integrating the effect of many genes is possible at the cellular level, but becomes too complex at plant level. The authors propose to trace the main hubs at the lower levels of organization and quantify their effects at the higher levels. They also state it is not necessary to represent the action of each gene, but rather the action of an entire gene group by a model parameter. The number of parameters in a process-based model can be thus restrained.

Hammer *et al.* (2004) suggest that not focusing on the complex gene networks, but on

higher order control, might be more appropriate when the goal is to understand overall plant performance. It is the flow of information across the different plant organs that allows the plant to adapt to the prevailing environment. Although this information is contained in the genetic make-up, there is a lot of redundant information in the genome that accumulated through evolution. Tardieu (2003) started this vision by stating that a plant will react in a predictable way to a given environmental condition and that we only need to find the highest level of organization which still explains the variability. He called this a 'meta-mechanism'.

In future light, integrating multi-scale models into ecophysiological models can help explaining the complex interplay between different spatial and temporal environmental influences and the genetic control of agronomically important traits (Baldazzi *et al.*, 2016). It might even identify interesting molecular mechanisms useful for breeding techniques, or can offer a framework for interpreting omics data, all at a low computational cost. See Section 2.9 for more explanation.

2.8   Modelling drought

Some important efforts have been made in characterizing major gene loci that are important for drought in wheat (see summary Table in Farooq *et al.* (2014)). These include for example QTLs for osmoregulation, leaf senescence, grain number, etc. Yet efforts to include these in models have been absent. The genetic basis for drought resistance has never been implemented in a wheat crop model, even though a lot of research has been done on the genetic control and networks in model plants (see paragraph 2.2.2).

For maize (*Zea mays*) and *Arabidopsis thaliana*, there have been some efforts to analyse the genetic response of water deficit and implementing this in an ecophysiological model (Reymond *et al.*, 2003; Tardieu, 2003). When modelling drought resistance, one has to decide what the application of the model will be. Because dependent on the phenological stage and the duration of the drought stress, the plant will administer different strategies and therefore probably also different genetic or signalling pathways. When water deficit lasts for only a short period, plants that maintain their growth, photosynthesis and development and empty their water supply, will result in better yields. However, when drought stress persists, these plants will reach death before the end of the crop cycle. Plants that save water during the first stages of their development at the expense of biomass accumulation will survive these conditions. But then, these plants risk being overgrown by plants with faster water use and development (Tardieu, 2003).

In maize (*Zea mays*), the effect of temperature, VPD and soil water status on the leaf elongation rate (LER) has been established. Response curves were drafted for different recombinant inbred lines. By then linking the slopes of these curves to a QTL analysis, the QTLs influencing the dependency of the environment on the LER could be determined. This way, 74 % of the variability of LER could be accounted for (Reymond *et al.*, 2003).
Reuning *et al.* (2015) identified the QTLs influencing the minimum stomatal conductance in *Arabidopsis thaliana*, important for transpiration. This was done both in dry and wet conditions to include variation across environments.

These examples, however, situate at the fourth level of Table 2.1; the models contain QTLs, but they do not integrate our understanding of the genetic control of drought resistance. Pursuing

plant systems biology to simulate whole plants still proves to be too difficult, especially for wheat, where availability of data on genotypes and field performance still appears limiting (White, 2006).

2.9 Applications and benefits of modelling genes and crop system biology

The applications of integrating genomic information into ecophysiological models can be subdivided into roughly three classes. First, it can aid in genomic selection and marker assisted breeding. Second, it might simulate the impact of changing environments, managements and genotypes or cultivars. And last, it could give us new insights in underlying processes both on the sub-cellular level as on the crop level.

2.9.1 Breeding and genomic selection

In genomic selection, first a training set of genotypes is both phenotyped and genotyped based on genetic markers. Then, this data is translated into a statistical model. New superior genotypes can finally be chosen based on the phenotypic prediction that is made with genetic marker data from breeding material that has not been phenotyped (Hammer *et al.*, 2016). Up until now, these predictions where dependent on the environment the model was made for, because G×E interaction was not accounted for. But by integrating these statistical models into ecophysiological models, the phenotypic predictions are concordant in any environment. Marker-assisted selection (MAS) can also be accelerated by integrating crop modeling. When the markers are chosen as parameters in the model, they can be ranked according to their contribution to the desired trait. Gu *et al.* (2014b) used a marker-based version of the GECROS model to rank the markers that determined yield component traits. By using this model, they could identify additional markers that a multiple regression method did not detect.

The reverse is also possible; by performing a sensitivity analysis, the genotype-specific parameters that are most important for the development of the trait of interest, can be identified (for examples, see Semenov & Halford, 2009; Suriharn *et al.*, 2011; Singh *et al.*, 2012). This is also called 'dissecting a complex trait into physiological component traits' (Yin *et al.*, 2016), whereby a genotype-specific parameter is such a component trait. Among complex traits, we understand for example yield, nutrient use efficiency, total height or total biomass. These complex traits are often integrated, cumulative outcomes, dependent on many fluctuating processes over time (Boote *et al.*, 2016).
Hammer *et al.* (2016) termed this 'shortening the phenotypic distance'. For complex traits, the phenotypic distance is often too large, meaning it is impossible to scale the gene network to the phenotype or to predict the phenotype based directly on the genetic information. This is due to the complexity and the magnitude of the regulating gene network and the G×E interactions (Sinclair *et al.*, 2004). When a single-gene transformation directly affects the plant phenotype however, the phenotypic distance is said to be short (Hammer *et al.*, 2016). The phenotypic distance can be shortened by dissecting complex traits to more robust sub-traits, or component traits. Often these component traits are difficult to phenotype using the normal phenotyping methods, but they can be modelled based on easily phenotyped traits that are used as inputs in crop ecophysiology and functional whole plant modelling.

For example, Gu *et al.* (2014b) dissected yield into seven easily measured physiological input parameters, like seed dry weight and maximum plant height. QTL loci for these parameters were then identified. To find direct loci for the yield trait would have been nearly impossible.

Since the complex traits are often cumulative outputs, another way of dissecting these traits would be to consider the derivatives, or in other words, the rate of change. An example of this approach, is the research by Reymond *et al.* (2003) and Tardieu *et al.* (2005). They modelled the reduction in leaf area under water deficit. The QTLs found for leaf area were dependent on the growing environment, meaning that at least one environmental variable was not accounted for in their model. Instead, the leaf expansion rate was only dependent on temperature, VPD and the plant water status. All these variables were addressed in the model, so by moving from the level of leaf area to the leaf expansion rate, the environment context dependency was eliminated (Hammer *et al.*, 2016).

The genes influencing these component traits can thus be sought after. Or one can first assess the potential value of a trait via modelling. Then, a direct search for alleles that lead to this trait will accelerate the breeding process. One can even look for expression of the trait in existing germplasm (Sinclair *et al.*, 2016), eliminating the need to develop a segregating population which takes a significant amount of time. Sinclair *et al.* (2016) performed such simulation studies to assess the potential benefit of the limited-transpiration trait in soybean (*Glycine max* L.), mentioned in Section 2.8. When they found candidate lines with this component trait in existing germplasm, they investigated the physiology of the trait. These candidate lines resulted in breeding lines with a superior performance under water-limited conditions.

Another interesting application of a quantitative genetic analysis is virtual breeding (Xu & Buck-Sorlin, 2016). In these methods, 'virtual chromosomes' containing the QTL-information along with recombination frequencies are recombined according to the rules of sexual reproduction. This way, it is possible to produce a large number of recombinant genotypes. By combining this method with growth models, the performances of the genotypes can be tested under different (virtual) climatic conditions. Xu *et al.* (2011) integrated QTL information on internode extension into an ecophysiological model of rice (*Oryza sativa*). In a follow-up study (Xu *et al.*, 2012), the model was extended for virtual breeding and named *Ricebreeder* (Xu & Buck-Sorlin, 2016).

Very important in breeding is the design and testing of ideotypes: genotypes that are specifically adapted to a set of environmental conditions or management practices of particular interest (Donald, 1968; Andrivon *et al.*, 2013). This subject is further discussed in Section 2.9.2.

2.9.2   Simulating the effect of new environments or new genotypes

As mentioned before, combining quantitative genetics and growth models can accelerate traditional breeding (Uptmoor *et al.*, 2008). The development of different phenotypes can not only be modelled under observed conditions, but also environmental conditions that have not been experimentally tested. Even new genotypes that only exist *in silico* can be virtually tested in different environments (Reymond *et al.*, 2004). The effect of mutations can be monitored, even before genetic manipulations are performed (Tardieu, 2003; Génard *et al.*, 2010, 2016).

This will lead to the identification of ideotypes. See Génard *et al.* (2016) for examples of the

design of ideotypes via process-based simulation models (PBSM). With the integration of a growth model, one can now virtually test ideotypes with a wide adaptation to a wide set of environments versus ideotypes that have a narrow adaptation to a limited set of environments. In traditional breeding, the decision of developing a widely adapted versus narrow adapted plant has to be made in advance of the breeding program.

Integrated models can also be used to assess whether a trait can be improved within the existing germplasm (Chenu *et al.*, 2009; Luquet *et al.*, 2016). When the regulating genes (or QTLs) for a certain trait have been identified, the different existing alleles can be recombined to give non-existing genotypes, but genotypes that cán be generated by marker-assisted breeding. Thus, large hypothetical recombinant populations can be assembled. Their respective hypothetical phenotypes can then be simulated by a process-oriented crop model. This was done by Chenu *et al.* (2009) for the QTLs controlling the leaf elongation rate (LER) and the anthesis-silking-interval (ASI) in maize (*Zea mays*). They identified new QTL combinations that were advantageous or disadvantageous to yield under multiple environments (Boote *et al.*, 2016). A similar approach was used by Luquet *et al.* (2016), only here, not genes but cultivar-specific parameters were recombined into a new, virtual population. After all, these parameters can be regarded as genotype-dependent traits. The parameters were chosen within the observed range of the real plants. Both real and virtual rice plants were subjected to three water treatments. The authors concluded that there is a substantial margin for potential genetic improvement of vigour with unchanged drought resistance.

Stam (1998) and Yin *et al.* (2016) express however their concerns regarding this approach. The assumption that genes, QTLs or alleles (or representative cultivar-specific parameters) can be recombined at will in a single genotype is not appropriate. It ignores the possible existence of constraints, feedback mechanisms and correlations among the traits. Examples are a tight linkage between the genes so they cannot be easily separated during breeding, or pleiotropy, the fact that a single gene can affect multiple traits (Yin *et al.*, 2016). This might reduce the interest of breeders to adopt the results of model-based approaches in their breeding programs. Therefore, a profound understanding of the inheritance of the model parameters within the breeding framework is required (Stam, 1998).

The impact of a changing environment, management or cultivar can be simulated on a large scale. For example, Sinclair *et al.* (2010) simulated the impact of the limited-transpiration trait (mentioned in Section 2.9.1) on the soybean production in the USA.
In the face of climate change and global warming, crop modeling and crop systems biology will become increasingly important to breeders. Developing a new cultivar usually takes 10 to 12 years and, faced with the rapid climate change, breeders do not have access yet to the climatic conditions of even the near future (Semenov & Halford, 2009). Modelling techniques can help quantify future threats.

2.9.3 Understanding physiological processes

By integrating the effects of alleles or genes over time and space, one can easily evaluate the effect of changes in a single gene or trait (Gu *et al.*, 2014a; Yin *et al.*, 2016). In the model, the other traits can simply be kept constant, something that is impossible in a 'real' experiment. For example, by upscaling the effect of an increased leaf photosynthetic rate to the crop level, Gu *et al.* (2014a) could prove that crop yield can be improved significantly. Such a correlation

between crop yield and leaf photosynthetic rate was long disputed in literature.

G×E interactions (see Section 2.4) could show where interaction between a physiological trait and the environment is present. This can lead to a better understanding of the regulation of certain cellular processes.

Co-localization of genes or QTLs for different traits might provide some insight in the processes that control them. For example, Quilot *et al.* (2005) found that the QTLs for peach fruit quality co-localized on the genetic map with QTL for fruit size and sugar content. Similarly, because the QTLs for leaf elongation and anthesis-silking interval in maize co-localized, Welcker *et al.* (2007) hypothesized that the traits might be regulated by the same process. Chenu *et al.* (2009) used these genes to produce a hypothetical recombinant population (see Section 2.9.2).

2.10   Future prospects of crop systems biology

Yin & Struik (2007) proposed a two-step road map for crop systems biology. Currently we are only in the juvenile phase of the first step (Yin & Struik, 2016).

The first step will mainly consist in improving our simulation models so they describe the individual processes more mechanistically (Yin & Struik, 2016). They should be detailed in their biochemical and physical description of the processes at the cellular level. Then, these processes should be integrated and scaled up to the crop level so that only conservative mechanisms such as energy and water transfer and carbon and nitrogen metabolism are at the basis of the processes. At the cellular level, these conservative models will be applicable to all different crops. The parts of mechanisms that show genetic variation can be modified according to the crop and the genetic information available.

In conclusion, the models should be robust for a variety of genotypes, species and environments, while at the same time allow easy phenotyping of the component traits, preferably in a high-throughput manner.

The second step mainly abides in the 'omics'-progression (Yin & Struik, 2016). As our understanding of genomic, transcriptomic and proteomic methods and outputs improves and high-throughput technologies become available, the modelling can go down to lower organizational levels. Summary models of only a particular metabolism or process will increasingly become available (Yin & Struik, 2016). It is then only a matter of time before they are embedded into crop systems biology models. It will thus become possible to model complete genetic regulatory pathways and metabolite networks in an environmental context and go down to lowest level possible.

Many different submodels will have to be combined, all having different temporal, spacial and structural scales. So multi-scale modelling will become inevitable in crop systems biology. Ultimately, it may develop into a highly computer-intensive discipline (Yin & Struik, 2016).

The benefits and applications of the integration of genetic profiles into ecophysiological models are endless. Not only can it provide a biological interpretation of the molecular control of plant processes and phenomena such as genotype-by-environment (G×E) interaction, epistatis and pleiotropy, its applications in breeding programs, crop management and genetic engineering are numerous.

Chapter 3

Model description

In this study, two models were built that are linked through only one variable: the leaf water potential, ψ_{leaf}^x. The first is a combination of the Penman-Monteith evapotranspiration model (Allen *et al.*, 1998) and the Cropsyst water uptake model (adopted from Camargo & Kemanian, 2016). This model simulates the actual transpiration of the plant based on a few atmospheric measurements and the soil water potential.

The second model is a variation on the water flow and storage model HydGro developed in Steppe *et al.* (2006) and Steppe *et al.* (2008). In the model, the wheat plant is divided into three main compartments: the stem, the leaves (simulated as one big leaf) and the head, consisting of the peduncle and the ear. The roots are not considered. The leaf and the head are both linked to the stem (Figure 3.1). The HydGro model simulates water transport between the different compartments and calculates the related water potentials and diameters of the stem and the head (or rather the peduncle).

The model was implemented using the plant modelling software PhytoSim (Phyto-IT BVBA, Mariakerke, Belgium). This software also provides modules for simulation, sensitivity and identifiability analysis, calibration and uncertainty analysis.

3.1 Penman-Monteith, the evapotranspiration submodel

Penman-Monteith (PM) is a widely known and often used model for estimating crop evapotranspiration based on environmental data. The Food and Agricultural Organization of the United Nations (FAO) developed a standard PM method known as the FAO-56 PM (Allen *et al.*, 1998). This model calculates the reference potential evapotranspiration ($ET_{0,pot}$) of a standard hypothetical crop using input data of solar radiation, air temperature, relative humidity and wind speed. By using a genotype-specific parameter, the crop coefficient (K_{crop}), this $ET_{0,pot}$ is then scaled to the crop of interest. The standard model however calculates the evapotranspiration on a daily basis and per area of crop, so the calculated $ET_{0,pot}$ was altered to $\mathrm{g\,h^{-1}}$ instead of $\mathrm{mm\,day^{-1}}$ and was divided by the density of the crop to result in values that apply to a single plant.

The resulting Penman-Monteith equation is

$$\lambda ET_{0,pot} = \frac{\Delta(R_n - G) + \rho_a c_p \frac{VPD}{r_a}}{\Delta + \gamma(1 + \frac{r_s}{r_a})} \frac{k}{d_{crop}} \tag{3.1}$$

with λ the latent heat of water vaporization at air temperature ($MJ\,kg^{-1}$), R_n the net radiation ($W\,m^{-2}$), G the soil heat flux ($W\,m^{-2}$), VPD the vapour pressure deficit of the air (kPa), ρ_a the air density at constant pressure ($kg\,m^{-3}$), c_p the specific heat of the air ($MJ\,kg^{-1}\,°C^{-1}$), Δ the slope of the saturation vapour pressure curve at air temperature ($kPa\,°C^{-1}$), γ the psychrometric constant ($kPa\,°C^{-1}$), r_s and r_a the bulk surface and aerodynamic resistances respectively ($s\,m^{-1}$), k the conversion factor to the unit $g\,h^{-1}$ and d_{crop} the density of the crop (m^{-2}), in this case the density of the plants in the pot.
This equation will calculate the potential evapotranspiration of a hypothetical reference crop with an assumed height of $0.12\,m$ and an albedo of 0.23. By making these assumptions, the different parameters in equation 3.1 can be determined solely based on relative humidity, wind speed and air temperature. The equations for Δ, λ, γ and ρ_a were taken from the model by Zweifel *et al.* (2002) and Zweifel *et al.* (2007) and will not be repeated here.

The soil heat flux G is often small compared to R_n, so it will be ignored in this study.
The VPD is calculated according to Jones (1992):

$$e_s = 0.6108 \exp(\frac{17.27 * T_{air}}{T_{air} + 237.3}) \tag{3.2}$$

$$e_a = e_s \frac{RH}{100} \tag{3.3}$$

$$VPD = e_s - e_a \tag{3.4}$$

with e_s the saturated vapour pressure (kPa), e_a the actual vapour pressure (kPa), T_{air} the measured air temperature (°C) and RH the measured relative humidity.
The aerodynamic resistance (r_a) is estimated based on the reference grass and becomes

$$r_a = \frac{208}{u_{wind}} \tag{3.5}$$

with u_{wind} the wind speed ($m\,s^{-1}$). This variable was measured at three time points in the greenhouse and each time measured at $0.00\,m\,s^{-1}$. To avoid numerical errors, the value was taken at a constant value of $0.005\,m\,s^{-1}$.
The bulk surface resistance (r_s) is approximated by

$$r_s = \frac{r_l}{LAI_{active}} \tag{3.6}$$

with r_l the bulk stomatal resistance of a well-illuminated leaf ($s\,m^{-1}$) and LAI_{active} the leaf area actively contributing to the surface heat and vapour transfer ($m^2\,m^{-2}$). Since the pot containing the plants was not surrounded by other plants, heat and vapour transfer was not greatly hindered and LAI_{active} was simply approximated by the LAI (Leaf Area Index). Both r_l and LAI were used as constant values based on measurements during a previous experiment. However, these values only apply to well-watered conditions and are expected to change

radically during the drought treatment since stomatal resistance will increase significantly and LAI will decrease as early senescence progresses. Normally, a moving window calibration would neutralize this accumulating error. New values for K_{crop} are then calculated each day. This genotype-specific parameter will then not be constant, but changing every day representing the variable stomatal resistance and LAI. Unfortunately, a moving window calibration was not possible for reasons explained in Chapter 6.

The actual plant potential evapotranspiration is then simply determined as follows

$$ET_{pot} = K_{crop} \times ET_{0,pot} \tag{3.7}$$

3.2 Cropsyst, the transpiration submodel

Cropsyst is a cropping systems simulation model that simulates growth and yield of different crops in different soil types and different management systems (Stöckle & Nelson, 2003). There are many similar models available, but what made Cropsyst interesting to use alongside the HydGro model, is that it uses water potentials to calculate certain variables. For example, it estimates the water potential of the leaves based on soil moisture data to determine when the stomata will close. Since the leaf water potential is simulated more accurately by HydGro, this variable was used instead of Cropsysts own calculations.

Cropsyst equations were used to calculate the actual plant transpiration from the potential evapotranspiration. This was done in two steps. In the first step, the potential transpiration Tr_{pot} is calculated via Stöckle & Nelson (2003):

$$Tr_{pot} = Fract_{cover,green} \times ET_{pot} \tag{3.8}$$

where $Fract_{cover,green}$ is the fraction of incident radiation intercepted by the crop green leaf area. Tr_{pot} is expressed in $g\,h^{-1}$, like ET_{pot}.
The actual transpiration Tr_{act} (also in $g\,h^{-1}$) is then determined in the second step by the stomatal conductance. When the leaf water potential ψ_{leaf} falls under a certain threshold ψ_{Lsc}, transpiration is reduced as the stomata are (partially) closed. For leaf water potentials under the permanent wilting point (ψ_{Lpwp}), transpiration stops (Camargo & Kemanian, 2016). This is expressed as

$$Tr_{act} = \begin{cases} Tr_{pot}, & \psi_{leaf}^x > \psi_{Lsc} \\ Tr_{pot}\frac{\psi_{leaf}^x - \psi_{Lpwp}}{\psi_{Lsc} - \psi_{Lpwp}}, & \psi_{leaf} < \psi_{Lsc} \\ 0, & \psi_{leaf} < \psi_{Lpwp} \end{cases} \tag{3.9}$$

with ψ_{Lsc} the leaf water potential at stomatal closure (MPa) and ψ_{Lpwp} the leaf water potential at permanent wilting point (MPa). ψ_{leaf}^x (MPa) is the leaf xylem water potential, als simulated by HydGro (see secion 3.3).

3.3   HydGro, the water storage submodel

HydGro is a water transport and storage model originally developed for trees (Steppe *et al.*, 2006, 2008), but the main principles should be applicable to all plants. The model consists of two submodels. The first submodel uses measurements of sap flow and soil water potential to describe water transport between the different plant organs and between the xylem and storage tissue within one organ.
The second submodel simulates the variation in stem diameter, as these organs will shrink and grow daily when the storage tissues are depleted and refilled again (reversible grow) or when irreversible growth occurs. Measurements of this diameter variation can then be used for calibration of the model.

In the wheat model, three different plant compartments are considered (Figure 3.1). Each plant organ consists of a xylem compartment (flow path) and of a storage compartment, which consists of all the living cells around the xylem vessels that are able to store water. Water will flow from the soil through the roots (not considered here) to the stem xylem. This flow rate is represented by F_{stem} and expressed in $\mathrm{g\,h^{-1}}$. In a similar way, F_{head} represents the flow rate from the stem xylem to the peduncle and ear xylem and F_{leaf} is then the flow rate to the leaf xylem.
Within each plant organ, water flow is also possible between the storage tissue and the xylem, since these tissues are hydraulically connected (Simonneau *et al.*, 1993; Génard *et al.*, 2001; Steppe *et al.*, 2006). These flows can attribute to the daily transpiration stream and are represented by f_{stem}, f_{head} and f_{leaf} for the stem, head and leaf, respectively, and also expressed in $\mathrm{g\,h^{-1}}$. These flows contribute to the filling and depletion of the storage tissue, which means they must have a variable water content. These are represented by W_{stem}, W_{head} and W_{leaf} and expressed in g.

One of the main concepts in the sap flow model, is the van den Honert (1948) principle based on Ohm's law. It states that water is transported from a high to a low water potential (read more negative) over a hydraulic resistance, R^x ($\mathrm{MPa\,h\,g^{-1}}$). All different compartments are therefore characterized by a water potential (ψ^x_{organ} for the xylem compartments and ψ^s_{organ} for the storage compartments) and expressed in MPa. The water flow between the organs can thus be expressed as

$$F_{stem} = \frac{\psi_{root} - \psi^x_{stem}}{R^x} \tag{3.10}$$

$$F_{head} = \frac{\psi_{stem} - \psi^x_{head}}{R^x} \tag{3.11}$$

$$F_{stem} = \frac{\psi_{stem} - \psi^x_{leaf}}{R^x} \tag{3.12}$$

where ψ_{root} is the water potential in the roots (MPa). Since this organ is not modelled, an estimation based on ψ_{soil} is made by multiplying its value with k_{soil}, a proportionality parameter that is to be calibrated (De Pauw *et al.*, 2008). This results in

$$\psi_{root} = k_{soil}\psi_{soil} \tag{3.13}$$

This correction is dual. First, it takes into account the fact that the water in the soil surrounding the roots will be addressed and depleted first when water uptake starts (Tuzet
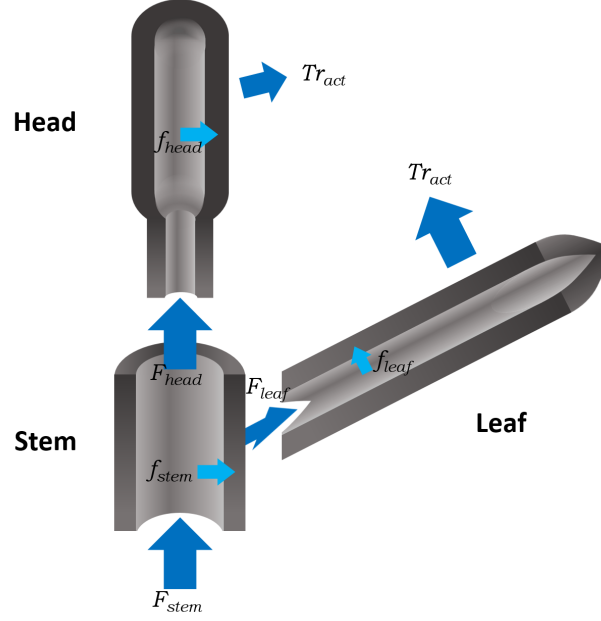
Figure 3.1: Scheme of the water flow and storage in the wheat model. Light grey areas represent the xylem compartments, while dark grey the storage compartments.

et al., 2003). The soil water potential in that region will therefore be lower than that in the bulk soil. Second, it considers the decrease in water potential due to water transport through the roots.

In earlier models, the hydraulic resistance within the xylem, R^x, was considered a constant parameter. Baert *et al.* (2015) improved this by stating that the hydraulic resistance is related to ψ_{soil}, or rather ψ_{root} according to

$$R^x = r_1 \exp((\psi_{root})^2 r_2) \tag{3.14}$$

with r_1 and r_2 proportionality parameters.

In a similar way as the xylem water transport, the water flow between the xylem and storage tissues can be expressed as

$$f_{organ} = \frac{\psi^x_{organ} - \psi^s_{organ}}{R^s} \tag{3.15}$$

with R^s the hydraulic exchange resistance ($\mathrm{MPa\,h\,g^{-1}}$) taken as a constant parameter. This flow is positive when the storage tissues are refilled and negative when water is withdrawn. The water potential in the storage compartments ψ^s_{organ} is calculated according to its water content W_{organ}. HydGro is a hydraulic system approach, which means it assumes a variable capacitance (Steppe *et al.*, 2006). This capacitance changes with the water content of the storage compartment, as represented by a desorption curve. ψ^s_{organ} is then calculated according to Zweifel *et al.* (2000) and Zweifel *et al.* (2001).

$$\psi^s_{organ} = \frac{\psi^s_{min,organ}}{1 + \exp(\frac{W_{organ} - k_{1,organ}}{k_{2,organ}})} \tag{3.16}$$

with $\psi^s_{min,organ}$ (MPa) the minimal water potential of the storage compartment, $k_{1,organ}$ the amount of stored water at the inflection point and $k_{2,organ}$ an index for the rate of change of ψ^s_{organ} at the inflection point. As suggested by Zweifel *et al.* (2001), these parameter values were chosen different for the stem and head compartment. Since there are no measurements of the leaf thickness, the parameters for the desorption curve of the leaf are impossible to determine. They were therefore equalised to the stem parameters.

The variable capacitance of the storage tissues can be calculated as follows

$$C_{organ} = \frac{\mathrm{d}W_{organ}}{\mathrm{d}\psi^s_{organ}} \qquad (3.17)$$

This expresses the ratio of the change in water mass to the change in water potential in the storage tissues.
As water flows from and to the storage tissues, their water content will change according to

$$\frac{\mathrm{d}W_{organ}}{\mathrm{d}t} = f_{organ} \qquad (3.18)$$

The preceding equations all apply to a single plant organ. How the submodules are connected is as follows. Root water potential ψ_{root} and stem sap flow F_{stem} are used to calculate the different variables and flows in the stem segment leading to values for the stem xylem water potential ψ^x_{stem}.
These values together with the measurements of the peduncle sap flow, F_{head}, are used as inputs to calculate the dynamics in the head segment.
Stem xylem water potential is also used for the simulation of the leaf. However, no measurements of leaf sap flow, F_{leaf}, are available. This variable is simply determined by a water mass balance over the stem segment:

$$F_{leaf} = F_{stem} - f_{stem} - F_{head} \qquad (3.19)$$

This of course, assumes no transpiration losses by the wheat stem.

In the second submodel of HydGro, the diameter variation of the base of the stem and of the peduncle is simulated to compare with the measured diameter values for calibration. These variables are implemented in the model as $D_{outer,stem}$ and $D_{outer,head}$ respectively, but will be denoted as simply D_{stem} and D_{head} in this report. Steppe *et al.* (2006) made the simplification of representing the xylem and the storage compartment as two coaxial cylinders. This is apt for trees since there, the xylem is indeed cylindrical and surrounded by the storage tissues. In wheat, however, the vascular tissue is arranged in bundles surrounding a hollow core (Hamman *et al.*, 2005). The bundles are embedded within the storage tissue. This could imply that the diameter of wheat changes differently with water potential compared to trees.
Since the equations for this submodel remained almost unchanged compared to Steppe *et al.* (2006), they will not be repeated here. Instead, a short explanation on the mechanism and dynamics is given.

When water is transported into the storage compartments of the plant, the water potential will increase (i.e. a smaller negative value). The turgor pressure (positive pressure potential) will also increase, pushing cells and the diameter outwards. This process is reversible as water can

flow back from the storage cells to the xylem. When the turgor however, reaches a threshold value Γ (MPa), the cells grow irreversibly. These calculations are based on Lockhart's equation (1965).

The pressure potential, $\psi_{p,organ}^s$, is calculated based on the simulated values for the water flow to the storage compartments, f_{organ}, in the first submodel of HydGro. As long as f_{organ} is positive, water flows to the storage cells and the pressure potential increases. These values in turn serve for the calculation of the diameter variation of the xylem compartment (inner cylinder) and the stem (outer cylinder).

In the model, the same parameter values were used for the stem compartment and for the head compartment, as they both simulate diameters of the stem. The only exception was the parameter ε_0, a proportionality constant determining how strongly the tissue responds to changes in the pressure potential. During test simulations, it became clear that the peduncle and the main stem respond differently to changes in sap flow making it necessary to distinguish both responses by considering separate parameters: $\varepsilon_{0,stem}$ and $\varepsilon_{0,head}$.

As mentioned above, the diameter changes in wheat stems could differ significantly from those in trees. This quickly became clear during test simulations. Simulated diameter variation was much larger than what was measured. A factor, $f_{diameter}$ was therefore included in the equations to reduce this simulated variation and make calibration possible. An interpretation of this factor is given in Chapter 6.

Chapter 4

Materials and methods

4.1 Plant material and experimental setup

In this experiment, 18 wheat plants of the Hartog cultivar were used immediately after the heading stage. Twenty wheat plants were sown on January 30, 2017 (Day of Year; DOY 30) in two pots containing 4 L potting soil. They were grown in a phytotron with a constant ambient temperature of 20 °C and a day/night cycle of 13/11 h. Only nine plants per pot grew. At the elongation stage, the plants were refertilised with NPK 6-6-7 suspension fertiliser. The ears appeared between March 29, 2017 and April 3, 2017 (DOY 93). At this point the plants were transferred to a small glasshouse compartment (2 m width × 2.5 m length × 4 m height) at the faculty of Bioscience Engineering in Ghent. Temperature in the glasshouse was controlled at a minimum of 21 °C. Along with the natural solar radiation in the glasshouse, the plants were also illuminated with artificial light (SON-T, Philips, Eindhoven, Netherlands) at a day/night cycle of 12/12 h.
One pot was used for the control treatment (further called 'control plant') and stood in a layer of water at all times to minimize influences in sap flow measurements. Soil moisture was kept at a constant value of 60 % (volumetric soil moisture level).
The second pot was used for the drought treatment (further called 'drought-stressed plant'). In this pot, soil moisture was kept at 60 % for 8 days and between April 11, 2017 and April 19, 2017 these plants were watered only a few times to start the drying process. On April 19, 2017 the sensors showed stable measurements and the plants were watered for the last time.

4.2 Microclimatic and soil measurements

Microclimate

For the PM submodel (Section 3.1), several atmospheric input variables that have a major impact on plant development are necessary. Temperature and relative humidity were measured with a humidity/temperature sensor (type EE08, E+E Elektronik, Engerwitzdorf, Austria). The sensor was installed 1 m above the plants. Photosynthetically active radiation (PAR) was measured using a quantum sensor (QS2-715, Delta-T Devices, Cambridge, U.K.). Net radiation was measured with a net radiometer (Q-7.1, Campbell Scientific, Logan, UT-US). The quantum sensor and net radiometer were installed just above the ears. Finally, atmospheric CO_2 concentration was measured using a carbon dioxide probe (CARBOCAP GMP343,

Vaisala, Vanha Nurmijärventie, Finland) placed at the height of the leaves, $30\,\mathrm{cm}$ away from the plants.

All continuous measurements mentioned here and below were scanned with a data logger (CR1000 and AM16/32 Multiplexer, Campbell Scientific, Logan, UT-US).

Soil moisture

An input of the HydGro submodel in Chapter 3 is the soil water potential, ψ_{soil}. This can be measured using a tensiometer, but since this device is rather large it could not be used in our experiments. Instead, the volumetric water content (VWC) was measured using soil moisture sensors (VWC EC5, Decagon, Pullman, WA-US). These sensors need to be calibrated for each soil type. To this end, the potting soil was dried in an oven to reach a moisture level of $0\,\%$. Water was then added in discrete steps to eventually reach the maximum moisture level. At each step, the signals of the sensors (in mV) were recorded and two samples of the same volume were taken. The exact gravimetric moisture level of the samples was determined by weighing and drying. To obtain the VWC, the results were multiplied by the density of the potting soil ($0.343\,\mathrm{g/cm^3}$). This way, a linear relation could be deduced between the volumetric moisture levels and the measured volt signal. The calibrations used are listed in Table 4.1.

Table 4.1: Calibration of the EC5 soil moisture sensors. x represents the measured signal in mV, while y represents the volumetric soil moisture level.

Sensor	Calibration	$\mathbf{R}^2$
EC5/1	$y = 0.0011865x - 0.4242$	0.9652
EC5/2	$y = 0.0011570x - 0.4139$	0.9624
EC5/3	$y = 0.0011650x - 0.4101$	0.9677
EC5/4	$y = 0.0012373x - 0.4454$	0.9618

To deduce the water potential from the VWC, a water retention curve (or pF curve) should be used. There are several models available for sand, clay and loamy soils (Tuller & Or, 2003), but for potting soil, a pF curve has to be determined empirically.

In the laboratory of Plant Ecology, such data for potting soil was available and used here to calculate the soil water potential. The relation between pF and VWC was determined empirically based on data points.

$$pF = 0.5687\,VWC^{-1.053} \tag{4.1}$$

$$\psi_{soil} = -10^{pF} \tag{4.2}$$

with VWC, the volumetric water volume (between 0 and 1) and ψ_{soil} the soil water potential (MPa).

4.3 Plant measurements

4.3.1 Continuous measurements

For each treatment, one plant was equipped with *in situ* physiological measurements. The sensors were installed on April 7, 2017 (DOY 97). A schematic layout of these sensors is presented in Figure 4.1a, whereas Figure 4.1b shows a picture of the practical installation. Sap flow rates were measured using custom 3D-printed miniaturized sap flow sensors (ExoBeat). Two sensors per plant were installed: one at the base of the main stem just above the second leaf (F_{stem}) and one on the peduncle (above the flag leaf, F_{head}).

Right above these sap flow sensors, stem diameter variations were measured using dendrometers (Solartron type DF5.0, Solartron Metrology, Bognor Regis West Sussex, UK) and leaf clips (Leaf Sensor, Leaf-Sen, Petach Tikva, Israel). The Solartrons measured the diameter variation at the base of the stem (D_{stem}), while the leaf clips measured the peduncle diameter variation (D_{head}). The sensors were tightly attached to metal rods using strings (Figure 4.1b). A few experiments showed that a tight mounting system was required to avoid anomalies when disturbing the plants for watering and sampling (data not shown). Initial values of the stem diameters were measured with an electronic calliper (RS Pro 150 mm Digital Calliper, RS Componants, Corby, UK).

In a side experiment, two types of dendrometers were tested for temperature dependency: Ecomatik (type DF, Ecomatik, Munich, Germany) and Solartron. To this end, the dendrometers were installed on a stainless steel rod, of which the exact diameter change could be calculated. The Ecomatiks often measured constant values for periods of 12 hours, which could not be explained and which did not appear in the Solartron measurements. This led us to decide to use the Solartrons in the final experiment. The Solartrons were calibrated for temperature according to von der Crone *et al.* (non published). The value for the thermal sensor coefficient (σ_{Sol}) determined by von der Crone *et al.* (non published) could not be adopted as it resulted in an overcorrection. Its value was therefore determined for each Solartron in the test set up by minimising the SSE (sum of squared errors of prediction). This resulted in a value of 2.57 $\times$ 10^{-4} mm °C^{-1} for the Solartron on the stem of the control plant and 2.90 $\times$ 10^{-4} mm °C^{-1} for the Solartron on the stem of the drought treated plant.

Because the Solartrons on the peduncles of both plants were heavily influenced by the temperature in the greenhouse, two additional leaf clips were mounted on these peduncles. Their temperature dependence was established in another side experiment, where the leaf clips were attached to an aluminium plate. In a similar manner, the thermal sensor coefficients, σ_{LC}, of the leaf clips were determined at 2.23 $\times$ 10^{-4} mm °C^{-1} for the leaf clip on the control plant and -2.43 $\times$ 10^{-4} mm °C^{-1} for the leaf clip on the drought treated plant.

The temperature calibration results in the following correction:

$$d_{real} = d_{meas} + \sigma(T_{air} - T_{ref}) \tag{4.3}$$

where d_{real} is the true diameter (mm), d_{meas} is the output of the leaf clip (mm) or in case of the Solartron the output after the first temperature correction by von der Crone *et al.*(non published), T_{air} is a moving window average of the ambient temperature with a window of 20 min, as specified by von der Crone *et al.* (non published). T_{ref} is the reference temperature, taken at 21 °C.

(a)   **(b)**
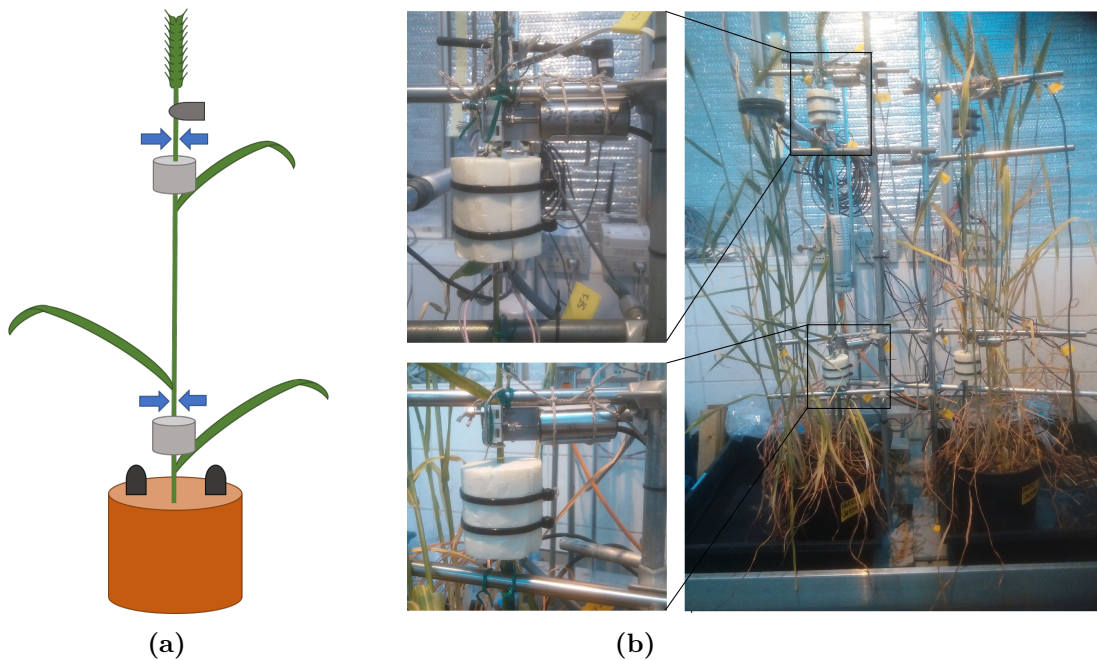
Figure 4.1: Layout of the different sensors for the *in situ* plant measurements. (a) Schematic representation. The light grey cylinders represent the sap flow sensors, blue arrows represent dendrometers, the dark grey shape the leaf clip and the black shapes the soil moisture sensors. (b) Practical installation of the different sensors.

4.3.2   Point measurements

To be able to estimate more parameters in the model, a few variables simulated by the model were also measured at different time points.

Leaf water potential, ψ_{leaf}^x, was measured destructively with a thermocouple psychrometer (HR 33T, Wescor, Logan, UT-US). Four to five replicate samples were taken from the flag leaf of each plant. Time points at which leaf samples were taken depended on the time points for protein sampling, since taking leaf samples would injure the plant, invoke a defence response and therefore contaminate any protein sample taken subsequently. As there were not many plants available, we were forced to use the same plants for first determining the leaf water potential and then taking protein samples. So both time points had to coincide theoretically. In practice, we left less than half an hour between sampling. The leaf samples were then enclosed in the chambers of the WESCOR and left for stabilization. Previous experiments showed that waiting 75 minutes was enough to stabilize the measurements (data not shown). Measurements were recorded with LoggerLite 1.9.1 (Vernier Software and Technology, Beaverton, OR-US). The water potential was calculated based on the volt signal 19 to 21 sec after the cooling circuit started (according to calibration data available).

Actual transpiration by the leaves (Tr_{act}) was measured with the LI-6400XT Portable Photosynthesis System (LI-COR, Lincoln, NE-US). Since this device measures parameters non-destructively, its measuring time points were not influenced by other factors. Transpiration was measured on the flag leaf for a few hours each day with 5 minutes intervals. Measured

values were 15 sec averages. Measurements for the control and the drought treatment were alternated each day.

To mimic the atmosphere as accurately as possible, the air transported to the chamber was not filtered of CO_2 or H_2O. The CO_2 levels and humidity were therefore equal to the atmosphere. Incoming radiation was measured with a quantum sensor on the sensor head and was used as input for the LEDs, but even so the set PAR in the chamber was about $20\,\mu\mathrm{mol\,m^{-2}\,s^{-1}}$ higher than what was measured by the quantum sensor in the glasshouse.

The temperature settings could not be linked to the ambient temperature, so to keep the influence of the temperature fluctuation during the day, the air in the chamber was not cooled. This gave the same temperature profile, but $3\,°\mathrm{C}$ higher than the true air temperature.

The measured transpiration values (in $\mu\mathrm{mol\,s^{-1}\,cm^{-2}}$) were upscaled to the whole plant and converted to $\mathrm{g\,h^{-1}}$ by multiplying it with the leaf surface, measured in a previous experiment. But even after this transformation, the values were considerably lower than the measured sap flows. If one considers that $97\,\%$ of the water taken up by the plant is transpired again, then these values should be the same on a daily basis. Moreover, the transpiration measurements were an underestimation of the true transpiration, since the PAR and the temperature in the chamber were too high. This caused the stomatal resistance to be higher than normal. For this reason and because the magnitude of the sap flow matched with reported literature (Langensiepen *et al.*, 2014), a scaling factor was used to bring the transpiration values to the same level as the sap flow measurements. Daily sums were taken since sap flow lags behind transpiration and an instant ratio would be deceptive. Averaging the ratio of these sums over the five days where transpiration measurements were available, led to a scaling factor of $16.9(\pm2.6)$.

4.4 Model settings

4.4.1 Parameter and initial values

The model described in Chapter 3 contains 29 parameters (listed in Table 4.2), of which only some can be calibrated. For a few of these, parameter values are available in literature and when measurements were possible, parameters were determined that way.

The parameters Γ and ϕ were not included for calibration, since wheat plants in the grain filling stage do not grow any more and the value of these parameters have no influence on the final output of the model. So these parameters were set at values found in Génard *et al.* (2001) and Steppe *et al.* (2008).

The minimum water potential in the storage compartments, $\psi^s_{min,organ}$, necessary in the HydGro submodel (Section 3.3), was set at -4 MPa for the leaf and -3.5 MPa for the head (Dougherty, 1974). Even though no information was available for the stem, its value was equalised to that of the head. These values found in literature were not specific for storage compartments, but were adopted due to the lack of more appropriate values. The value for the water potential in the leaf at the permanent wilting point, ψ_{Lpwp}, necessary in the Cropsyst submodel (Section 3.2) was also set at -4 MPa (Dougherty, 1974).

For the derived variables in the model, initial values are necessary. The initial stem diameters were set at the first values of the input files used in the model. Initial values for W_{organ} were set at their simulated values 24 h later in the simulation. Initial values for the second part

of the HydGro model were calculated according to Steppe *et al.* (2006). Since there was no way of determining the initial values of the pressure potential in the storage compartments, $\psi^s_{p,stem}$ and $\psi^s_{p,head}$, these values were included in the sensitivity analysis and calibration.

4.4.2   Sensitivity analysis

Because the final data of the Solartrons (D_{stem}) did not show the expected pattern in diameter variation (see Figure 5.2b), we decided to perform the sensitivity analysis and calibration solely based on the measurements of Tr_{act}, ψ^x_{leaf} and D_{head}.
The sensitivity analysis (SA) was performed with PhytoSim. The SA module uses the parameters at their given values and a 1% deviation from this value. It then uses the deviation on the simulated output variables to calculate a sensitivity index and the identifiability of the parameters (De Pauw *et al.*, 2008).

A first quick local sensitivity with identifiability analysis was performed with the 16 parameters that were hard to measure or to find in literature. This way, all identifiable parameters for which calibration was possible could be selected. In this first analysis the parameters $Fract_{cover,green}$, $\varepsilon_{0,stem}$, $k_{1,head}$ and $\psi^s_{p,stem}$ were included with the 12 other parameters that were eventually calibrated. This analysis easily showed that only 12 of the 16 parameters included could be identified. K_{crop} and $Fract_{cover,green}$ were highly correlated. Looking at the model, this seems logic as they both simply multiply subsequent variables. Since it was easier to choose the parameter $Fract_{cover,green}$, its value was set at 0.90. This means that 90% of the incident radiation was captured by the leaves. This is just an estimate, as almost no leaves were shadowed by other leaves. Thus the parameter K_{crop} was left for calibration.
Also the parameters $\varepsilon_{0,stem}$ and $\psi^s_{p,stem}$ appeared to be non-identifiable. This also seemed logic as these parameters are used to calculate D_{stem} and no calibration data was used anymore for this variable. The value of $\psi^s_{p,stem}$ was therefore set equal to the calibrated value of $\psi^s_{p,head}$ in the model, while $\varepsilon_{0,stem}$ was set to $800\,\mathrm{m}^{-1}$, a value that led to good simulations.
Even though calibration data for the head compartment was available, $k_{1,head}$ could not be calibrated either. Its value was also chosen at a value of 1.2 to give good simulations, since this led to better simulation outputs than simply taking the calibrated value of $k_{1,stem}$.

4.4.3   Calibration and simulation

For calibration, the Simplex method (local search) was used with an accuracy of 0.001 and a maximum evaluations of 1000. Calibration was first performed with the calibration data of the drought-stressed plant. The parameters ψ_{Lsc}, k_{soil}, R^s, r_1 and r_2 could be determined better with this dataset, since the measurements of Tr_{act}, ψ_{soil} and D_{head} showed a larger variability in this dataset than in the control dataset. These parameter values were then fixed during calibration of the control dataset. After 514 evaluations for the drought data and 358 evaluations for the control data, the requested accuracy was obtained.
After calibration, simulations were performed with the parameter values listed in Table 4.2. Simulations were performed with a fourth order variable step size (Runge-Kutta method), an accuracy of 10^{-6} and a maximum step size of $0.01\,\mathrm{h}$.

Table 4.2: Symbol, unit and description of the model parameters

Symbol	Description	Value	Unit	Reference
Penman-Monteith				
d_{crop}	Planting density of the crop	280	m^{-2}	measured
K_{crop}	Genotype specific evapotranspiration coefficient (control/drought)	2.68/2.58	unitless	calibrated
LAI	Leaf area index	49	$m^2\,m^{-2}$	measured
P	Air pressure	90	kPa	Zweifel et al. (2002)
r_l	Stomatal resistance of a single leaf (in well watered conditions)	200	$s\,m^{-1}$	measured
u_{wind}	Windspeed in the greenhouse	0.005	$m\,s^{-1}$	measured
Cropsyst				
$Fract_{cover,green}$	Fraction of the incident radiation by the crop green leaf area	0.90	unitless	estimated
ψ_{Lpwp}	Leaf water potential at the permanent wilting point	-4	MPa	Dougherty (1974)
ψ_{Lsc}	Leaf water potential at the onset of stomatal closure	-1.01	MPa	calibrated
HydGro				
a	Allometric parameter	0.002968	m^{-1}	Génard et al. (2001)
b	Allometric parameter	32	m^{-1}	Génard et al. (2001)
$f_{diameter}$	Conversion parameter (control/drought)	0.0115/0.0142	unitless	calibrated
k_{soil}	Conversion parameter	4.00	unitless	calibrated
$k_{1,stem}$	Amount of stored water at the inflection point of the desorption curve (control/drought)	1.50/1.49	g	calibrated
$k_{1,head}$	Amount of stored water at the inflection point of the desorption curve	1.2	g	chosen
$k_{2,stem}$	Index for the rate of change of ψ^s_{stem} at the inflection point (control/drought)	0.73/.62	unitless	calibrated
$k_{2,head}$	Index for the rate of change of ψ^s_{head} at the inflection point (control/drought)	0.10/0.16	unitless	calibrated
l_{head}	Length of the peduncle (control/drought)	0.110/0.088	m	measured
l_{stem}	Lenght of the stem segment up to the peduncle (control/drought)	0.641/0.602	m	measured
R^s	Exchange resistance between a xylem and storage compartment	1.81	$MPa\,h\,g^{-1}$	calibrated
r_1	Proportionality parameter	0.600	$MPa\,h\,g^{-1}$	calibrated
r_2	Proportionality parameter	0.288	Mpa^{-2}	calibrated
$\varepsilon_{0,head}$	Proportionality constant	800	m^{-1}	chosen
$\varepsilon_{0,stem}$	Proportionality constant (control/drought)	170/114	m^{-1}	calibrated
Γ	Critical value for the pressure component which must be exceeded to produce (positive) growth in the storage compartment	0.9	MPa	Génard et al. (2001)
ϕ	Extensibility of cell walls in relation to non-reversible dimensional changes (water storage)	0.000448	$MPa^{-1}\,h^{-1}$	Steppe et al. (2008)
$\psi^s_{min,stem}$	Minimal water potential of the stem storage compartment	-3.5	MPa	(Dougherty, 1974)
$\psi^s_{min,head}$	Minimal water potential of the head storage compartment	-3.5	MPa	(Dougherty, 1974)
$\psi^s_{min,leaf}$	Minimal water potential of the leaf storage compartment	-4	MPa	(Dougherty, 1974)

4.5   Construction of a drought index

Drought stress can have two origins: drought because of a high atmospheric demand, or drought because of soil water deficit. Most of the time, these drought origins have to coincide to really affect the plant, but they can also occur independently. The information captured in the PM and Cropsyst submodel, together with the measured sap flow data, is enough to distinguish both origins.

The simulation output of the PM submodel shows how much water the wheat plant should lose through transpiration under the current circumstances in the glasshouse when the stomata are completely open and stomatal resistance is close to zero (Tr_{pot}, see Section 3.1). The simulation output of the Cropsyst submodel then calculates how much water is actually lost when the virtual plant is allowed to close its stomata (Tr_{act}, see Section 3.2). Since the control plant experiences no soil water deficit, its stem sap flow also represents this loss through transpiration. After all, what comes in (F_{stem}) must come out (Tr_{act}). This is especially true for cereals in their grain filling stage, as the plant does not grow any more and no water is used to increase the turgor pressure for growth. Thus the control plant experiences drought stress caused by a high atmospheric demand.
Since the drought-stressed plant is located in the same environment as the control plant, it experiences the same 'atmospheric drought stress'. However, the drought-stressed plant also suffers from soil water deficit. So the difference between the sap flows of the control and the drought-stressed plant represents this 'soil water deficit stress'.

The drought index that is constructed calculates differences between daily sums of the mentioned variables. A smaller time frame for the drought index was not possible because of the hysteresis between transpiration and sap flow. The index is normalised by dividing the differences by the maximum water loss, that is Tr_{pot}. This results in the following equations:

$$Atmospheric\ drought = \frac{\sum Tr_{pot} - \sum F_{stem,control}}{\sum Tr_{pot}} \tag{4.4}$$

$$Soil\ Water\ deficit = \frac{\sum F_{stem,control} - \sum F_{stem,drought}}{\sum Tr_{pot}} \tag{4.5}$$

An alternative calculation of this drought index is possible with the simulations of the Cropsyst submodel:

$$Atmospheric\ drought = \frac{\sum Tr_{pot} - \sum Tr_{act}}{\sum Tr_{pot}} \tag{4.6}$$

$$Soil\ Water\ deficit = \frac{\sum Tr_{act} - \sum F_{stem,drought}}{\sum Tr_{pot}} \tag{4.7}$$

To avoid numerical problems, all summations that resulted in negative values were adjusted to zero.

4.6 Proteomic analysis

4.6.1 Protein sampling and extraction

Samples for protein extraction were taken no more than half an hour after damaging the plant for the leaf water potential sampling. The ear, leaves and stem were flash-frozen in liquid nitrogen to stop all biochemical processes. They were manually ground with a pestle and mortar to a fine powder and stored separately at -80 °C until further use. Only the stem samples taken at around 3 p.m. on five different days were used for further analysis.

About 0.5 g of powder was used for protein extraction. Protein extraction, tryptic digestion and phosphopeptide enrichment were all done according to Vu *et al.* (2016). Since the wheat plants were at the end of their life cycle, the plant tissues were more fibrous than the seedling samples used in Vu *et al.* (2016). The samples were therefore sonicated for 30 sec and centrifuged at 4000×g instead of 2500×g. Instead of resuspending the proteins in guanidinium hydrochloride, we used 8 M ureum solubilised in 50 mM triethylammonium bicarbonate (TEAB) buffer.

After extraction, the protein concentration was measured with Nanodrop (Thermo Fisher Scientific). The proteins were not pre-digested with EndoLysC (Wako Chemicals). Since there were no replicate samples in our experimental design, this step was not necessary.

After the tryptic digestion, the samples were split in two for both a proteomic analysis and a phospoproteomic analysis. For the elution of the phosphopeptides after enrichment, a 5 % instead of a 1 % NH$_4$OH solution was used.

4.6.2 Mass spectrometry and data processing

The samples were analysed via LC-MS/MS (liquid chromatography, mass spectrometry) on an Ultimate 3000 RSLC nano LC (Dionex, Thermo Fisher Scientific) in-line connected to a Q-Exactive mass spectrometer (Thermo Fisher Scientific). Samples were processed according to Vu *et al.* (2016), with a few alterations. To minimize processing time, the samples were separated with a 30 min gradient instead of 170 min. Dynamic exclusion time was 50 s instead of 20.

Also the processing of the data was done according to Vu *et al.* (2016). The MS/MS spectra were searched against a wheat proteomic data base (Duncan *et al.*, 2017).

4.7 Heat map

To compare the proteomic data to the physiological variables of the plant, heat maps were created with 22 variables in the model and all proteins found in the samples. The heat map with the model variables quickly shows the difference between the control plant and the water-stressed plant and their dynamics. It gives a virtual profile fingerprint (Génard *et al.*, 2016).

The physiological variables were extracted from the model on the exact same time points as the samples were taken for protein analysis. This was around 3 p.m. on DOY 111, 114, 115, 116 and 117. One hour averages were taken to avoid outliers, since the sap flow data did show rather large instant variation. The simulated sap flows to the storage compartments, f_{organ},

were not included in the heat map, since on some time points their values were negative, while on others positive. This made the calculations, mentioned below, impossible.

For normalisation, all values were compared to the first time point in the control plant (DOY 111) and these resulting ratios were log-2 transformed. Unfortunately, no other pre-processing of the data like a Z-score as in Vu *et al.* (2016) or a background correction were possible due to the lack of replicates.

The proteins and their phosphosite intensities were processed the same way as the physiological variables (log-2 transformation of the ratio to the first time point in the control plant). When biological replicates are available, one would normalise the phosphosite intensities to their respective protein intensity. However, since this was not the case in this research, this might result in errors, e.g. the protein intensity being lower than a phosphosite intensity.

All transformed values were processed in a heat map with R, whereby the plant variables, proteins or phosphosites were clustered.

Chapter 5

Results

5.1 Observed measurements

5.1.1 Atmospheric measurements

Figure 5.1 shows the daily variation in atmospheric data variables that were used as an input for the PM submodel. At night, the temperature (T_{air}) fluctuated around $21\,°C$ but during warm days ambient temperature could rise up to $33\,°C$ in the glasshouse (Figure 5.1a). High temperatures corresponded with a strong decrease in relative humidity (RH). On colder days, relative humidity remained unchanged as in DOY 111 (Figure 5.1b). Net radiation, R_n, showed less variation between days (Figure 5.1c).

5.1.2 Plant measurements

Soil VWC and water potential, ψ_{soil}, are shown in Figure 5.2a, while sap flow of the stem and the head compartments, F_{stem} and F_{head}, are depicted in Figure 5.2b. These are the input variables for the HydGro submodel.

For the control, the soil moisture stayed constant at $64.2\,\%$. This corresponds to a water potential of -0.008 MPa. For the stressed plant, water levels decreased to $23.2\,\%$ or -0.45 MPa at the end of the experiment. Even though at DOY 108, the drought-stressed plants already looked paler than the control plants, this was not yet visible in the measured physiology of the plant at that time.

Sap flow measurements ranged between 0 and $1.8\,\mathrm{g\,h^{-1}}$, which is similar to the reported values of Langensiepen *et al.* (2014). Sap flow intensities in the control and drought-stressed plant are similar in the beginning of the experiment. Only at DOY 112, sap flow reduced in the stem of the drought-stressed plant compared to the control plant and was severely hindered at the end of the experiment (DOY 117). The sap flow through the peduncle (F_{head}) is about a tenth of that through the main stem (F_{stem}). What is remarkable is that the peduncle sap flow did not show a decreasing trend in the drought-stressed plant.

The measured wheat stem diameters, D_{stem} and D_{head}, used for calibrating the HydGro submodel are depicted in Figure 5.3. An immediate observation of these diameters is their declining trend. The overall shrinkage of the stem is $1.21\,\%$ for the control plant and $2.04\,\%$ for the drought-stressed plant. For the peduncle (part of the head), this is $1.82\,\%$ and $3.22\,\%$

respectively.

This matches the grain filling stage, as the plant does not grow any more but invests all its energy and nutrients in the developing kernels. WSC (water-soluble carbohydrates) are retranslocated from the leaves and stem to the ear (Blum, 1998; Rebetzke *et al.*, 2008). As the drought becomes severe from DOY 114 onwards, the diameters shrink even more (Figure 5.3b).

The daily variations in stem diameter are only clearly visible in the data of the leaf clips (peduncle diameters; D_{head}). This is why calibration was performed only with this data. During the day, stem diameters reduce to increase again at the end of the day. During the night, they stay constant.
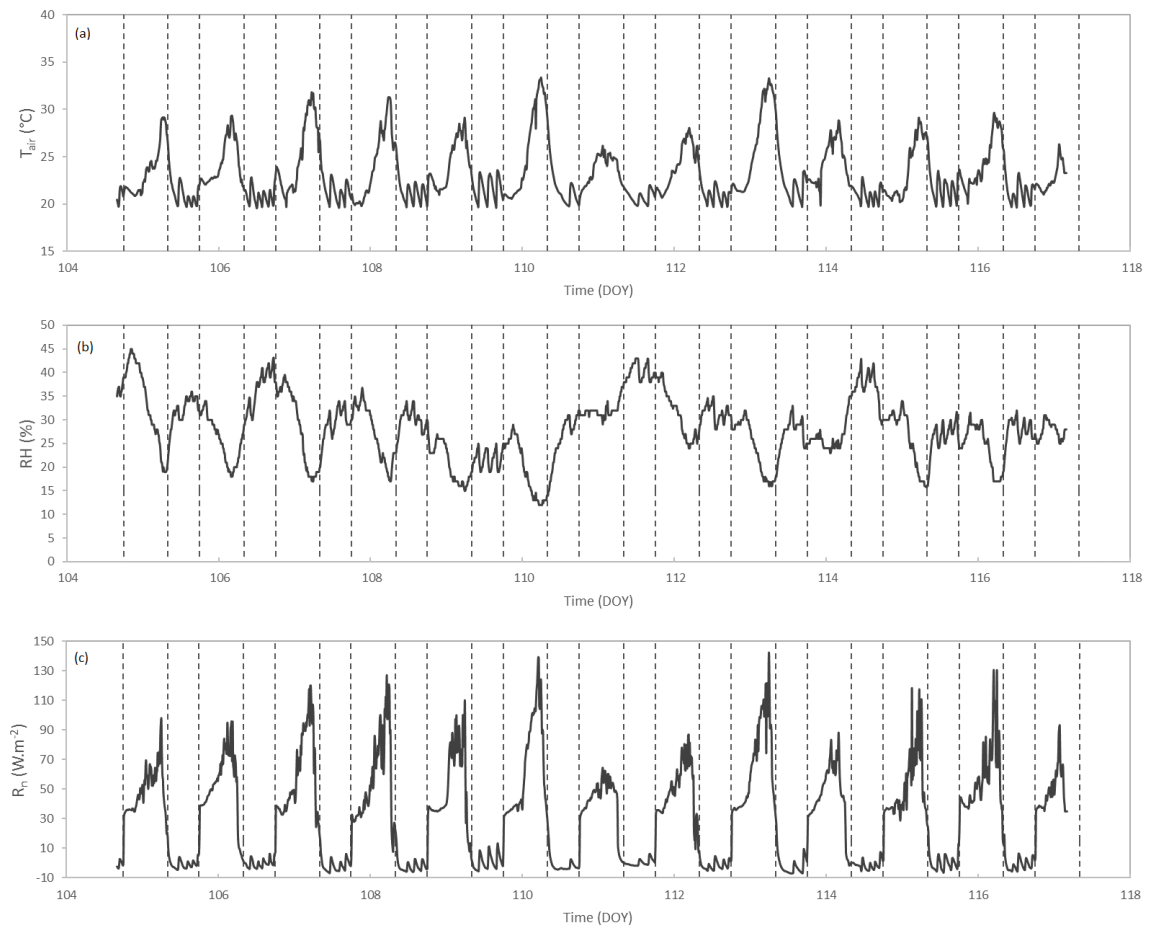
Figure 5.1: The varying atmosphere in the glasshouse used as input for the Penman-Monteith submodel. (a) air temperature (T_{air}), (b) relative humidity (RH) and (c) net radiation (R_n). Vertical dotted lines represent the beginning and end of the daytime (a combination of artificial light and solar radiation).
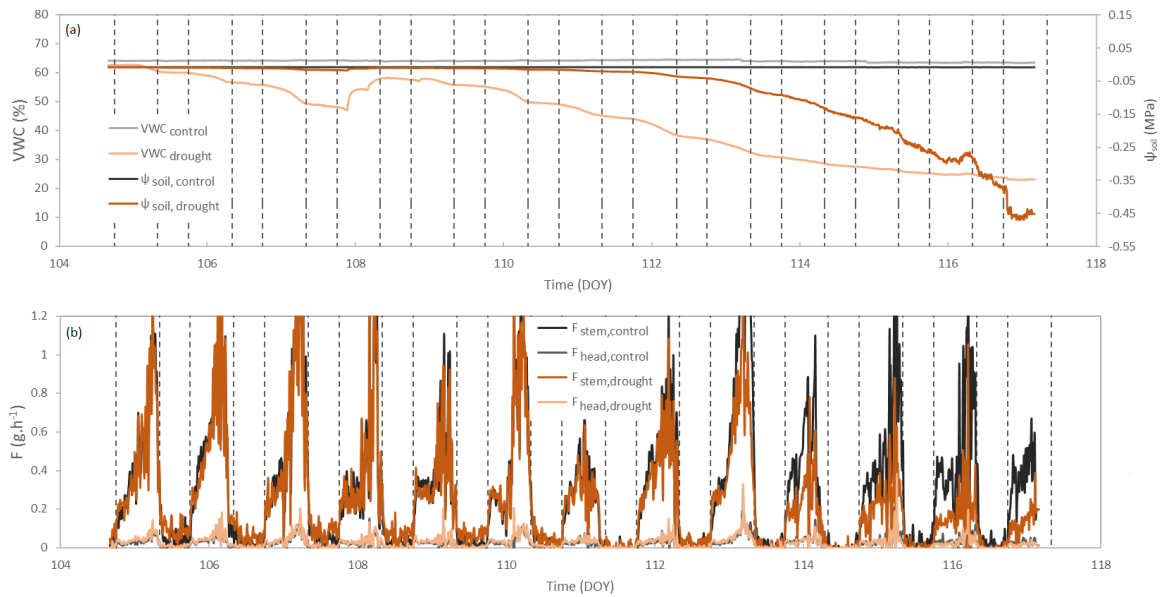
Figure 5.2: Input data for the HydGro submodel for both the control plant and the drought-stressed plant. (a) volumetric soil moisture content (VWC) and (b) sap flow (F_{stem} or F_{head}). Measurements of the control plant are always depicted in black and grey, while those of the drought-stressed plant in red and orange. Vertical dotted lines represent the beginning and end of the daytime.
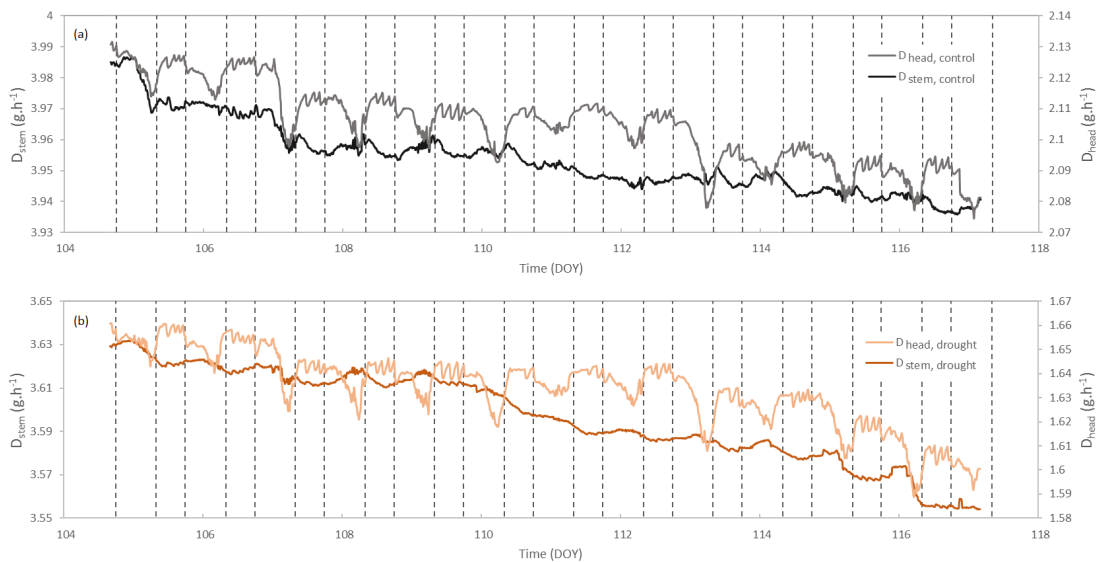
Figure 5.3: Calibration data for the HydGro submodel. (a) control plant and (b) drought-stressed plant. The stem diameter, measured with the Solartrons, is depicted in a darker colour. The peduncle diameter, measured with the leaf clips, is depicted in a lighter colour. Both diameters are represented on different axes. Vertical dotted lines represent the beginning and end of the daytime.

5.1.3   Transpiration

When comparing actual transpiration with stem sap flow (Figure 5.4), one can see that the daily pattern is captured by both independent measuring techniques. From morning until noon, transpiration is higher than sap flow. Around midday, sap flow has caught up and remains equal to, or even a little higher than transpiration.

Transpiration and sap flow in the control plant increase slightly when net radiation is maximal (Figure 5.4a,b between 2 p.m. and 5 p.m.) and the magnitude hereof remains the same between days. Sap flow in the control plant even reaches values of $1 \, \mathrm{g \, h^{-1}}$ on top moments.

The first day of transpiration measurements in the drought-stressed plant (Figure 5.4c) is not a good one to compare to the other days, as net radiation and temperature were low that day, and sap flow in the control plant was also lower than average (see Figure 5.2b at DOY 111). During DOY 114 and 116 (Figures 5.4d and e, respectively), sap flow in the control plant was comparable to the other days, but strongly reduced in the drought-stressed plant, only reaching values of 0.1-$0.4 \, \mathrm{g \, h^{-1}}$. An increased transpiration or sap flow is also absent when radiation increases during the day. This indicates stomatal closure.
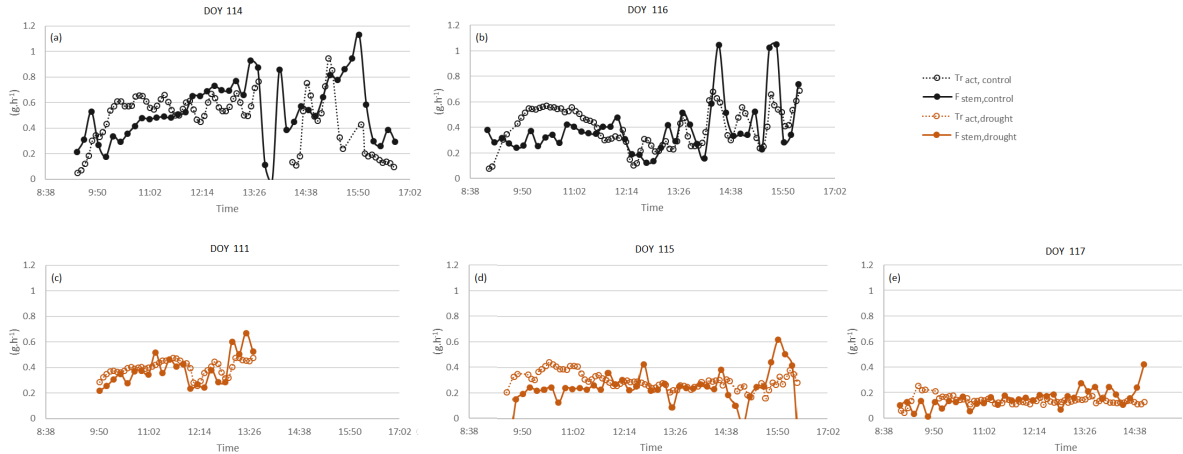
Figure 5.4: Comparison of measured transpiration (Tr_{act}, dotted line and empty circles) and measured stem sap flow (F_{stem}, continuous line and filled circles). (a,b) control plant on DOY 114 and 116 respectively and (c,d,e) the drought-stressed plant on DOY 111, 115 and 117 respectively. For the convenience of comparing, all axes were set to the same range.

5.2   Calibration

An overview of the values of the calibrated parameters for the control and drought data set is given in Table 5.1. The results of the different simulations are shown and described in Section 5.4.

Table 5.1: Values of the calibrated parameters for the control and drought dataset

Parameter	Control	Drought	Unit
$f_{diameter}$	0.0115	0.0142	
K_{crop}	2.68	2.58	
k_{soil}	4.00*	4.00	
$k_{1,stem}$	1.50	1.49	g
$k_{2,stem}$	0.73	0.62	
$k_{2,head}$	0.10	0.16	
R^s	1.81*	1.81	MPa h g^{-1}
r_1	0.60*	0.60	MPa h g^{-1}
r_2	0.29*	0.29	Mpa^{-2}
$\varepsilon_{0,stem}$	170	114	m^{-1}
ψ_{Lsc}	-1.01*	-1.01	MPa
$\psi^s_{p,head}$	0.019	0.120	MPa

* Value not calibrated, but taken from the calibration of
the drought dataset.

5.3 Sensitivity analysis

A sensitivity analysis identifies the important parameters in prediction imprecision of the outcome variables (Blower & Dowlatabadi, 1994). This gives the opportunity to prioritize parameters before their estimation. Parameters having no (or only a small) effect on the model outputs can be set to fixed values, resulting in model simplification: less parameters have to be estimated (Génard *et al.*, 2016).
The identifiability analysis described in De Pauw *et al.* (2008) not only checks whether a parameter has sufficient influence on the model output but also if it is not correlated with other model parameters.

Since the sensitivity index is dependent on the given parameter values and different parameter values are used for the control and the drought data set, these calculated indices will be different for the control and the drought data. An overview of the ranked parameters is given in Figure 5.5.
This figure explains why $\varepsilon_{0,stem}$ and the initial value of $\psi^s_{p,stem}$ are non-identifiable (see also Section 4.4.2). The parameters simply do not influence the simulated output variables. Consequently, their values do not matter. It can also be noted that K_{crop} and $Fract_{cover,green}$ have the exact same sensitivity for reasons already explained in Section 4.4.2. The value of $k_{1,head}$ does however influence the simulation output, so it is unfortunate that its value could not be calibrated. The chosen value will therefore have a large impact on the results of the simulations.
What is also remarkable is that the parameters did not appear to have much influence on the simulations of D_{head} compared to ψ^x_{leaf} and Tr_{act}. It is not that their sensitivity indices are zero, they are just small compared to the other values. This means that D_{head} is simulated quite accurately, while there is a lot of variation in the simulations of ψ^x_{leaf} and Tr_{act}.
The differences between Figure 5.5a and b indicate that when drought is simulated, the parameter values of r_1, R^s and $k_{2,head}$ are much more sensitive. This means that these values

can be calibrated more precisely with the drought data set. The values of r_1 and R^s were indeed used for simulations with the control data set.
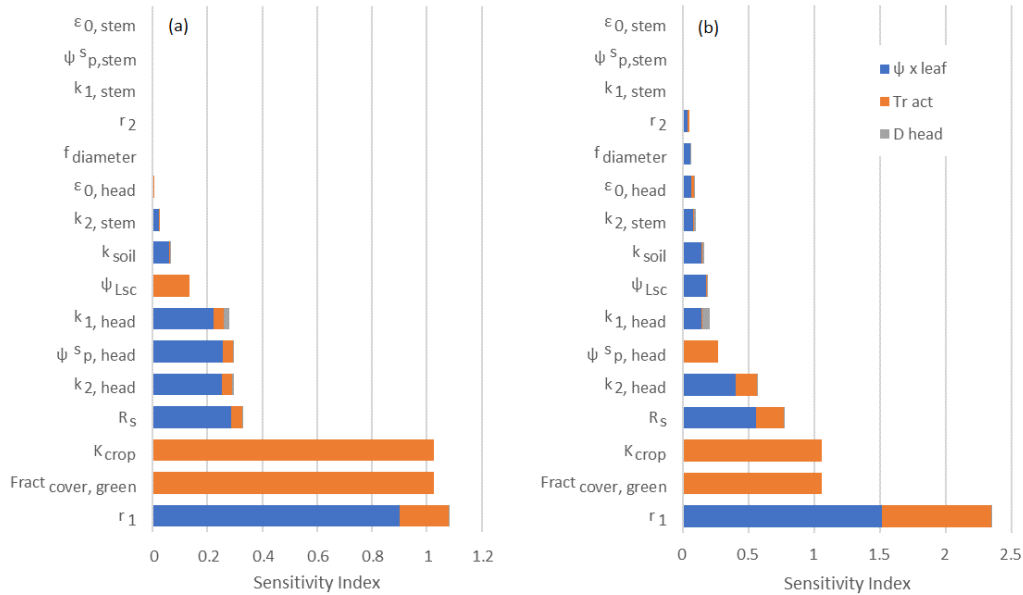
Figure 5.5: Sensitivity indices of the different parameters for the different target components (output variables used for calibration). (a) sensitivity indices when parameters are set at the calibrated values for the control data set. (b) same as (a) but for the drought data set.

5.4   Final simulation

Figure 5.6 depicts the environmental factors that can cause drought in a plant. A high atmospheric demand, represented by a high VPD, causes the plant to lose a lot of water through transpiration. To counteract this, a plant will close its stomata. This is a first indication of drought stress.

When less water is available in the soil, the water potential will decrease (Figure 5.6b). At the end of the experiment, the plant roots experienced water potentials as low as -1.8 MPa. This means that the water potential within the root xylem has to be even lower to allow water transport inside the plant. The plant leaves have to dry out almost completely to produce water potential values that low.

The measured and simulated sap flows are depicted in Figure 5.7. On the left are the sap flows in the control plant (Figure 5.7a,b,c), on the right the sap flows in the drought-stressed plant (Figure 5.7d,e,f). Almost all water imported by the stem (F_{stem}, Figure 5.7a,d) is transported to the leaves (F_{leaf}, Figure 5.7c,f) where it is transpired. Xylem sap flow in the stem and the leaves decreases significantly as drought becomes more severe, but the sap flow pattern to the ear stays remarkably constant (compare F_{head} in Figure 5.7b and e).
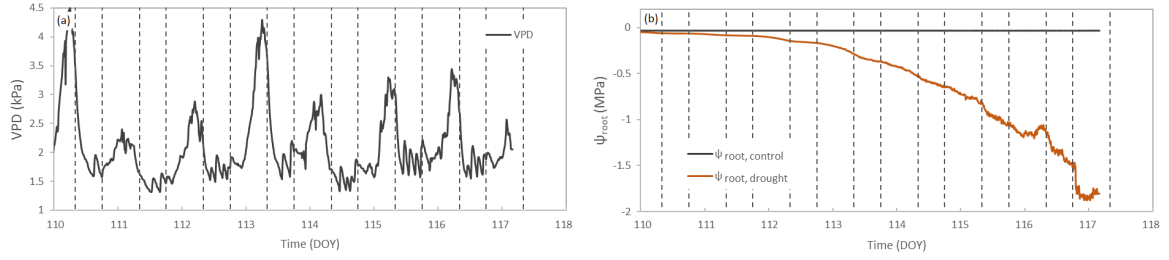
Figure 5.6: Factors influencing drought, simulated as explained in Chapter 3. (a) VPD, calculated according to Jones (1992). (b) ψ_{root}, water potential as experienced by the roots. Vertical dotted lines represent the beginning and end of the daytime.
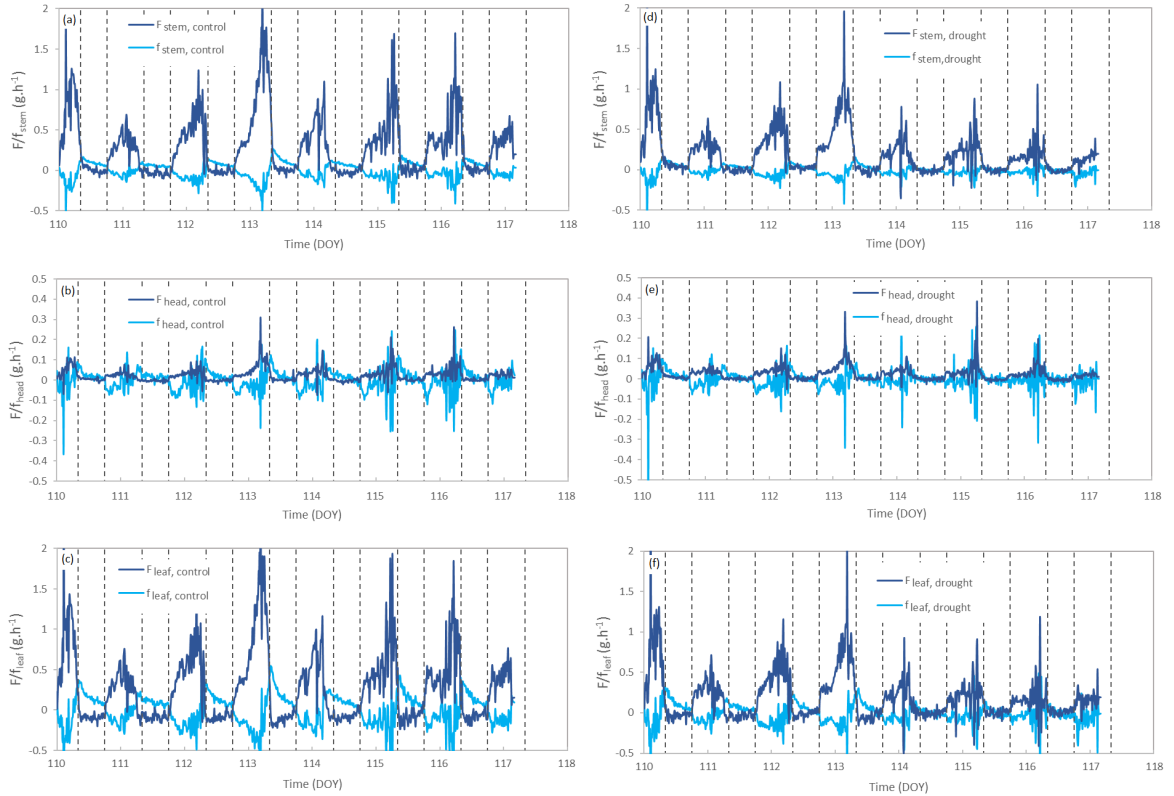
Figure 5.7: Sap flow within the different organs of the wheat plant. (a,b,c) control plant (d,e,f) drought-stressed plant. Dark blue lines represent sap flows between the xylem compartments of different organs (F_{organ}), while light blue lines represent sap flows from the xylem to the storage tissue within an organ (f_{organ}). See also Figure 3.1 for a schematic representation. Only F_{stem} and F_{head} are measured variables, the other variables are simulated as explained in Section 3.3. Vertical dotted lines represent the beginning and end of the daytime.

When looking at the sap flows from and to the storage tissues (light blue lines, Figure 5.7), one can see that in the morning, there is sap flowing from the storage to the xylem as transpiration

starts before water is taken up by the roots. The water that is transpired in the morning is thus coming from the storage tissues. During midday, when VPD is highest, the storage tissues are being depleted. Their water content decreases consequently throughout the day (Figure 5.8a). When the evening falls and transpiration ceases, the storage tissues are filled again (a positive f_{organ} in Figure 5.7 and an increasing water content in Figure 5.8).

What Figures 5.7 and 5.8 also show, is that the storage tissues of the stem are not utilized as much as those from the head and the leaves. This can be seen as the reduced diel variation in W_{stem} compared to W_{leaf} in Figure 5.8 and as the relatively smaller f_{stem} compared to f_{leaf} in Figure 5.7.
The amount of stored water in the stem and the leaves is very similar, but both are much larger than the amount in the head compartment.
During drought, the stored water continues to decline in the stem and the leaves, but stays rather constant in the head (Figure 5.8b).
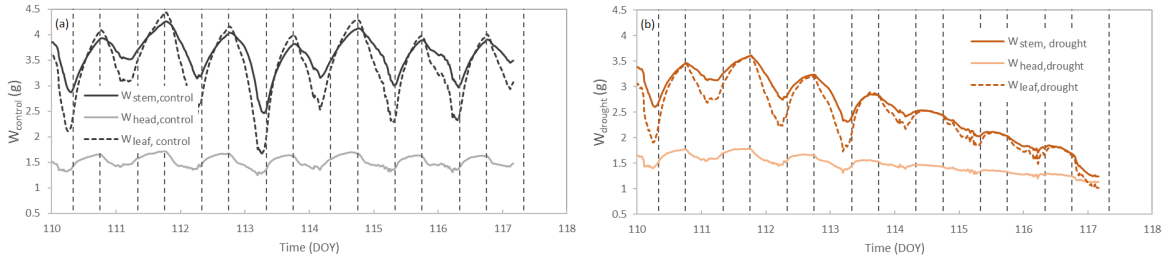
Figure 5.8: Water content within the different organs of the wheat plant. (a) control plant (b) drought-stressed plant. Vertical dotted lines represent the beginning and end of the daytime.

To allow flow from one compartment to another, differences in water potential values are required. These are depicted in Figure 5.9a,b,c for the control plant and Figure 5.9d,e,f for the drought-stressed plant. Measured leaf water potential values are also plotted with their respective standard deviation.
When VPD is highest and transpiration at its maximum, the leaf tissues reach a simulated water potential of -2 MPa (Figure 5.9c). This exerts a suction power on the water column in the xylem vessels through which water is pulled up. Transpiration also occurs in the head, although to a lesser extent. Simulated water potential there reaches values of only -1 MPa (Figure 5.9b). The model assumes no transpiration losses by the stem, so the loss in suction power, represented by a higher water potential (read less negative), can only be ascribed to friction losses in the xylem vessels.

In the mornings, water potential values are always lower in the xylem compartments (ψ^x_{organ}) than in the storage tissue compartments (ψ^s_{organ}), since transpiration removes water from the xylem. This is the driving force for the water flow out of the storage tissues. During the night, it is the other way around and the storage tissues can be refilled. At 5 a.m. (alternating dotted lines, Figure 5.9), the water potential values of the xylem and storage tissue are equal, meaning that no sap flow is possible and the plant is in an equilibrium state.
When high VPDs require a sap flow that cannot be met due to a soil water deficit, the tissues

cannot be refilled adequately and water potential keeps decreasing (Figure 5.9d,e,f). Figures 5.4d and e show that the stomata do not close completely and a minimal transpiration is still allowed. This lowers the leaf water potential to -2.5 MPa and the head and stem water potential to -2.2 MPa. The diurnal differences between xylem and storage tissue water potential also disappear as the storages tissues are emptied and no sap flow is possible.
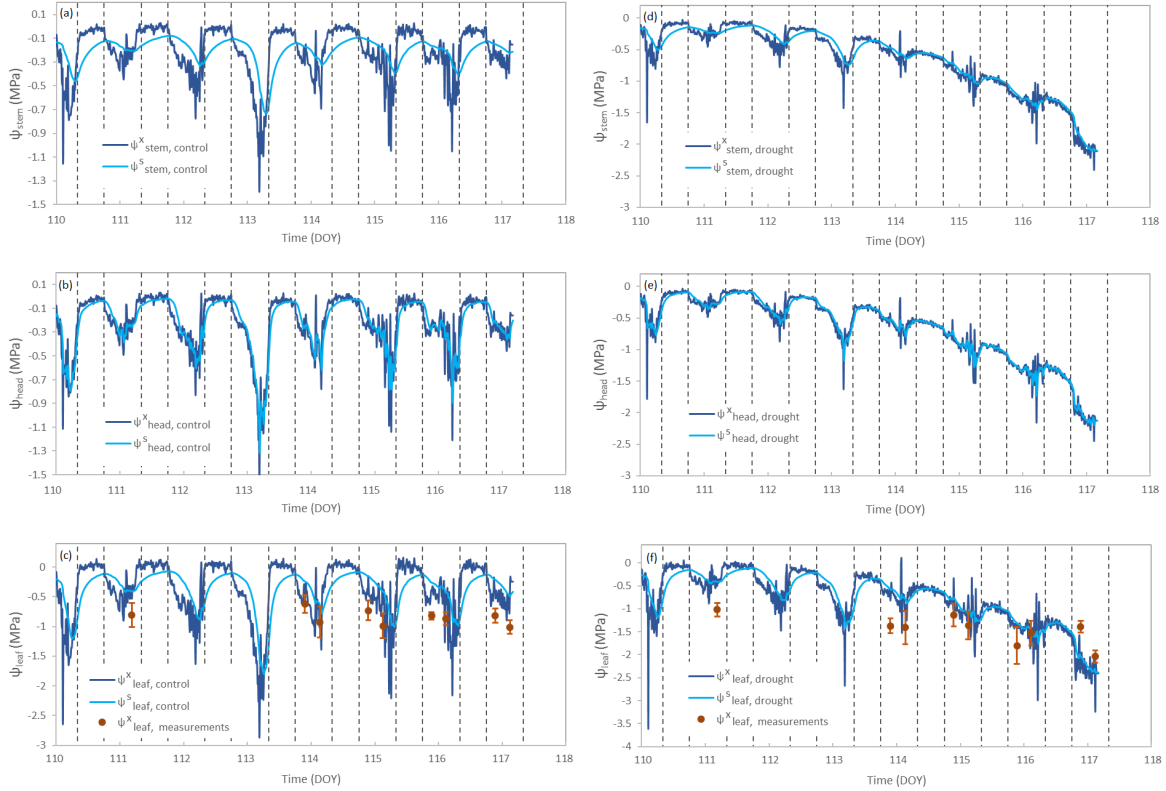
Figure 5.9: Water potential values within the different organs of the wheat plant. (a,b,c) control plant (d,e,f) drought-stressed plant. Dark blue lines represent xylem water potential values (ψ^x_{organ}), while light blue lines represent storage water potential values (ψ^s_{organ}). Measured leaf water potential values are plotted as red dots with their respective standard deviation. Vertical dotted lines represent the beginning and end of the daytime.

The variable capacitance is depicted in Figure 5.10. At night, the capacitance increases and reaches a maximum. On those moments, more water can be stored per unit pressure drop in the storage pools (Steppe *et al.*, 2006). Physiologically it means that at low water potential (read less negative), the available water in the plant is stored as capillary water in the intercellular spaces and easily reachable. During the day, the capacitance decreases as water is only stored within the cells of the storage tissues. When the plant dries out (Figure 5.10b), the capacitance stays small as the intercellular spaces are never used for the storage of water. At the end of the experiment, the capacitance is extremely low which means that a high potential difference is necessary to reach the stored water.

The differences between the different organs should be interpreted with care, as the calibrated parameters are not yet optimal (see discussion in Section 6.1).
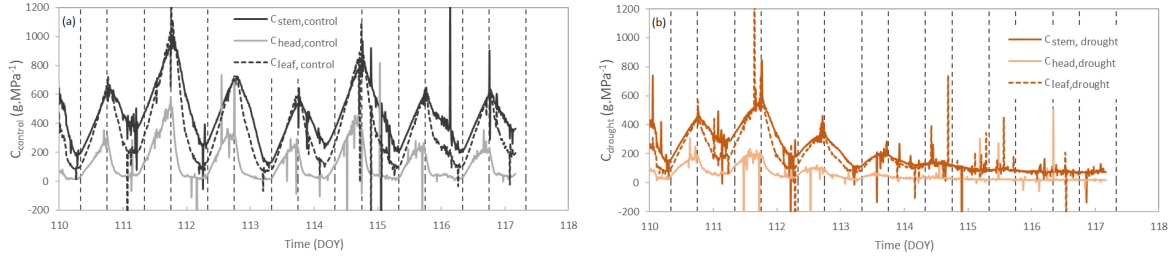
Figure 5.10: Variable capacitance of the different organs in the wheat plants. (a) control plant (b) drought-stressed plant. Vertical dotted lines represent the beginning and end of the daytime.

Figure 5.11 shows the simulated peduncle diameter compared to the measured diameter of the control and drought-stressed plant. As can be seen, the diel variation is captured by the model. When the storage tissues are depleted of their water content during the day to enter the transpiration stream, the diameters shrink. At night the storage tissues are refilled again and the diameter expands. The measured data show a fluctuating diameter during the night, but this is due to the temperature fluctuation in the glasshouse and its influence on the leaf clips.

Since in the grain filling stage, the plant does not invests energy in growth, the pressure potential of the storage tissues, $\psi^s_{p,organ}$, never exceeds the threshold value Γ (data not shown) and the simulated diameter is not able to increase gradually. The overall declining trend of the diameters indicating grain filling could not be simulated by the model. Instead, the simulated diameter of the control plant remains constant, apart from the diel variation. However, a decreasing diameter due to drought stress could be simulated accurately (Figure 5.11b). Still, the diel variation during drought is larger than simulated by the model. This indicates that the storage tissues are more utilized under drought stress than is simulated by the model.

5.5   Drought index

Figure 5.12 compares the data variables that are used for the construction of the drought index. The potential transpiration, Tr_{pot}, simulated by the PM submodel (Section 3.1) and the actual transpiration of the drought-stressed plant, $Tr_{act,drought}$, simulated by the Cropsyst submodel (Section 3.2), are almost similar to the sap flow in the control plant. $Tr_{act,drought}$ is generally equal to the potential transpiration. Only the last few days of the experiment, the simulated transpiration declined, but not to the level of the sap flow in the drought-stressed plant.

One can see that in the morning, transpiration starts before sap flow but also reduces earlier (Figure 5.12b, DOY 113 and 115). This shows the need for a daily integration of the variables in the construction of the drought index.

In the same figure, the effect of drought on sap flow is also visible. Especially when VPD is high, the difference between $F_{stem,control}$ (black lines) and $F_{stem,drought}$ (orange lines) becomes more pronounced. This translates to a positive 'soil water deficit' component of the drought index (Figure 5.13a). When the daily sap flow in the control plant falls under the daily potential transpiration (Tr_{pot}, dark blue lines in Figure 5.12), the 'atmospheric drought' component becomes positive (Figure 5.13a). This indicates the closure of the stomata.
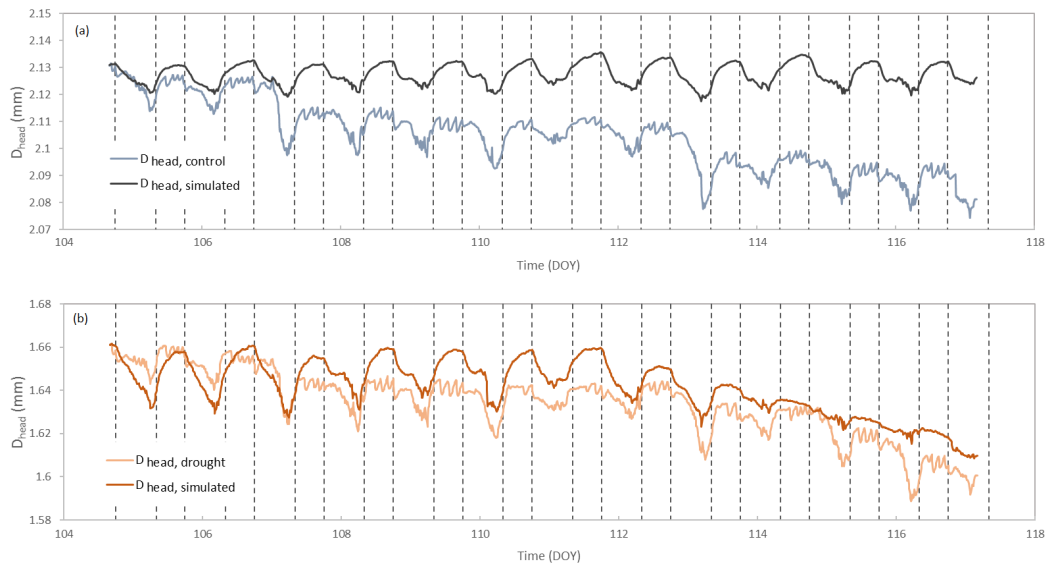
Figure 5.11: Measured and simulated diameters of the wheat peduncle, which is part of the head. (a) control plant (b) drought-stressed plant. Vertical dotted lines represent the beginning and end of the daytime.
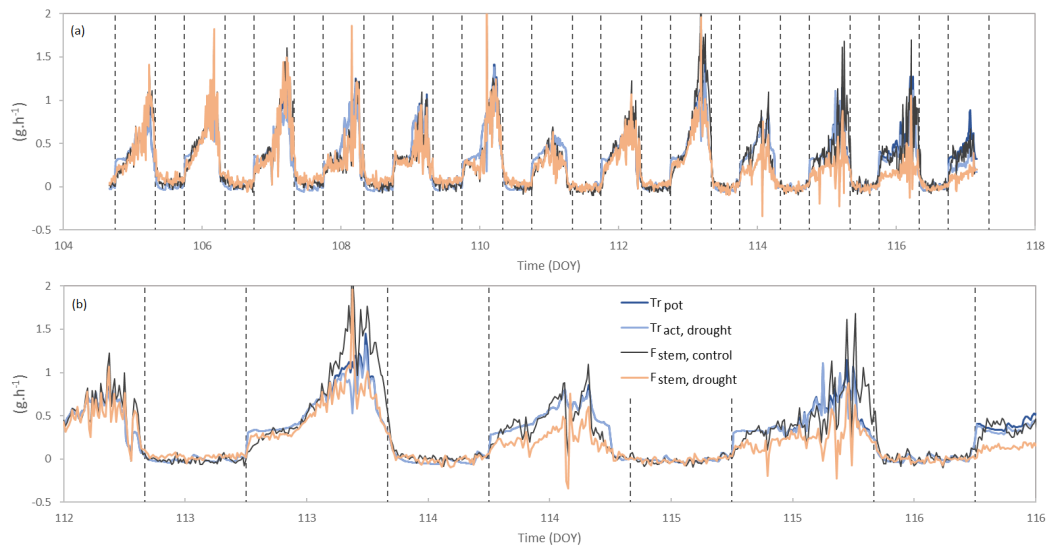
Figure 5.12: Data used for the construction of the drought index. Tr_{pot} is simulated by the PM submodel (Section 3.1) and $Tr_{act,drought}$ by the Cropsyst submodel using the drought dataset (Section 3.2). The dark blue lines of Tr_{pot} are often not visible when it coincides with Tr_{act}, in light blue. This means that Cropsyst simulates no stomatal closure. (a) full data set. (b) selection of (a) for clarification. Vertical dotted lines represent the beginning and end of the daytime.

An alternative of using sap flow measurements in a control plant is the use of the Cropsyst simulation output, $Tr_{act,drought}$ (Figure 5.12, light blue lines). This variable simulates the closure of the stomata and thus the 'atmospheric drought' (Figure 5.13b). Because the sap flow of the drought-stressed plant is now compared to the simulated actual transpiration, the 'soil water deficit' component of the drought index is also influenced.
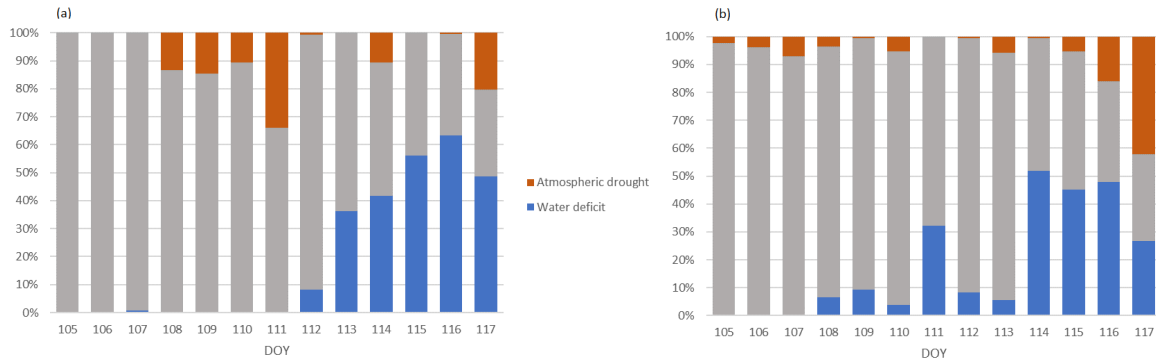
Figure 5.13: Drought index calculated for the stressed plant on a daily basis with the data from Figure 5.12. The index differentiates between atmospheric drought stress (red) and soil water deficit stress (blue). (a) drought index calculated according to equations 4.4 and 4.5. (b) drought index calculated according to equations 4.6 and 4.7.

It should be mentioned here that DOY 117 is not a complete day. Measurements and simulations were available until 4 p.m., so it is likely that the drought index deviates from what is depicted in Figure 5.13. Since potential and actual transpiration starts and stops before sap flow, these former variables will be too large in relation to the latter variables. Thus the 'soil water deficit' component on DOY 117 in Figure 5.13 is an underestimation.

5.6   Proteomic analysis

Since there are no replicates of the protein samples available, no statistic analyses could be performed. Instead, the results of the proteomic analysis are merely indicative. The heat map of the simulated and measured plant physiological variables is shown in Figure 5.14, while Figure 5.16 shows the heat map of the proteins and their phosphosites.

The largest observed change in physiological variables due to drought is in water potential of all compartments. They all increase in magnitude and are therefore clustered together. All other variables decrease in magnitude in the drought-stressed plant. The decrease in pressure potential ($\psi^s_{p,organ}$) and capacitance (C_{organ}) are most pronounced.

Figure 5.15 shows a heat map of the protein intensities found in the stem samples of the control and drought-stressed plant. As can be seen on DOY 117, six days after the sap flow slowed down, a remarkable change in protein content is visible. The proteins denoted with $*$ are clearly more upregulated on DOY 117 in the drought-stressed plant compared to the control plant.
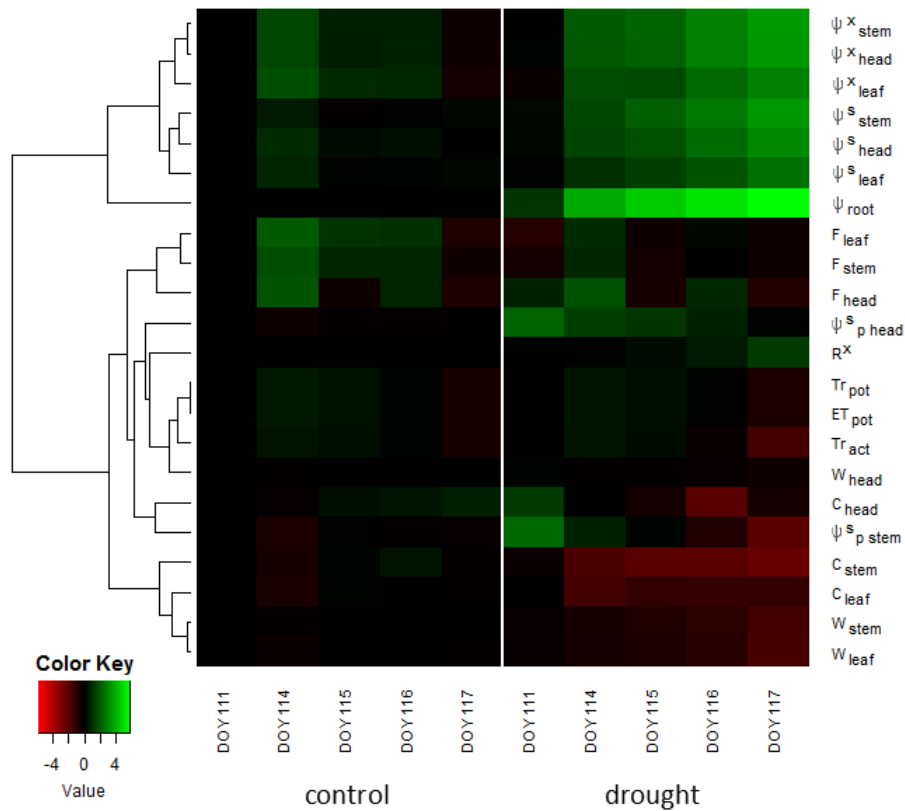
Figure 5.14: Heat map of the measured and simulated plant physiological variables.

A downregulation compared to the control plant is visible in the proteins on DOY 116 and 117 (marked with ∗∗) but it is hard to say whether this is significant or not since it does not apply for that many proteins and the intensities should be interpreted with care.

The phosphorylated sites of the proteins showed no significant changes between the control and drought-stressed plant (Figure 5.16). DOY 111 of the drought-stressed plant resembles thad of the control plant the most.
The upper part of the heat map shows phosphorylation sites that are more (all green) or less (all red) phosphorylated in both the control and the drought-stressed plant compared to DOY 111 in the control plant. The lower half of the figure shows less significant changes in phosphorylation.
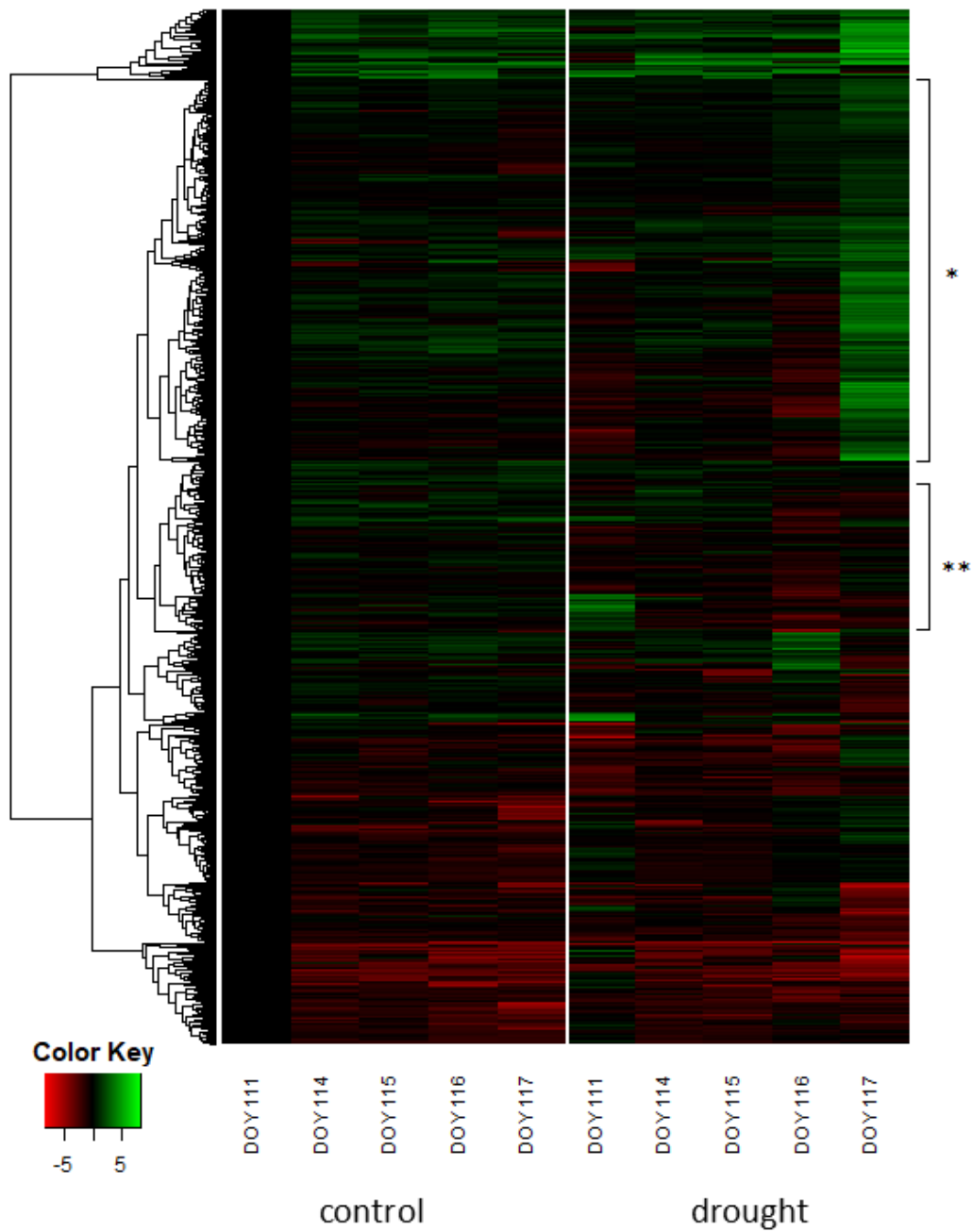
Figure 5.15: Heat map of the proteins in the stem.
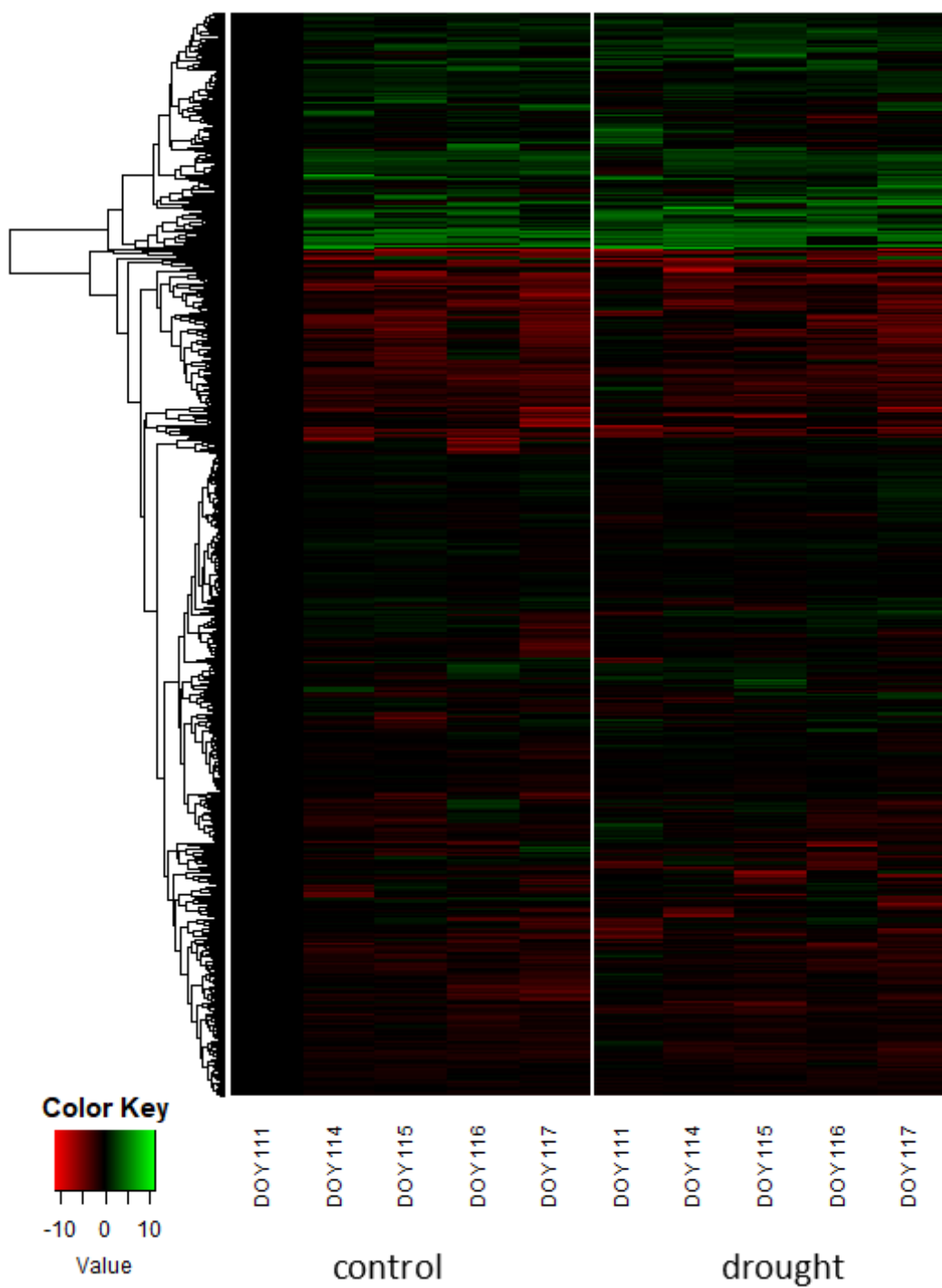
Figure 5.16: Heat map of the phosphorylation of proteins.

Chapter 6

Discussion

6.1 The wheat model

The calibrated wheat model that was developed in Chapter 3 shows promising results for future use in research on drought in wheat. The model makes it possible to determine variables that are cumbersome or even impossible to measure. With only a few sensors and limited effort, a vast amount of data can be gathered. The simulated variables enable us to understand how a plant responds to drought. With only measured data, some patterns would be harder to explain.
The model and its simulated variables can be used in many research topics to support other phenotyping data or to link to genomic data, like in this report.
Because the model is based on processes and principles that are universal, only a few adaptations of the HydGro model were necessary before applying the model to wheat. The switch from trees to wheat is rather drastic, but this means that adaptation of the model to other crops will be even less significant. So with few alterations, the model could be applicable to a whole range of plants.
Not only in research, but also in agriculture and horticulture, this model can be used (see also Section 6.2).

The wheat model paves the way for research on drought in wheat, but is certainly not optimal yet. A moving window calibration is normally necessary to estimate the changing values of K_{crop}, since the simulated variable Tr_{pot} is based on fixed values of the stomatal resistance, r_l, and LAI. During drought, these parameters are expected to change but only one measurement was available. A changing value of K_{crop} could adjust for these errors.
However, no moving window calibration was eventually performed for K_{crop} as there simply was not enough transpiration data. A complete data set from DOY 105 to 117 for both the control and the drought-stressed plant would have been required, while this was only available for five days in total.

In Chapter 5, it becomes clear that a key process is missing to properly simulate the decreasing diameters. In Figure 5.11a, calibration starts adequately, but deviation with the measured diameter becomes so large after DOY 107, that the simulated values do not even come within the range of the diel variation. For the drought data set (Figure 5.11b), this deviation is less pronounced because a declining diameter can be simulated under drought. But nevertheless, between DOY 105 and 112, the simulations start under and end above the actual diameter.

Moreover, a moving window calibration was performed with the parameters R_s, r_1, r_2 and $f_{diameter}$ (data not shown), but even then, the model could not simulate a declining trend in the diameter. This proves that the model does not contain any process that can simulate a declining diameter under well-watered conditions. This is thus a process that should be included in the future.

The diameter deviation has its consequences further downstream. Because slight alterations in the parameter values during calibration do not result in better simulations, the results of the calibration should not be interpreted too strictly. Moreover, confidence information could not be calculated because of this.

Nevertheless, some conclusions can be made on the different values and simulations of the model.

As mentioned in Section 3.3, it became clear during test simulations that the values of $\varepsilon_{0,head}$ and $\varepsilon_{0,stem}$ had to be different to result in acceptable simulations of the diameter. $\varepsilon_{0,head}$ turned out to be 5 to 7 times larger than $\varepsilon_{0,stem}$ (Table 4.2). The part of the HydGro model where this parameter belongs to, was not explained in Chapter 4, but the parameter should be interpreted as follows: $\varepsilon_{0,organ}$ determines how strongly the pressure potential in the storage tissues ($\psi_{p,organ}^s$) respond to a changing water content. A high value means that a slight alteration in water content results in a relatively large change in pressure potential.

Applied to the wheat plant, this can be interpreted as the peduncle storage tissue cells being more rigid and/or smaller than those of the stem. After all, when the cells are smaller or more rigid, the same amount of water imported brings about a larger increase in pressure potential. Nevertheless, the pressure potentials in the head and the stem storage tissues are the same (simulation data not shown), because the amount of water stored in the stem is two to three times larger than in the head (Figure 5.8).

Even though the stem contains the same amount of water than the leaves, it is the water stored in the leaves that is first utilized. This is why f_{leaf} in Figure 5.7 is large (-0.5 g h^{-1} when VPD is high) and why the leaf water content displays such large diel variation (W_{leaf} in Figure 5.8).

When a wheat plant is exposed to a drying environment, the plant will maintain functionality as long as possible. Only when water potential in the soil surrounding the roots reached a value of -0.3 MPa, sap flow slowed down. At values of -1 MPa, sap flow was significantly hindered. This reduction in water transport happens quite quickly. Within two or three days, it is about 60 % of what it should be without water deficit in the soil (Figure 5.13).

To maintain a normal grain filling as long as possible, the sap flow to the ear was not influenced within the time frame of the experiment. Figure 5.7 shows that the sap flow through the peduncle (F_{head}) remains constant while its stem and leaf flow (F_{stem} respectively F_{leaf}) clearly decrease.

During drought, the stomata do not close completely and transpiration continues, although to a lesser extent (Figure 5.4). Transpiration causes the leaf water potential to drop to a value of -2.5 MPa (Figure 5.9f). The transpired water comes from the stem and leaf storage tissues, as their water content continually decreases (Figure 5.8b). The water content in the soil is insufficient to refill these storage tissues leading to only small negative values of f_{organ} (Figure 5.7d and f, light blue lines). This explains why the water potential in the storage tissues and their respective xylem vessels is equal (Figure 5.9d,f). Capacitance continues to

decrease during drought which means that larger potential differences are needed to refill the storage tissues.

Remarkably, the water content in the ear decreases only slightly (Figure 5.8b), indicating again that the grain filling process is preserved even when the plants reserves get depleted.

Even though the water content in the head storage tissues only decrease slightly, this reduction must mainly abide in the peduncle, since its diameter does shrink visibly during drought (Figure 5.11b). This is confirmed by the relatively higher overall diameter shrinkage of the head compartment compared to the stem.

The diel changes in the peduncle diameter are larger during drought than what is expected by the model simulations, which means that water ís transported in and out the storage tissues of the head and to a larger extent than is simulated in Figure 5.7e.

This coincides with the unaffected water supply during drought stress into the head (see the constant $F_{head,drought}$ in Figures 5.2b and 5.7e). This is again proof that the wheat plant will maintain a normal grain filling as long as possible and that it is a process that the model cannot simulate. This is logic, since the model was developed for trees and they do not know a grain filling stage.

What will be interesting to see, is whether the diel diameter variation of the base of the stem will also be smaller than expected, since the sap flow through the stem base does decrease under drought stress. Unfortunately, the Solartron measurements were inadequate to test this (Figure 5.3).

As mentioned in Section 3.3, the measured diameter variation was much smaller than what was simulated by the original model. A scaling parameter, $f_{diameter}$ had to be implemented to reduce the simulated diameter variation. Calibration showed that its value is roughly 1 % (Table 5.1). The true value of this parameter is hard to determine because of reasons mentioned before, but nevertheless it can be concluded that the actual diameter variation in wheat is merely a fraction of what was originally simulated.

This can be linked to the fact that the HydGro model was originally built for trees and not for annual plants. The wheat stem contains a hollow core (Hamman *et al.*, 2005), so it is hypothesized that the majority of the stem expansion occurs to the inside of the stem. That way, a more rigid outer epidermis can be produced by the plant to optimize pathogen protection and lodging resistance.

While in trees, one would expect a continuous growth in stem diameter, in annual plants, this does not have to be the case. Especially during the grain filling stage, which is the last phenological stage, the plant will not invest energy in growth. Instead, even carbohydrates (WSC) stored in the stem are retranslocated (remobilized) to the ear (Blum, 1998; Rebetzke *et al.*, 2008). This can be seen as the declining diameter that cannot be explained by the model (Figure 5.11). This occurs under non-stress conditions, but literature suggests that during drought in the grain filling stage, this process is even more noticeable (Blum *et al.*, 1994; Palta *et al.*, 1994; Yang *et al.*, 2001; Plaut *et al.*, 2004).

Since the HydGro submodel can only simulate a diameter reduction due to drought stress, this would mean that the measured diameter shrinks even faster than the model would simulate during drought. After all, a sugar transport process is not included in the model.

In Figure 5.11b one can see that the declining trend of both the simulated and the measured diameter from DOY 113 onwards is the same. This means the measurements imply that the

retranslocation only continues as long as drought is not too severe and that remobilization stops when drought becomes so intense that sap flow is hindered. The shrinkage of the diameter can then only be ascribed to the depletion of water from the storage tissues.

6.2   Drought index

The drought index is only as accurate as the model simulations. A steep drop in the plants diameter indicates that the storage tissues are needed excessively to meet the transpiration demand. A high transpiration is caused by a high atmospheric demand, meaning a high VPD. A high transpiration happens at DOY 110 and 113 (Figure 5.11). On these days, VPD is indeed higher compared to other days (Figure 5.6). Also sap flow reaches maximum values (Figure 5.7a). However, on these days the flaws in the PM model become visible. The simulations of Tr_{pot} are quite close to the measured sap flow in the control plant on DOY 110 and 113 (Figure 5.12). This means that, according to the PM model, the stomatal resistance increases only slightly and the plant does not experience 'atmospheric drought stress'. But this stress is recorded in the declining diameter and the increased sap flow. The result is that the drought index does not indicate the atmospheric drought as intensely as should be (Figure 5.13a).
Vice versa, on DOY 111 the differences between the sap flows in the control and drought-stressed plant are negligible (Figure 5.12a). This means that soil water deficit is not influencing the drought-stressed plant yet, which is correctly indicated by the index in Figure 5.13a. When using the alternative drought index, no atmospheric drought is predicted (Figure 5.13b). This is logic, because the net radiation was low that day (Figure 5.2) and the VPD was minimal (Figure 5.6). So there is indeed a lot of probability that the stomata did not close. But then the potential transpiration is estimated too high and the reduced sap flow of the drought-stressed plant is thus falsely ascribed to a soil water deficit. So on warm days with a high VPD, PM underestimates the potential transpiration, while on colder days it overestimates the potential transpiration.

The differences between Figure 5.13a and b show that the Cropsyst simulation of stomatal closure is also not yet optimal, even with the incorporation of the leaf water potential from HydGro (ψ_{leaf}^x). Figure 5.4 shows that measured transpiration and stem sap flow are very similar, yet the simulated values of Tr_{act} are almost always an overestimate of the real transpiration (Figure 5.12b). Increasing the water potential at which the stomata close (ψ_{Lsc}) was not an option, since this resulted in simulations at which transpiration stops completely almost every afternoon (data not shown). This indicates that the Cropsyst model lacks some key processes to simulate stomatal closure accurately.

Furthermore, the interaction of the atmospheric drought and drought by soil water deficit is not included in the drought index that is based on two sap flow measurements (Figure 5.13a). That is to say, when a plant experiences soil water deficit stress, the leaf water potential values are lower than normal, and the stomata will close at lower VPDs than usual. This can be interpreted as follows: a plant that suffers from soil water deficit will experience atmospheric drought stress much more quickly. This quicker response is not included in the data from the control plant.
When using the simulations of $Tr_{act,drought}$, this problem is nullified, since the leaf water potential is calculated based on the sap flow of the drought-stressed plant. Thus, with an

optimisation of both the PM and the Cropsyst submodel, the drought index solely based on one sap flow sensor has the potential to be more accurate than the drought index based on two sap flow sensors.

To be accurate in the simulations of the stomatal regulation, an accurate determination of the leaf water potential is necessary. This makes the use of the HydGro model indispensable, but it means that a calibration is required before any practical usage of the drought index.

The application of such an index in agriculture or horticulture could be beneficial and even cost-effective. Of course, the model should then be adapted to the plant species of interest. But with only a soil moisture and a sap flow sensor on the main stem of one plant, the farmer will be able to distinguish the main origin of drought stress when his plants show symptoms, given that data of the microclimate in the greenhouse or on the field is available. When the farmer's plants show drought symptoms, he can then make the appropriate decision based on the index. If the 'soil water deficit' component is dominant, a higher irrigation is in place. However, when atmospheric drought dominates, it is more appropriate to open a few windows in the greenhouse to drop the temperature and increase the wind speed or to sprinkle water in the air to increase relative humidity.

For a prior calibration, only measurements with a dendrometer are necessary. Values for ψ_{Lsc} are available in literature, but are preferably also calibrated with measurements of the actual transpiration.

6.3 Proteomics

Since not enough plants were available to analyse duplicate samples, several remarks have to be made concerning the proteomic analysis.

First of all, no statistic analyses of the MS/MS data was possible due to the lack of both biological and technical replicates. This means that no conclusions can be made on the intensity data of the different proteins. At most, an increasing or decreasing trend in intensity can be used.

Second, because of the absence of biological replicates, there is no way to normalise for micro-climatic fluctuations. Yin *et al.* (2016) already cautioned that these fluctuations can obscure genetic effects.

In other drought experiments, like the one of Liu *et al.* (2017), at least three replicates were analysed. Moreover, the research by Ford *et al.* (2011) shows that the protein response to drought even differs between two tolerant varieties due to their difference in physiological response. So even with replicates, any conclusion on particular proteins cannot necessarily be extrapolated to other varieties.

Six days after sap flow slows down in the drought-stressed plant, a significant upregulation in protein content was seen (Figure 5.15). Because this concerns so many proteins, it is safe to say that this effect is significant. A substantial downregulation was harder to identify, but is likely to be also present, and already five days after sap flow decreased.

Some similarities can be found between Figure 5.14 and Figure 5.15. For instance, the capacitance in the head (C_{head}) shows a downregulation in the drought plant on DOY 116, but not on DOY 117. There are several proteins that show a similar trend. Whether this is causal or coincidence, further research should point out.

The phosphorylation state of a protein tells us something about its activity and conformation. A change in phosphorylation indicates a change in protein activity or cellular location and thus a change in the phenotype of a plant. The results of the phoshoproteomic analysis were, however, disappointing. No immediate trends in phosphorylation were visible (Figure 5.16) or showed a similar trend as the model variables in Figure 5.14.

When the model variables were included together with the phosposites in a heat map, they clustered between the phosphorylated proteins (see Figure B.1), indicating that there are phosphorylations showing the same trend as the model variables. These are however not numerous and are more likely to be ascribed to coincidence than true phenotypic change. Moreover, since there were no replicates, all intensity values should be interpreted with caution, so any trend that is present in Figure 5.16 might be erroneous.

As a consequence, there is no point in identifying the proteins that showed a similar trend as the model variables, since there is no statistical evidence that these protein changes are truly drought-induced.

Ford *et al.* (2011) performed a very similar proteomics analysis. They found that proteins involved in ROS scavenging increased and proteins involved in photosynthesis and the Calvin cycle decreased as the wheat plant experienced more drought stress. So the photosynthetic apparatus is broken down to avoid oxidative stress and ROS species. An increase in protein folding proteins was also found.

Chapter 7

Future prospects

In the previous chapters, it became clear that the model and the associated experiment can still be improved.

First of all, additional experiments are necessary to see what the real magnitude of the transpiration or sap flow is. In this report transpiration was upscaled to the magnitude of the sap flow based on a few observations, but there was no actual proof that this was correct.

Second, an independent technique is required to prove the hypothesis that the stem does indeed expands towards the hollow core and to determine the true magnitude of this inwards expansion compared to the outwards expansion. The results of this experiment suggest that this ratio is 99 to 1, but other influencing factor might contribute to the value of $f_{diameter}$ that were not mentioned in this report.

To be able to perform a moving window calibration, continuous measurements of the true transpiration are also necessary. This might already lead to a first improvement of the PM submodel.

Furthermore, biological replicates of the proteins samples will contain much more information and allow statistical analysis. Of course, this means that a lot more plants will have to be sown and grown, making these experiments a lot less practical, especially if many cultivars are studied simultaneously (see further).

The model itself can be vastly improved by incorporating other mechanisms.

First and foremost, a process should be included for the retranslocation of WSCs during grain filling, since inclusion of this process will lead to the observed continuous shrinking of the stem. The storage tissue volume should hereby reduce even under well-watered conditions.

As discussed in Chapter 6, the diameter measurements combined with the model simulations imply that when sap flow declines, the retranslocation of WSC is arrested an not increased as literature proposes. Inclusion of a sugar transport model should provide insight into this matter and determine if this retranslocation really ceases, or if it is merely small compared to the water depletion of the storage tissues.

Of course, other processes that are important during drought could also improve model simulations significantly.

Cavitation, the replacement of water by water vapour in the xylem, is an important source of increased hydraulic resistance values (Tyree & Sperry, 1988) and plays a major role in the drought response of the plant. Inclusion of cavitation in the future might lead to better estimates of the hydraulic resistance in drought conditions.

Also photosynthesis and stomatal regulation are two important processes in the plant that will influence its water balance, but are not yet considered in this research. These processes should improve not only the HydGro simulation of the water potential values in the leaves, but also the simulations of Tr_{act} in the Cropsyst submodel and thus the drought index presented in this report.

So far, the roots are not included in any of the submodels, as is often done in literature. However, Tuzet *et al.* (2003) proved that the roots have a major impact on how water deficit in the soil is experienced by the plant.

Of course, not all processes mentioned here can be combined into one single model. Enough processes should be modelled so that enough variability of the phenotypic traits of interest are explained. One should balance the risk of over-parametrization with the risk of over-simplification. Processes should be added until model calibration becomes cumbersome or is no longer possible (Xu & Buck-Sorlin, 2016).

When the model is able to properly simulate the desired variables, it can be used for experimental design. This means that the time points at which certain measurements or samples have to be taken, can be determined beforehand so as to contain as much information as possible.

Because we were restricted by the number of plants and the fact that each plant had to provide two different measurements, this was not performed in our experiment.

No validation was performed in this report, but this is absolutely necessary to confirm and further correct the model. However, this is best done after the declining diameter can be simulated properly. First of all, a validation on the same cultivar is needed to detect aberrations in the model. Then both calibration and validation data of other cultivars is necessary to check whether the model is applicable to wheat in general.

Because of time limitations and the novelty of this research, we could only focus on one genotype. We were therefore forced to take protein samples at different time points. An experimental design like this only enables the identification of important proteins during water deficit. These proteins are, however, very likely to be general proteins and thus ubiquitous in all wheat species. They will probably be only important to physiologists and modellers, and not for geneticist since they have probably been selected already by breeders in their breeding programs. The genetic variability concerning those genes will thus have been strongly reduced (Prioul *et al.*, 1997).

In the future, it might be more advantageous to monitor different wheat cultivars and take only one, or a few, protein samples at key points in the drought response. This way, the differences between cultivars can be denoted. This knowledge could then be useful in breeding programs.

If one would switch from analysing proteins to analysing the genes themselves, the amount samples would reduce to only one per cultivar since the genetic background remains identical, regardless of the conditions. Of course, this would require knowledge on the genes already present in the cultivars, for designing primers, unless a DNA fingerprinting technique is used. Another possibility is the rather new technique of RNAseq. This high-throughput technique allows the sequencing of the entire transcriptome, eliminating the need to design primers. The benefit of analysing RNA is that it includes information on the activation of genes and

provides concentration differences. Of course, this means that the time point at which the sample(s) is (are) taken becomes important again. The major drawback of this technique is of course its high cost. Again, a cheaper RNA fingerprinting technique is also possible and can be used as a cheap screening method.

As mentioned in the preface, the goal of this master thesis was unfortunately not accomplished, but is still possible in the future: using genetic (or proteomic) information to better estimate genotype-specific parameters (GSP).

To this end, it is necessary to study many different cultivars. Using their genetic fingerprints, the most sensitive parameters of the model (r_1, K_{crop}, R^s and $k_{2,head}$) could be estimated solely based on this genetic data.

At the same time, identification of the key regulating genes or proteins that differentiate a resistant cultivar from a non-resistant one is possible. Having one genetic sample per cultivar, one could adopt the method of Reymond *et al.* (2003) to implement its information into the ecophysiological model. For each cultivar, a reaction norm (which is the phenotypic response curve of a genotype to different environments) can be established. The slopes of these curves should be parameters in the model. The parameters can then be estimated in two ways: by individual calibration of the model to the response curve of each genotype and by using the genetic data. Combining the two methods for all cultivars should be able to point out the key regulating genes. A regression model can then be constructed with these genes to predict the parameter value.

The genetic data, whether obtained by analysing proteins, RNA or DNA, do not restrict themselves to one parameter. The same raw data can be used in exactly the same way for multiple parameters. In this research, we could for example determine the hydraulic resistance in the storage compartments, R^s, based on the presence of certain genes, but also all other genotype-specific parameters in the model like K_{crop}, r_1, r_2, k_1 and k_2.

If a regression model can be constructed for all parameters, model calibration could become redundant as in the research of Hoogenboom *et al.* (2004).

Chapter 8

Conclusion

In this research, a wheat model was built based on a combination of Penman-Monteith, Cropsyst and HydGro that can simulate transpiration and water flow and storage within a wheat plant. Even though improvements of the model are necessary in the future, a few strong conclusions could already be made from the data and simulations acquired in this research.

When a wheat plant (*Triticum aestivum* L.) experiences drought, transpiration and thus photosynthesis, are being reduced. However, these processes are not arrested immediately, leading to significant water losses in the plant that cannot be replenished as long as drought perseveres. Sap flow through the stem decreases as water in the soil becomes harder to reach. More and more water is coming from the plants reserves. However, only the water reserves from the stem and the leaves are used to maintain grain filling functionality as long as possible. The reserves in the head section, being the peduncle with the ear, remain untouched as long as possible. Also sap flow to the ear remains consistent.

During the grain filling stage, carbohydrates are remobilized to the ear. This was noticeable as a declining diameter that could not be explained by the model. Several sources mention that this retranslocation of carbohydrates increases during drought to accelerate the grain filling stage. However, during severe drought the rate of decline wás predicted accurately by the model. This suggests that the reduction in diameter at that moment could only be ascribed to the loss of water in the storage tissues and that retranslocation stops.

Further research is necessary to see whether the increased retranslocation is indeed only occurring when drought is not severe and arrests when sap flow becomes limiting. Comparison of diameter measurements and model simulations in both mild and severe drought conditions might already give an answer to this question. Inclusion of a sugar transport model could show us what really happens in the ear during drought.

To accurately simulate the diameter variation of the wheat peduncle, a scaling factor had to be used that was not present in the original model. Since the HydGro model was originally developed for trees, it was not surprising that the diameter simulations did not match our measured data at first. The diel variation in the simulations was far too large for the wheat plant. Since wheat stems contain a hollow core, it was hypothesized that the majority of the expansion occurs to the inside of the stem. This enables the plant to construct a more rigid epidermis for protection.

Further research with independent techniques is necessary to confirm this hypothesis.

In a second part of this report, a first draft was made for a drought index that can differentiate between drought caused by a high atmospheric demand and drought caused by a soil water deficit. Inclusion of an improved stomatal regulation model within the Penman-Monteith and Cropsyst model will be crucial for an adequate performance of the index. But this report already shows promising results for its application in greenhouse horticulture.

With measurements of the atmosphere in the greenhouse along with soil moisture levels and a single sap flow sensor on the base of the stem, the index can already be calculated. A prior calibration of the model is however necessary. To this end, stem diameter variation data, and preferably also photosynthesis data, is required for a plant of the same cultivar that experienced drought.

Even though no conclusions could be made on particular proteins, or their concentration due to the lack of replicates, this master thesis sets the base for a larger experiment in which more genotypes and more plants per genotype should be analysed and sampled.

With a few alteration in the methodology, the genotype-specific parameters of the model could be estimated based on proteomic data, possibly eliminating the need for calibration.

At the same time, the model allows to detect genotype by environment interaction, making it possible to identify key regulating proteins.

Bibliography

ABE, H., YAMAGUCHI-SHINOZAKI, K., URAO, T., TOSHISUKE, I., HOSOKAWA, D., *et al.*
1997. Role of *Arabidopsis* MYC and MYB homologs in drought- and abscisic acid-regulated
gene expression. *Plant Cell* , **9**(10), 1859–1868.

ABE, H., URAO, T., ITO, T., SEKI, M., SHINOZAKI, Y., *et al.* 2003. *Arabidopsis* AtMYC2
(bHLH) and AtMYB2 (MYB) functions as transcriptional activators in abscisic acid signaling.
Plant Cell , **15**(1), 63–78.

ADIE, B.A.T., PEREZ-PEREZ, J., PEREZ-PEREZ, M.M., GODOY, M., SANCHEZ-SERRANO,
J.J., *et al.* 2007. ABA is an essential signal for plant resistance to pathogens affecting JA
biosynthesis and the activation of defenses in Arabidopsis. *Plant Cell* , **19**(5), 1665–1681.

ALI, M., JENSEN, C.R., MOGENSEN, V.O., ANDERSEN, M.N., & HENSON, I.E. 1999. Root
signalling and osmotic adjustment during intermittent soil drying sustain grain yield of field
grown wheat. *Field Crops Research* , **62**(1), 35–52.

ALLEN, R.G., PEREIRA, L.S., RAES, D., & SMITH, M. 1998. FAO Penman-Monteith
equation. *In: Crop evapotranspiration - Guidelines for computing crop water requirements -
FAO Irrigation and drainage paper 56*. FAO - Food and Agriculture Organization of the
United Nations.

AMELONG, A., GAMBIN, B., SEVERINI, A.D., & BORR'AS, L. 2015. Predicting maize kernel
number using QTL information. *Field Crops Research* , **172**, 119–131.

ANDRIVON, D., GIORGETTI, C., BARANGER, A., CALONNEC, A., CARTOLARO, P., *et al.*
2013. Defining and designing plant architectural ideotypes to control epidemics? *European
Journal of Plant Pathology*, **135**(3), 611–617.

ARAUS, J.L., GUSTAVO, G.A., ROYO, C., & SERRET, M.D. 2008. Breeding for Yield
Potential and Stress Adaptation in Cereals. *Critical Reviews in Plant Sciences*, **27**(6),
377–41.

ASSENG, S., TURNER, N.C., BOTWRIGHT, T., & CONDON, A.G. 2003. Evaluating the
impact of a trait for increased specific leaf area on wheat yields using a crop simulation
model. *Agronomy Journal* , **95**(1), 10–19.

BAERT, A., DE SCHEPPER, V., & STEPPE, K. 2015. Variable hydraulic resistances and their
impact on plant drought response modelling. *Tree Physiology* , **35**, 439–449.

BAKER, R.J. 1988. Tests for crossover genotype-environmental interactions. *Canadian Journal
of Plant Science* , **68**(2), 405–410.

BALDAZZI, V., BERTIN, N., GENARD, M., GAUTIER, H., DESNOUES, E., *et al.* 2016. Challenges in Integrating Genetic Control in Plant and Crop Models. *In:* YIN, X., & STRUIK, P.C. (eds), *Crop Systems Biology: Narrowing the Gaps between Crop Modelling and Genetics* . Springer.

BAND, L.R., UBEDA-TOMÁS, S., DYSON, R.J., MIDDLETON, A.M., HODGMAN, T.C., *et al.* 2012. Growth-induced hormone dilution can explain the dynamics of plant root cell elongation. *Proc. Natl. Acad. Sci. U.S.A.* , **109**(19), 7577–7582.

BARNABAS, B., JAEGER, K., & FEHER, A. 2008. The effect of drought and heat stress on reproductive processes in cereals. *Plant Cell and Environment* , **31**(1), 11–38.

BAZARGANI, M.M., SARHADI, E., BUSHEHRI, A.A., MATROS, A., MOCK, H.P., *et al.* 2011. A proteomics view on the role of drought-induced senescence and oxidative stress defense in enhanced stem reserves remobilization in wheat. *Journal of Proteomics* , **74**(10), 1959–1973.

BEEMSTER, G.T.S., VERCRUYSSE, S., DE VEYLDER, L., KUIPER, M., & INZÉ, D. 2006. The arabidopsis leaf as a model system for investigating the role of cell cycle regulation in organ growth. *Journal of Plant Research*, **119**(1), 43–50.

BERNARDO, R. 2004. What proportion of declared QTL in plants are false. *Theoretical and Applied Genetics*, **109**(2), 419–424.

BLOWER, S.M., & DOWLATABADI, H. 1994. Sensitivity and uncertainty analysis of complex-models of disease transmission - an HIV model, as an example. *International Statistical Review* , **62**(2), 229–243.

BLUM, A. 1998. Improving wheat grain filling under stress by stem reserve mobilisation. *Euphytica* , **100**(3), 77–83.

BLUM, A. 2005. Drought resistance, water-use efficiency, and yield potential– are they compatible, dissonant, or mutually exclusive? *Australian Journal of Agricultural Research*, **56**(11), 1159–1168.

BLUM, A. 2006. Drought adaptation in cereal crops: a prologue. *Pages 3–15 of:* RIBAUT, J.M. (ed), *Drought Adaptation in Cereals.* Binghamton, NY: The Haworth Press, Inc .

BLUM, A. 2009. Effective use of water (EUW) and not water-use efficiency (WUE) is the target of crop yield improvement under drought stress. *Field Crops Research* , **112**(2-3), 119–123.

BLUM, A., SINMENA, B., MAYER, J., GOLAN, G., & SHPILER, L. 1994. Stem reserve mobilization supports wheat grain filling under heat stress. *Australian Journal of Agricultural Research*, **21**(6), 771–781.

BLUM, A., ZHANG, J.X., & NGUYEN, H.T. 1999. Consistent differences among wheat cultivars in osmotic adjustment and their relationship to plant production. *Field Crops Research* , **64**(3), 287–291.

BOGARD, M., RAVEL, C., PAUX, E., BORDES, J., BALFOURIER, F., *et al.* 2014. Predictions of heading date in bread wheat (*Triticum aestivum* L.) using QTL-based parameters of an ecophysiological model. *Journal of Experimental Botany* , **65**(20), 5849–5865.

BOOTE, J.K., JONES, J.W., HOOGENBOOM, G., & PICKERING, N.B. 1998. The CROPGRO model for grain legumes. *Pages 99–128 of:* TSUJI, G.Y., HOOGENBOOM, G., & THORNTON, P.K. (eds), *Understanding Options for Agricultural Production.* Dordrecht: Springer Netherlands.

BOOTE, K.J., VALLEJOS, C.E., JONES, J.W., & CORRELL, M.J. 2016. Crop Modeling Approaches for Predicting Phenotype of Grain Legumes with Linkage to Genetic Information. *In:* YIN, X., & STRUIK, P.C. (eds), *Crop Systems Biology: Narrowing the Gaps between Crop Modelling and Genetics* . Springer.

BRUNEL, S., TEULAT-MERAH, B., WAGNER, M.H., HUGUET, T., POSPERI, J., *et al.* 2009. Using a model-based framework for analysing genetic diversity during germination and heterotrophic growth of *Medicago truncatula. Annals of Botany* , **103**(7), 1103–1117.

BUSTOS-KORTS, D., M.MALOSETTI, CHAPMAN, S., & VAN EEUWIJK, F. 2016. Modelling of Genotype by Environment Interaction and Prediction of Complex Traits across Multiple Environments as a Synthesis of Crop Growth Modelling, Genetics and Statistics. *In:* YIN, X., & STRUIK, P.C. (eds), *Crop Systems Biology: Narrowing the Gaps between Crop Modelling and Genetics* . Springer.

CAMARGO, G.G.T., & KEMANIAN, A.R. 2016. Six crop models differ in their simulation of water uptake. *Agricultural and Forest Meteorology*, **220**, 116–129.

CARUSO, G., CAVALIERE, C., FOGLIA, P., GUBBIOTTI, R., SAMPERI, R., *et al.* 2009. Analysis of drought responsive proteins in wheat (*Triticum durum*) by 2D-PAGE and MALDI-TOF mass spectrometry. *Plant Science* , **17**(6), 570–576.

CHAPMAN, S.C. 2008. Use of crop models to understand genotype by environment interactions for drought in real-world and simulated plant breeding trials. *Euphytica* , **161**(1-2), 195–208.

CHAPMAN, S.C., COOPER, M., & HAMMER, G.L. 2002. Using crop simulation to generate genotype by environment interaction effects for sorghum in water-limited environments. *Asutralian Journal of Agricultural Research*, **53**(4), 379–389.

CHARMET, G. 2000. Power and accuracy of QTL detection: simulation studies if one-QTL models. *Agronomie*, **20**(3), 309–323.

CHENG, M.C., LIAO, P.M., KUO, W.W., & LIN, T.P. 2013. The Arabidopsis ETHYLENE RESPONSE FACTOR1 regulates abiotic stress-responsive gene expression by binding to different cis-acting elements in response to different stress signals. *Plant Physiology*, **162**(3), 1566–1582.

CHENU, K., CHAPMAN, S.C., TARDIEU, F., MCLEAN, G., WELCKER, C., *et al.* 2009. Simulating the yield impacts of organ-level quantitative trait loci associated with drought response in maize: a "gene-to-phenotype" modeling approach. *Genetics* , **183**(4), 1507–1523.

CHOI, H.I., PARK, H.J., PARK, J.H., KIM, S., IM, M.Y., *et al.* 2005. Arabidopsis calcium-dependent protein kinase AtCPK32 interacts with ABF4, a transcriptional regulator of abscisic acid-responsive gene expression, and modulates its activity. *Plant Physiology* , **139**(4), 1750–1761.

CHRISTMANN, A., MOES, D., HIMMELBACH, A., YANG, Y., TANG, Y., *et al.* 2006. Integration of abscisic acid signalling into plant responses. *Plant Biology* , **8**(3), 314–325.

CHRISTMANN, A., WEILER, E.W., STEUDLE, E., & GRILL, E. 2007. A hydraulic signal in root-to-shoot signalling of water shortage. *Plant Journal* , **52**(1), 167–174.

COWAN, I.R., & FARQUHAR, G.D. 2012. Stomatal function in relation to leaf metabolism and environment. *Pages 471–505 of:* JENNINGS, D.H. (ed), *Integration of Activity in the Higher Plant.*

CROSSA, J., YANG, R.C., & CORNELIUS, P. 2004. Studying crossover genotype x environment interaction using linear-bilinear models and mixed models. *Journal of Agricultural Biological and Environmental Statistics*, **9**(3), 362–380.

CROSSA, J., DE LOS CAMPOS, G., PÉREZ, P., D.GIANOLA, BURGUENO, J., *et al.* 2010. Prediction of Genetic Values of Quantitative Traits in Plant Breeding Using Pedigree and Molecular Markers. *Genetics*, **186**(2), 713–724.

CUSHMAN, J.C., & BOHERT, H.J. 2000. Genomic approaches to plant stress tolerance. *Current Opinion in Plant Biology*, **3**(2), 117–124.

DE PAUW, D.J.W., STEPPE, K., & DE BAETS, B. 2008. Identifiablilty analysis and improvement of a tree water flow and storage model. *Mathematical Biosciences*, **211**, 314–332.

DE SWAEF, T., VERBIST, K., CORNELIS, W., & STEPPE, K. 2012. Tomato sap flow, stem and fruit growth in relation to water availability in rockwool growing medium. *Plant Soil*, **350**, 237–252.

DEWITT, T.J., & SCHEINER, S.M. 2004. *Phenotypic plasticity: functional and conceptual approaches.* Oxford University Press.

DIAS, A.S., & LIDON, F.C. 2009. Evaluation of Grain Filling Rate and Duration in Bread and Durum Wheat, under Heat Stress after Anthesis. *Journal of Agronomy and Crop Science*, **195**(2), 137–147.

DISTELFELD, A., LI, C., & DUBCOVSKY, J. 2009. Regulation of flowering in temperate cereals. *Current Opinion in Plant Biology* , **12**(2), 178–184.

DONALD, C.M. 1968. The breeding of crop ideotypes. *Euphytica*, **17**(3), 385–403.

DOUGHERTY, C.T. 1974. The relationship between solar radiation, soil water, and water potential of ears of wheat. *New Zealand Journal of Agricultural Research*, **17**(4), 459–463.

DUNCAN, O., TRÖSCH, J., FENSKE, R., TAYLOR, N.L., & MILLAR, A.H. 2017. Resource: Mapping the *Triticum aestivum* proteome. *Plant Journal*, **89**, 601–616.

DUNCAN, W.G., MCCLOUD, D.E., MCGRAW, R.L., & BOOTE, K.J. 1978. Physiological aspects of peanut yield improvement. *Crop Science* , **18**(6), 1015–1020.

EDMEADES, G.O., MCMASTER, G.S, WHITE, J.W., & CAMPOS, H. 2004. Genomics and the physiologist: bridging the gap between genes and crop response. *Field Crops Research*, **90**(1), 5–18.

ELFVING, D.C., KAUFMANN, M.R., & HALL, A.E. 1972. Interpreting Leaf Water Potential Measurements with a Model of the Soil-Plant-Atmosphere Continuum. *Physiologia Plantarum* , **27**(2), 161–168.

ELWELL, D.L., CURRY, R.B., & KEENER, M.E. 1987. Determination of Potential Yield-Limiting Factors of Soybeans using SOYMOD/OARDC. *Agricultural systems* , **24**(3), 221–242.

FAN, X.W., LI, F.M., XIONG, Y.C., AN, L.Z., & LONG, R.J. 2008. The cooperative relation between non-hydraulic root signals and osmotic adjustment under water stress improves grain formation for spring wheat varieties. *Physiologia Plantarum* , **132**(3), 283–292.

FAROOQ, M., HUSSAIN, M., & SIDDIQUE, K.H.M. 2014. Drought Stress in Wheat during Flowering and Grain-filling Periods. *Critical Reviews in Plant Sciences*, **33**(4), 331–349.

FINKELSTEIN, R., GAMPALA, S.S.L., LYNCH, T.J., THOMAS, T.L., & ROCK, C.D. 2005. Redundant and distinct functions of the ABA response loci ABA-INSENSITIVE(ABI)5 and ABRE-BINDING FACTOR (ABF)3. *Plant Molecular Biology* , **59**(2), 253–267.

FINKELSTEIN, R.R., GAMPALA, S.S.L., & ROCK, C.D. 2002. Abscisic acid signaling in seeds and seedlings. *Plant Cell* , **14**, S15–S45.

FINLAY, K.W., & WILKINSON, G.N. 1963. The analysis of adaptation in a plant-breeding programme. *Asutralian Journal of Agricultural Research*, **14**(6), 742–754.

FORD, K.L., CASSIN, A., & BACIC, A. 2011. Quantitative proteomic analysis of wheat cultivars with differing drought stress tolerance. *Frontiers in Plant Science* , **2**(44).

GEBHARDT, C., BALLVORA, A., WALKEMEIER, B., OBERHAGEMANN, P., & SCHULER, K. 2004. Assessing genetic potential in germplasm collections of crop plants by marker-trait association: a case study for potatoes with quantitative variation of resistance to late blight and maturity type. *Molecular Breeding*, **13**(1), 93–102.

GÉNARD, M., FISHMAN, S., VERCAMBRE, G., HUGUET, J.G., BUSSI, C., *et al.* 2001. A Biophysical Analysis of Stem and Root Diameter Variations in Woody Plants. *Plant Physiology*, **126**(1), 188–202.

GÉNARD, M., BERTIN, N., GAUTIER, H., LESCOURRET, F., & QUILOT, B. 2010. Virtual profiling: a new way to analyse phenotypes. *Plant Journal* , **62**(2), 344–355.

GÉNARD, M., MEMMAH, M.M., QUILOT-TURION, B., VERCAMBRE, G., BALDAZZI, V., *et al.* 2016. Modelling of Genotype by Environment Interaction and Prediction of Complex Traits across Multiple Environments as a Synthesis of Crop Growth Modelling, Genetics and Statistics. *In:* YIN, X., & STRUIK, P.C. (eds), *Crop Systems Biology: Narrowing the Gaps between Crop Modelling and Genetics* . Springer.

GU, J., YIN, X., STOMPH, T.J., & STRUIK, P.C. 2014a. Can exploiting natural genetic variation in leaf photosynthesis contribute to increasing rice productivity? A simulation analysis. *Plant Cell and Environment* , **37**(1), 22–34.

GU, J., YIN, X., ZHANG, C., WANG, H., & STRUIK, P.C. 2014b. Linking ecophysiological modelling with quantitative genetics to support marker-assisted crop design for improved rice (*Oryza sativa* L.) yields under drought stress. *Annuals of Botany* , **114**(3), 499–511.

GUILFOYLE, T.J., & HAGEN, G. 2007. Auxin response factors. *Current Opinion in Plant Biology* , **10**(5), 453–460.

HAAKE, V., COOK, D., RIECHMANN, J.L., PINEDA, O., THOMASHOW, M.F., *et al.* 2002. Transcription factor CBF4 is a regulator of drought adaptation in *Arabidopsis*. *Plant Physiology* , **130**(2), 639–648.

HACKETT, C.A. 2002. Statistical methods for QTL mapping in cereals. *Plant Molecular Biology*, **48**(5), 585–599.

HAGEN, G., & GUILFOYLE, T. 2002. Auxin-responsive gene expression: genes, promoters and regulatory factors. *Plant Molecular Biology* , **49**(3-4), 373–385.

HAJHEIDARI, M., EIVAZI, A., BUCHANAN, B.B., WONG, J.H., MAJIDI, I., *et al.* 2007. Proteomics uncovers a role for redox in drought tolerance in wheat. *Journal of Proteome Research* , **6**(4), 1451–1460.

HAMMAN, K.D., WILLIAMSON, R.L., STEFFLER, E.D., WRIGHT, C.T., HESS, J.R., *et al.* 2005. Structural Analysis of Wheat Stems. *Applied Biochemistry and Biotechnology*, **121**, 71–80.

HAMMER, G., MESSINA, C., VAN OOSTEROM, E., CHAPMAN, S., SINGH, V, *et al.* 2016. Molecular Breeding for Complex Adaptive Traits: How Integrating Crop Ecophysiology and Modelling Can Enhance Efficiency. *In:* YIN, X., & STRUIK, P.C. (eds), *Crop Systems Biology: Narrowing the Gaps between Crop Modelling and Genetics* . Springer.

HAMMER, G.L., KROPFF, M.J., SINCLAIR, T.R., & PORTER, J.R. 2002. Future contributions of crop modelling - from heuristics and supporting decision making to understanding genetic regulation and aiding crop improvement. *European Journal of Agronomy*, **18**(1-2), 15–31.

HAMMER, G.L., SINCLAIR, T.R., CHAPMAN, S.C., & VAN OOSTEROM, E. 2004. On Systems Thinking, Systems Biology, and the in Silico Plant. *Plant Physiology*, **134**(3), 909–911.

HAMMER, G.L., COOPER, M., TARDIEU, F., WELCH, S., WALSH, B., *et al.* 2006. Models for navigating biological complexity in breeding improved crop plants. *Trends in Plant Science* , **11**(12), 587–593.

HAMMER, G.L., VAN OOSTEROM, E., MCLEAN, G., CHAPMAN, S.C., BROAD, I., *et al.* 2010. Adapting APSIM to model the physiology and genetics of complex adaptive traits in field. *Journal of Experimental Botany* , **61**(8), 2185–2202.

HESS, J.R., CARMAN, J.G., & BANOWETZ, G.M. 2002. Hormones in wheat kernels during embryony. *Journal of Plant Physiology* , **159**, 379–386.

Hirel, B., Bertin, P., Quillere, I., Bourdoncle, W., Attagnant, C., *et al.* 2001. Towards a better understanding of the genetic and physiological basis for nitrogen use efficiency in maize. *Plant Physiology*, **125**(3), 1258–1270.

Ho, L.C. 1988. Metabolism and compartmentation of imported sugars in sink organs in relation to sink strength. *Annual Review of Plant Physiology and Plant Molecular Biology*, **39**, 355–378.

Holmes, M.G., & Keiller, D.R. 2002. Effects of pubescence and waxes on the reflectance of leaves in the ultraviolet and photosynthetic wavebands: a comparison of a range of species. *Plant Cell and Environment*, **25**(1), 85–93.

Hoogenboom, G., White, J.W., Jones, J.W., & Boote, K.J. 1994. BEANGRO - A process-oriented dry bean model with a versatile user-interface. *Agronomy Journal*, **86**(1), 182–190.

Hoogenboom, G., White, J.W., & Messina, C.D. 2004. From genome to crop: integration through simulation modeling. *Field Crops Research* , **90**(1), 145–163.

IPCC. 2014. *Climate Change 2014, Synthesis Report, Summary for Policymakers.* Tech. rept. Intergovernmental Panel on Climate Change.

Izanloo, A., Condon, A.G., & Langridge, P. 2008. Different mechanisms of adaptation to cyclic water stress in two South Australian bread wheat cultivars. *Journal of Experimental Botany* , **59**(12), 3327–3346.

Johnson, R.R., Wagner, R.L., Verhey, S.D., & Walker-Simmons, M.K. 2002. The abscisic acid-responsive kinase PKABA1 interacts with a seed-specific abscisic acid response element-binding factor, TaABF, and phosphorylates TaABF peptide sequences. *Plant Physiology*, **130**(2), 837–846.

Jones, H.G. 1992. *Plants and Microclimate: A Quantitative Approach to Environmental Plant Physiology.* 2nd edn. Cambridge University Press.

Kamal, A.H.M., Kim, K.H., Shin, K.H., Choi, J.S., Baik, B.K., *et al.* 2010. Abiotic stress responsive proteins of wheat grain determined using proteomics technique. *Australian Journal of Crop Science* , **4**(3), 196–208.

Katul, G.G., Manzoni, S., Palmroth, S., & Oren, R. 2010. A stomatal optimization theory to describe the effects of atmospheric CO2 on leaf photosynthesis and transpiration. *Annals of Botany*, **105**(3), 431–442.

Kearsey, M.J., & Farquhar, A.G.L. 1998. QTL analysis in plants; where are we now? *Heredity*, **80**(2), 137–142.

King, C.A., Larry, L.C., & Brye, K.R. 2009. Differential Wilting among Soybean Genotypes in Response to Water Deficit. *Crop Science* , **49**(1), 290–298.

Kuchen, E.E., Fox, S., de Reuille, P.B., Kennaway, R., Bensmihen, S., *et al.* 2012. Generation of leaf shape through early patterns of growth and tissue polarity. *Science* , **335**(6072), 1092–1096.

LANDIVAR, J.A., BAKER, D.N., & JENKINS, J.N. 1983a. Application of GOSSYM to genetic feasibility studies. I. Analyses of fruit abscission and yield in okra-leaf cottons. *Crop Science* , **23**(3), 497–504.

LANDIVAR, J.A., BAKER, D.N., & JENKINS, J.N. 1983b. Application of GOSSYM to genetic feasibility studies. II. Analyses of increasing photosynthesis, specific leaf weight and longevity of leaves in cotton. *Crop Science* , **23**(3), 504–510.

LANGENSIEPEN, M., KUPISCH, M., GRAF, A., SCHMIDT, M., & EWERT, F. 2014. Improving the stem heat balance method for determining sap-flow in wheat. *Agricultural and Forest Meteorology*, **186**(5), 34–42.

LAPERCHE, A., DEVIENNE-BARET, F., MAURY, O., LE GOUIS, J., & NEY, B. 2006. A simplified conceptual model of carbon/nitrogen functioning for QTL analysis of winter wheat adaptation to nitrogen deficiency. *Theoretical and Applied Genetics*, **113**(6), 1131–1146.

LEVCHENKO, V., KONRAD, K.R., DIETRICH, P., ROELFSEMA, M.R.G., & HEDRICH, R. 2005. Cytosolic abscisic acid activates guard cell anion channels without preceding Ca2+ signals. *Proc. Natl. Acad. Sci. U.S.A.* , **102**(1), 4203–4208.

LEVITT, J. (ed). 1972. *Responses of Plants to Environmental Stresses.*

LIU, H., ABLE, A.J., & ABLE, J.A. 2016. Water-deficit stress responsive microRNAs and their targets in four durum wheat genotypes. *Functional and Integrative Genomics* , **17**(237).

LIU, H., ABLE, A.J., & ABLE, J.A. 2017. Genotypic water-deficit stress response in durum wheat: association between physiological traits, microRNA regulatory modules and yield components. *Functional Plant Biology*, **44**, 538–551.

LOCKHART, J.A. 1965. An analysis of irreversible plant cell elongation. *Journal of Theoretical Biology*, **8**(2), 264–275.

LUDWIG-MÜLLER, J. 2011. Auxin conjugates: their role for plant development and in the evolution of land plants. *Journal of Experimental Botany* , **62**(6), 1757–1773.

LUQUET, D., CLEMENT-VIDAL, A., & FABRE, D. 2008. Orchestration of transpiration, growth and carbohydrate dynamics in rice during a dry-down cycle. *Functional Plant Biology*, **35**(8), 689–704.

LUQUET, D., REBOLLEDO, C., ROUAN, L., SOULIE, J.C., & DINGKUHN, M. 2016. Heuristic Exploration of Theoretical Margins for Improving Adaptation of Rice through Crop-Model Assisted Phenotyping. *In:* YIN, X., & STRUIK, P.C. (eds), *Crop Systems Biology: Narrowing the Gaps between Crop Modelling and Genetics* . Springer.

MAMMADOV, J., AGGARWAL, R., BUYYARAPU, R., & KUMPATLA, S. 2012. SNP Markers and Their Impact on Plant Breeding. *International Journal of Plant Genomics* , **2012**.

MANZONI, S., VICO, G., KATUL, G., FAY, P.A., POLLEY, W., *et al.* 2011. Optimizing stomatal conductance for maximum carbon gain under water stress. *Functional Ecology* , **25**(3), 456–467.

MEDLYN, B.E., DUURSMA, R.A., EAMUS, D., ELLSWORTH, D.S., PRENTICE, I.C., *et al.* 2011. Reconciling the optimal and empirical approaches to modelling stomatal conductance. *Global Change Biology*, **17**(6), 2134–2144.

MERAH, O. 2001. Potential importance of water status traits for durum wheat improvement under Mediterranean conditions. *Journal of Agricultural Science* , **137**, 139–145.

MESSINA, C.D., JONES, J.W., BOOTE, K.J., & VALLEJOS, C.E. 2006. A gene-based model to simulate soybean development and yield responses to environment. *Crop Science* , **46**(1), 456–466.

MORGAN, J.M. 1984. Osmoregulation and Water-Stress in Higher Plants. *Annual Review of Plant Physiology and Plant Molecular Biology* , **35**, 299–319.

MUNNS, R. 1988. Why Measure Osmotic Adjustment? *Australian Journal of Plant Physiology* , **15**(6), 717–726.

MYERS, P.N., SETTER, T.L., MADISON, J.T., & THOMPSON, J.F. 1990. Abscisic acid inhibition of endosperm cell division in cultured maize kernels. *Plant Physiology*, **94**(3), 1330–1336.

NAKAGAWA, H., YAMAGISHI, J., MIYAMOTO, N., MOTOYAMA, M., YANO, M., *et al.* 2005. Flowering response of rice to photoperiod and temperature: a QTL analysis using a phenological model. *Theoretical and Applied Genetics*, **110**(4), 778–786.

PALTA, J.A., KOBATA, T., TURNER, N.C., & FILLERY, I.R. 1994. Remobilization of carbon and nitrogen in wheat as influenced by post anthesis water deficits. *Crop Science* , **34**(1), 118–124.

PALTA, J.A., N.C.TURNER, FRENCH, R.J., & BUIRCHELL, B.J. 2007. Physiological responses of lupin genotypes to terminal drought in a Mediterranean-type environment. *Annals of Applied Biology* , **150**(3), 269–279.

PANTIN, F., SIMONNEAU, T., ROLLAND, G., DAUZAT, M., & MULLER, B. 2011. Control of leaf expansion: a developmental switch from metabolics to hydraulics. *Plant Physiology* , **156**(2), 803–815.

PAPIN, J.A., PRICE, N.D., WIBACK, S.J., FELL, D.A., & PALSSON, B.O. 2003. Metabolic pathways in the postgenome era. *Trends in Biochemical Sciences* , **28**(5), 250–258.

PASSIOURA, J.B. 1977. Grain yield, harvest index, and water use of wheat. *Journal of the Australian Institute of Agricultural Science*, **43**(3-4), 117–120.

PENG, Z.Y., WANG, M.C., LI, F., LU, H.J., LI, C.L., *et al.* 2009. A proteomic study of the response to salinity and drought stress in an introgression strain of bread wheat. *Molecular and Cellular Proteomics*, **8**(12), 2676–2686.

PLAUT, Z., BUTOW, B.J., BLUMENTHAL, C.S., & WRIGLEY, C.W. 2004. Transport of dry matter into developing wheat kernels and its contribution to grain yield under post-anthesis water deficit and elevated temperature. *Field Crops Research*, **86**(2-3), 185–198.

PRENTICE, I.C., DONG, N., GLEASON, S.M., MAIRE, V., & WRIGHT, I.J. 2014. Balancing the costs of carbon gain and water transport: testing a new theoretical framework for plant functional ecology. *Ecology Letters* , **17**(1), 82–91.

PRIOUL, J.L., QUARRIE, S., CAUSSE, M., & DE VIENNE, D. 1997. Dissecting complex physiological functions through the use of molecular quantitative genetics. *Journal of Experimental Botany*, **48**(311), 1151–1163.

QUILOT, B., KERVELLA, J., GENARD, M., & LESCOURRET, F. 2005. Analysing the genetic control of peach fruit quality through an ecophysiological model combined with a QTL approach. *Journal of Experimental Botany* , **56**(422), 3083–3092.

RABBANI, M.A., MARUYAMA, K., ABE, H., KHAN, M.A., KATSURA, K., *et al.* 2003. Monitoring expression profiles of rice genes under cold, drought, and high-salinity stresses and abscisic acid application using cDNA microarray and RNA gel-blot analyses. *Plant Physiology*, **133**(4), 1755–1767.

RAGHAVENDRA, A.S., GONUGUNTA, V.K., CHRISTMANN, A., & GRILL, E. 2010. ABA perception and signalling. *Trends in Plant Science*, **15**(7), 395–401.

REBETZKE, G.J., VAN HERWAARDEN, A.F., JENKINS, C., WEISS, M., LEWIS, D., *et al.* 2008. Quantitative trait loci for water-soluble carbohydrates and associations with agronomic traits in wheat. *Australian Journal of Agricultural Research*, **59**(10), 891–905.

REUNING, G.A., BAUERLE, W.L., MULLEN, J.L., & MCKAY, J.K. 2015. Combining quantitative trait loci analysis with physiological models to predict genotype-specific transpiration rates. *Plant Cell and Environment*, **38**(4), 710–717.

REYMOND, M., MULLER, B., LEONARDI, A., CHARCOSSET, A., & TARDIEU, F. 2003. Combining quantitative trait loci analysis and an ecophysiological model to analyze the genetic variability of the responses of maize leaf growth to temperature and water deficit. *Plant Physiology*, **131**(2), 664–675.

REYMOND, M., MULLER, B., & TARDIEU, F. 2004. Dealing with the genotype x environment interaction via a modelling approach: a comparison of QTLs of maize leaf length or width with QTLs of model parameters. *Journal of Experimental Botany* , **55**(407), 2461–2472.

REYNOLDS, M.P., MUJEEB-KAZI, A., & SAWKINS, M. 2005. Prospects for utilising plant-adaptive mechanisms to improve wheat and other crops in drought- and salinity-prone environments. *Annals of Applied Biology*, **146**(2), 239–259.

RICHARDS, R.A. 2006. Physiological traits used in the breeding of new cultivars for water-scarce environments. *Agricultural Water Management* , **80**(1-3), 179–211.

RIERA, M., VALON, C., FENZI, F., GIRAUDAT, J., & LEUNG, J. 2005. The genetics of adaptive responses to drought stress: abscisic acid-dependent and abscisic acid-independent signalling components. *Physiologia Plantarum*, **123**(2), 111–119.

SADOK, W., & SINCLAIR, T.R. 2010. Genetic variability of transpiration response of soybean [*Glycine max* (L.) Merr.] shoots to leaf hydraulic conductance inhibitor AgNO3. *Crop Science*, **50**(4), 1423–1430.

Salvi, S., Corneti, S., Bellotti, M., Carraro, N., Sanguienti, M.C., *et al.* 2011. Genetic dissection of maize phenology using an intraspecific introgression library. *BMC Plant Biology*, **11**(4).

Sanguineti, M.C., Tuberosa, R., Landi, P., Salvi, S., Maccaferri, M., *et al.* 1999. QTL analysis of drought related traits and grain yield in relation to genetic variation for leaf abscisic acid concentration in field-grown maize. *Journal of Experimental Botany*, **50**(337), 1289–1297.

Schilling, C.H., Letscher, D., & Palsson, B.O. 2000. Theory for the systemic definition of metabolic pathways and their use in interpreting metabolic function from a pathway-oriented perspective. *Journal of Theoretical Biology*, **203**(3), 229–248.

Schon, C.C., Utz, H.F., Groh, S., Truberg, B., Openshaw, S., *et al.* 2004. Quantitative trait locus mapping based on resampling in a vast maize test cross experiment and its relevance to quantitative genetics for complex traits. *Genetics*, **167**(1), 485–498.

Schuster, S., Fell, D.A., & Dandekar, T. 2000. A general definition of metabolic pathways useful for systematic organization and analysis of complex metabolic networks. *Nature Biotechnology*, **18**(3), 326–332.

Seki, M., Narusaka, M., Abe, H., Kasuga, M., Yamaguchi-Shinozaki, K., *et al.* 2001. Monitoring the expression pattern of 1300 Arabidopsis genes under drought and cold stresses by using a full-length cDNA microarray. *Plant Cell*, **13**(1), 61–72.

Seki, M., Narusaka, M., Ishida, J., Nanjo, T., Fujita, M., *et al.* 2002. Monitoring the expression profiles of 7000 Arabidopsis genes under drought, cold and high-salinity stresses using a full-length cDNA microarray. *Plant Journal*, **31**(3), 279–292.

Semenov, M.A., & Halford, N.G. 2009. Identifying target traits and molecular mechanisms for wheat breeding under a changing climate. *Journal of Experimental Botany*, **60**(10), 2791–2804.

Serraj, R., & Sinclair, T.R. 2002. Osmolyte accumulation: can it really help increase crop yield under drought conditions? *Plant Cell and Environment*, **25**(2), 333–341.

Sharma, E., Sharma, R., Borah, P., Jain, M., & Khurana, J.P. 2015. Emerging roles of auxin in abiotic stress responses. *Pages 299–328 of:* Pandey, G.K. (ed), *Elucidation of abiotic stress signaling in plants.* Springer.

Sharp, R.E., Silk, W.K., & Hsiao, T.C. 1988. Growth of the maize primary root at low water potentials : I. Spatial distribution of expansive growth. *Plant Physiology*, **87**(1), 50–57.

Shinozaki, K., & Yamaguchi-Shinozaki, K. 2000. Molecular responses to dehydration and low temperature: differences and cross-talk between two stress signaling pathways. *Current Opinion in Plant Biology*, **3**(3), 217–223.

Shinozaki, K., & Yamaguchi-Shinozaki, K. 2007. Gene networks involved in drought stress response and tolerance. *Journal of Experimental Botany*, **58**(2), 221–227.

SHINOZAKI, K., YAMAGUCHI-SHINOZAKI, K., & SEKI, M. 2003. Regulatory network of gene expression in the drought and cold stress responses. *Current Opinion in Plant Biology* , **6**(5), 410–417.

SIEGEL, R.S., XUE, S.W., MURATA, Y., YANG, Y.Z., NISHIMURA, N., *et al.* 2009. Calcium elevation-dependent and attenuated resting calcium-dependent abscisic acid induction of stomatal closure and abscisic acid-induced enhancement of calcium sensitivities of S-type anion and inward-rectifying K+ channels in Arabidopsis guard cells. *Plant Journal* , **59**(2), 207–220.

SIMMONS, S., OELKE, E., & ANDERSON, P. 1995. *Growth and development guide for spring wheat.* University of Minnesota. `http://www.extension.umn.edu/agriculture/small-grains/growth-and-development/spring-wheat/.` (consulted 2-10-2016).

SIMMONS, S., OELKE, E., & ANDERSON, P. 2013. *Growth and development guide for spring barley.* University of Minnesota. `http://www.extension.umn.edu/agriculture/small-grains/growth-and-development/spring-barley/.` (consulted 2-10-2016).

SIMONNEAU, T., HABIB, R., GOUTOULY, J.P., & HUGUET, J.G. 1993. Diurnal changes in stem diameter depend upon variations in water content: direct evidence in peach trees. *Journal of Experimental Botany* , **44**, 615–621.

SINCLAIR, T., PURCELL, L., & SNELLER, C.H. 2004. Crop transformation and the challenge to increase yield potential. *Trends in Plant Science* , **9**(2), 70–75.

SINCLAIR, T.R., MESSINA, C.D., BEATY, A., & SAMPLES, M . 2010. Assessment across the United States of the benefits of altered soybean drought traits. *Agronomy Journal* , **102**(2), 475–482.

SINCLAIR, T.R., DEVI, J.M., & CARTER JR., T.E. 2016. Limited-Transpiration Trait for Increased Yield for Water-Limited Soybean: From Model to Phenotype to Genotype to Cultivars. *In:* YIN, X., & STRUIK, P.C. (eds), *Crop Systems Biology: Narrowing the Gaps between Crop Modelling and Genetics* . Springer.

SINGH, P., BOOTE, K.J., KUMAR, U., SRINIVAS, K., NIGAM, S.N., *et al.* 2012. Evaluation of genetic traits for improving productivity and adaptation of groundnut to climate change in India. *Journal of Agronomy and Crop Science* , **198**(5), 399–413.

SIRICHANDRA, C., WASILEWSKA, A., VLAD, F., VALON, C., & LEUNG, J. 2009. The guard cell as a single-cell model towards understanding drought tolerance and abscisic acid action. *Journal of Experimental Botany* , **60**(5), 1439–1463.

SLAFER, G.A., ARAUS, J.L., ROYO, C., & GARCIA DEL MORAL, L.E. 2005. Promising eco-physiological traits for genetic improvement of cereal yields in Mediterranean environments. *Annals of Applied Biology* , **146**(1), 61–70.

SNOUSSI, E.L. 1989. Qualitative dynamics of piecewise-linear differential equations: a discrete mapping approach. *Dynamics and Stability of Systems* , **4**(3-4), 565–583.

SPERRY, J.S., VENTURAS, M.D., ANDEREGG, W.R., M.MENCUCCINI, MACKAY, D.S., *et al.* 2016. Predicting stomatal responses to the environment from the of photosynthetic gain and hydraulic cost. *Plant Cell Environment.*

STAM, P. 1998. Crop physiology, QTL analysis and plant breeding. *In:* LAMBERS, H., & VAN VUUREN, M.M.I (eds), *Inherent variation in plant growth: physiological mechanisms and ecological consequences* . Backhuys Publishers, Leiden.

STEPPE, K., DE PAUW, D.J.W., LEMEUR, R., & VANROLLEGHEM, P.A. 2006. A mathematical model linking tree sap flow dynamics to daily stem diameter fluctuations and radial stem growth. *Tree Physiology*, **26**, 257–273.

STEPPE, K., DE PAUW, D.J.W., & LEMEUR, R. 2008. A step towards new irrigation scheduling strategies using plant-based measurements and mathematical modelling. *Irrigation Science*, **26**(6), 505–517.

STÖCKLE, C.L., & NELSON, R. 2003. *Cropping Systems Simulation Model User's Manual.* Washingtion State University, Biological Systems Engineering Department.

STÖCKLE, C.O., DONATELLI, M., & NELSON, R. 2003. CropSyst, a cropping systems simulation model. *European Journal of Agronomy*, **18**(3-4), 289–307.

STRUIK, X.Y. YIN P.C., TANG, J.J., QI, C.H., & LIU, T.J. 2005. Model analysis of flowering phenology in recombinant inbred lines of barley. *Journal of Experimental Botany*, **56**(413), 959–965.

SURIHARN, B., PATANOTHAI, A., BOOTE, K.J., & HOOGENBOOM, G. 2011. Designing a peanut ideotype for a target environment using the CSM-CROPGRO-peanut model. *Crop Science*, **51**(5), 1887–1902.

TAMBUSSI, E.A., BORT, J., & ARAUS, J.L. 2007. Water use efficiency in C3 cereals under Mediterranean conditions: a review of physiological aspects. *Annals of Applied Biology*, **150**(3), 307–321.

TARDIEU, F. 2003. Virtual plants: modelling as a tool for the genomics of tolerance to water deficit. *Trends in Plant Science*, **8**(1), 9–14.

TARDIEU, F., REYMOND, M., MULLER, B., SIMONNEAU, T., SADOK, W., *et al.* 2005. Linking physiological and genetic analyses of the control of leaf growth under changing environmental conditions. *Australian Journal of Agricultural Research* , **56**(9), 937–946.

TEULAT, B., THIS, D., KHAIRALLAH, M., BORRIES, C., RAGOT, C., *et al.* 1998. Several QTLs involved in osmotic adjustment trait variation in barley (*Hordeum vulgare* L.). *Theoretical and Applied Genetics*, **96**(5), 688–698.

TOMITA, M., HASHIMOTO, K., TAKAHASHI, K., SHIMIZU, T.S., MATSUZAKI, Y., *et al.* 1999. E-CELL: software environment for whole-cell simulation. *Bioinformatics*, **15**(1), 72–84.

TON, J., FLORS, V., & MAUNCH-MANI, B. 2009. The multifaceted role of ABA in disease resistance. *Trends in Plant Science*, **14**(6), 310–317.

TUBEROSA, R. 2012. Phenotyping for drought tolerance of crops in the genomics era. *Frontiers in Physiology*, **3**(UNSP 347).

TULLER, M., & OR, D. 2003. *Retention of water in soil and the soil water characteristic curve.*

Tuzet, A., Perrier, A., & Leuning, R. 2003. A coupled model of stomatal conductance, photosynthesis and transpiration. *Plant Cell and Environment* , **26**, 1097–1116.

Tyree, M.T., & Sperry, J.S. 1988. Mechanisms of water stress-induced xylem embolism. *Plant Physology* , **88**, 581–587.

Uptmoor, R., T.Schrag, Stuetzel, H., & Esch, E. 2008. Crop model based QTL analysis across environments and QTL based estimation of time to floral induction and flowering in *Brassica oleracea*. *Molecular Breeding* , **21**(2), 205–216.

Urao, T., Yamaguchi-Shinozaki, K., Urao, S., & Shinozaki, K. 1993. An *Arabidopsis myb* homolog is induced by dehydration stress and its gene product binds to the conserved MYB recognition sequences. *Plant Cell*, **5**(11), 1529–1539.

van den Honert, T.H. 1948. Water transport in plants as a caternary process. *Discussion of the Faraday Society* , **3**, 146–153.

van Eeuwijk, F.A., Malosetti, M., Yin, X., Struik, P.C., & Stam, P. 2005. Statistical models for genotype by environment data: from conventional ANOVA models to eco-physiological QTL models. *Asutralian Journal of Agricultural Research*, **56**(9), 883–894.

Vu, L.D., Stes, E., Van Bel, M., Nelissen, H., Maddelein, D., *et al.* 2016. Up-to-Date Workflow for Plant (Phospho)proteomics Identiefies Differential Drought-Responsive Phosporylation Events in Maize Leaves. *Journal of Proteome Research*, **15**, 4304–4317.

Welch, S.M., Roe, J.L., & Dong, Z. 2003. A genetic neural network model of flowering time control in *Arabidopsis thaliana*. *Agronomy Journal* , **95**(1), 71–81.

Welch, S.M., Dong, Z., & Roe, J.L. 2016. Modelling gene networks controlling transition to flowering in arabidopsis. *Pages 1–20 of:* adn N. Turner, A. Fischer, Angus, J.F., McIntyre, L, Robertson, M.J., Borrell, A.K., *et al.* (eds), *New directions for a diverse planet: proceedings for the 4th international crop science congress.*

Welcker, C., Boussuge, B., Bencivenni, C., Ribaut, J.M., & Tardieu, F. 2007. Are source and sink strengths genetically linked in maize plants subjected to water deficit? A QTL study of the responses of leaf growth and of anthesis-silking Interval to water deficit. *Journal of Experimental Botany* , **58**(2), 339–349.

White, J.W. 2006. From genome to wheat: Emerging opportunities for modelling wheat growth and development. *European Journal of Agronomy*, **25**(2), 79–88.

White, J.W., & Hoogenboom, G. 1996. Simulating effects of gens for physiological traits in a process-oriented crop model. *Agronomy Journal*, **88**(3), 416–422.

White, J.W., & Hoogenboom, G. 2003. Gene-based approaches to crop simulation: Past experiences and future opportunities. *Agronomy Journal*, **95**(1), 52–64.

Wittmann, D.M., Krumsiek, J., Saez-Rodriguez, J., Da, L., Klamt, S., *et al.* 2009. Transforming Boolean models to continuous models: methodology and application to T-cell receptor signaling. *BMC Systems Biology*, **3**(98).

XU, L., & BUCK-SORLIN, G. 2016. Simulating Genotype-Phenotype Interaction Using Extended Functional-Structural Plant Models: Approaches, Applications and Potential Pitfalls. *In:* YIN, X., & STRUIK, P.C. (eds), *Crop Systems Biology: Narrowing the Gaps between Crop Modelling and Genetics* . Springer.

XU, L., HENKE, M., ZHU, J., KURTH, W., & BUCK-SORLIN, G. 2011. A functional-structural model of rice linking quantitative genetic information with morphological development and physiological processes. *Annals of Botany*, **107**(5), 817–828.

XU, L., DING, W., ZHU, J., HENKE, M., KURTH, W., *et al.* 2012. Simulating superior genotypes for plant height based on QTLs: towards virtual breeding of rice. *Pages 447–454 of:* KANG, M., DUMONT, Y., & GUO, Y. (eds), *IEEE 4th international symposium on plant growth modeling, simulation, visualization and applications (PMA12)*.

YAMAGUCHI-SHINOZAKI, K., & SHINOZAKI, K. 1993. The plant hormone abscisic acid mediates the drought-induced expression but not the seed-specific expression of *rd22*, a gene responsive to dehydration stress in *Arabidopsis thaliana. Molecular and General Genetics* , **138**(1), 17–25.

YAMAGUCHI-SHINOZAKI, K., & SHINOZAKI, K. 1994. A novel *cis*-acting element in an Arabidopsis gene is involved in responsiveness to drought, low-temperature, or high-salt stress. *Plant Cell* , **6**(2), 251–264.

YAMAGUCHI-SHINOZAKI, K., & SHINOZAKI, K. 2005. Organization of *cis*-acting regulatory elements in osmotic- and cold-stress-responsive promoters. *Trends in Plant Science* , **10**(2), 88–94.

YAMAGUCHI-SHINOZAKI, K., & SHINOZAKI, K. 2006. Transcriptional regulatory networks in cellular responses and tolerance to dehydration and cold stresses. *Annual Review of Plant Biology* , **57**, 781–803.

YANG, J., ZHANG, J., WANG, Z., XU, G., & ZHU, Q. 2004. Activities of key enzymes in sucrose-to-starch conversion in wheat grains subjected to water deficit during grain filling. *Plant Physiology* , **135**(3), 1621–1629.

YANG, J.C., ZHANG, J.H., WANG, Z.Q., ZHU, Q.S., & WANG, W. 2001. Remobilization of carbon reserves in response to water deficit during grain filling of rice. *Field Crops Research*, **71**(1), 47–55.

YIN, X., & STRUIK, P.C. 2007. Crop systems biology: an approach to connect functional genomics with crop modelling. *In:* SPIERTZ, J.H.J., STRUIK, P.C., & VAN LAAR, H.H. (eds), *Scale and complexity in plant systems research: gene-plant-crop relations.* Springer, Dordrecht .

YIN, X., & STRUIK, P.C. 2016. Crop Systems Biology: Where Are We and Where to Go? *In:* YIN, X., & STRUIK, P.C. (eds), *Crop Systems Biology: Narrowing the Gaps between Crop Modelling and Genetics* . Springer.

YIN, X., STRUIK, P.C., GU, J., & WANG, H. 2016. Modelling QTL-Trait-Crop Relationships: Past Experiences and Future Prospects. *In:* YIN, X., & STRUIK, P.C. (eds), *Crop Systems Biology: Narrowing the Gaps between Crop Modelling and Genetics* . Springer.

YIN, X.Y., CHASALOW, S.D., DOURLEIJN, C.J., STAM, P., & KROPFF, M.J. 2000. Coupling estimated effects of QTLs for physiological traits to a crop growth model: predicting yield variation among recombinant inbred lines in barley. *Heredity*, **85**(6), 539–549.

ZEEVAART, J.A.D. 1980. Changes in the Levels of Abscisic Acid and Its Metabolites in Excised Leaf Blades of *Xanthium strumarium* during and after Water Stress. *Plant Physiology* , **66**(4), 672–678.

ZHANG, J.X., NGUYEN, H.T., & BLUM, A. 1999. Genetic analysis of osmotic adjustment in crop plants. *Journal of Experimental Botany* , **50**(332), 291–302.

ZHENG, B., BIDDULPH, B., LI, D., KUCHEL, H., & CHAPMAN, S. 2013. Quantification of the effects of *VRN1* and *Ppd-D1* to predict spring wheat (*Triticum aestivum*) heading time across diverse environments. *Journal of experimental botany*, **64**(12), 3747–3761.

ZHENG, B., CHENU, K., DOHERTY, A., & CHAPMAN, S. 2014. *The APSIM-Wheat Module (7.5 R3008)*.

ZHU, J.K. 2002. Salt and drought stress signal transduction in plants. *Annual Review of Plant Biology* , **53**, 247–273.

ZHU, S.Y., YU, X.C., WANG, X.J., ZHAO, R., LI, Y., *et al.* 2007. Two calcium-dependent protein kinases, CPK4 and CPK11, regulate abscisic acid signal transduction in Arabidopsis. *Plant Cell* , **19**(10), 3019–3036.

ZWEIFEL, R., ITEM, H., & HÄSLER, E. 2000. Stem radius changes and their relation to stored water in stems of young Norway spruce trees. *Trees*, **15**, 50–75.

ZWEIFEL, R., ITEM, H., & HÄSLER, E. 2001. Link between diurnal stem radius changes and tree water relations. *Tree Physiology*, **21**, 869–877.

ZWEIFEL, R., BÖHM, J.P., & HÄSLER, R. 2002. Midday stomatal closure in Norway spruce–reactions in the upper and lower crown. *Tree Physiology*, **22**, 1125–1136.

ZWEIFEL, R., STEPPE, K., & STERCK, F.J. 2007. Stomatal regulation by microclimate and tree water relations: interpreting ecophysiological field data with a hydraulic plant model. *Journal of Experimental Botany*, **58**(8), 2113–2131.

Appendix

A   PhytoSim code

```
// -----------------------------------------------------
// WHEAT WATER BALANCE MODEL
// -----------------------------------------------------

// Wheat water balance model: a combination of
// Penman-Monteith for evapotranspiration,
// Cropsyst for transpiration,
// HYDGRO for internal water balance and water potential values.

// last worked on: 10/05/2017

// -----------------------------------------------------
// COUNTER: Tracking days
// -----------------------------------------------------
HourCounter = (nounit(t)-1)%24
ThreeHourCounter = (nounit(t)-1)%3
PeriodCounter = if( previous(ThreeHourCounter)>ThreeHourCounter;
                previous(PeriodCounter) + 1; previous(PeriodCounter))
PeriodCounter = if( t < 65; 0 ;PeriodCounter)
DayNight = if(HourCounter<12; 1; 0)

// -----------------------------------------------------
// Initial section (calculated once at the start of a simulation)
// -----------------------------------------------------

// Thickness of the storage compartment (Génard et al., 2001)
initial( d_S_stem ) = a * ( 1 - exp( -b * initial( D_outer_stem ) ) )
initial( d_S_head ) = a * ( 1 - exp( -b * initial( D_outer_head ) ) )

// Initial value of the inner stem segment
initial( D_inner_stem ) = initial( D_outer_stem ) - 2 * initial( d_S_stem )
initial( D_inner_head ) = initial( D_outer_head ) - 2 * initial( d_S_head )
```

```
// ----------------------------------------------------------
// PENMAN-MONTEITH: Potential evapotranspiration
// ----------------------------------------------------------
// from http://www.fao.org/docrep/X0490E/x0490e06.htm

// Vapor pressure
Tc_nounit = degc2k( T_air )/K
e_s = 0.6108 * exp ( 17.27*T_air / (T_air + 237.3) ) * kPa
e_a = e_s * ( RH / 100 )

// Vapor pressure deficit
VPD = e_s - e_a

// Slope of the saturation vapor pressure curve at the actual temperature
delta = e_s * ( 17.269 / ( 237.3 + T_air ) ) * ( 1 - ( T_air / (237.3 + T_air )))

// Latent heat of vaporization of water
lambda = 2.5 * MJ/kg - 0.002361 * MJ/kg/C  * T_air

// Psychrometer coefficient
gamma = c_p * P / ( epsilon * lambda )

// Air density
rho_a = P / ( R_gas * ( ( degc2k( T_air ) ) / ( 1 - 0.378 * e_a / P ) ) )

// Canopy resistance
r_c = r_l / (0.5*LAI)

// Aerodynamic resistance
r_a = 208 / u_wind

// Potential evapotranspiration of reference grass crop
ET_pot_ref = ( ( delta * R_n + rho_a* c_p * J_MJ * VPD / r_a ) /
               ( delta + gamma *  ( 1 + r_c/r_a) ) )* k / ( lambda * J_MJ * d_crop)

// Potential evapotranspiration
ET_pot = K_crop * ET_pot_ref


// ----------------------------------------------------------
// pF CURVE: Soil water retention
// ----------------------------------------------------------

pF = c1 * (theta/100)^c2
psi_soil = -pow10(pF) * MPa_hPa


// ----------------------------------------------------------
// CROPSYST: Potential and actual transpiration
// ----------------------------------------------------------
// mainly from Camargo (2016). Instead of simulating psi leaf as the authors
// mentioned, we simply use psi_leaf as calculated from HYDGRO

// Potential transpiration
Tr_pot = Fract_cover_green * ET_pot
```

```
// Actual transpiration (should be changed depending on the stomatal conductance)
if (previous(psi_x_leaf) > psi_Lsc)
  {
  Tr_act = Tr_pot
  }
else
  {
  Tr_act = if (previous(psi_x_leaf) < psi_Lpwp; 0; Tr_pot *
              (previous(psi_x_leaf) - psi_Lpwp) / (psi_Lsc - psi_Lpwp))
  }
// Calculate drought indices
if (F_stem_drought > F_stem)
  {
  DroughtWaterDeficit =1
  }
else
  {
  DroughtWaterDeficit = if (F_stem_drought<0 || F_stem<0; 0;
                           F_stem_drought/F_stem)
  }
DroughtTotal = Tr_act/Tr_pot


// ---------------------------------------------------------
// HYDGRO: WATER BALANCE
// ---------------------------------------------------------
// from Steppe (2006)

// ----- Water transport submodel ---------

// stem compartment

   // Soil water potential as felt by the roots
   psi_root = k_soil * psi_soil
   // Water potential of the storage compartment
   psi_s_stem = psi_s_stem_min / (1+exp((nounit(W_stem) - k1_stem)/k2_stem))
   // Root to leaf hydraulic resistance (Baert et al. 2015)
   Rx = r1 * exp( ( psi_root * psi_root ) * r2 )
   // Stem xylem water potential
   psi_x_stem = psi_root - F_stem * Rx
   // Horizontal water transport between the stem xylem and storage compartment
   f_stem = (psi_x_stem - psi_s_stem) / R_s
   deriv(W_stem) = f_stem
   // Variable Capacity
   dpsi_stem = (previous(psi_s_stem)-psi_s_stem)/h


// head compartment

   // Water potential of the storage compartment
   psi_s_head = psi_s_head_min / (1+exp((nounit(W_head) - k1_head)/k2_head))
   // Head (peduncle) xylem water potential
   psi_x_head = psi_x_stem - F_head * Rx
   // Horizontal water transport between the head xylem and storage compartment
   f_head = (psi_x_head - psi_s_head) / R_s
   deriv(W_head) = f_head
   // Variable Capacity
   dpsi_head = (previous(psi_s_head)-psi_s_head)/h
```

```
// leaf compartment

    // Water potential of the storage compartment
    psi_s_leaf = psi_s_leaf_min / (1+exp((nounit(W_leaf) - k1_stem)/k2_stem))
    // Vertical water transport between the stem and the leaf compartment
    F_leaf = F_stem - F_head - f_stem
    // Leaf xylem water potential
    psi_x_leaf = psi_x_stem - F_leaf*Rx
    // Horizontal water transport between the leaf xylem and storage compartment
    f_leaf = (psi_x_leaf - psi_s_leaf)/R_s
    deriv(W_leaf) = f_leaf
    // Variable Capacity
    dpsi_leaf = (previous(psi_s_leaf)-psi_s_leaf)/h



// ----- Stem diameter variation submodel ---------

// for the stem section (up until the highest node)

    // Volume of the storage compartment
    V_stem = pi() * d_S_stem * D_inner_stem * l_stem
    // Change in pressure potential
    deriv( psi_s_stem_p ) = deriv( W_stem ) * Epsilon_0_stem * psi_s_stem_p
                                           * D_outer_stem / ( Rho_w * V_stem )
    // Check for growth
    if ( psi_s_stem_p > Gamma )
    // Stem diameter variation due to elastic changes and growth
    {
      deriv( D_outer_stem ) = f_diameter * 2.0 * d_S_stem * deriv( psi_s_stem_p )
                                    / ( Epsilon_0_stem * psi_s_stem_p * D_outer_stem)
                                    + ( d_S_stem * Phi * ( psi_s_stem_p - Gamma )
                                    / ( b * ( a - d_S_stem ) ) )

    }
    // Stem diameter variation due to elastic changes only
    else
    {
     deriv( D_outer_stem ) = f_diameter * 2.0 * d_S_stem * deriv( psi_s_stem_p )
                                    / ( Epsilon_0_stem * psi_s_stem_p * D_outer_stem )
    }
    // Bulk elastic modulus
    Epsilon_stem = Epsilon_0_stem * psi_s_stem_p * D_outer_stem
    // Osmotic water potential component
    psi_s_stem_o = psi_s_stem_p - psi_s_stem
    // Thickness change of the storage compartment
    deriv( d_S_stem ) = a * b * exp( -b * D_outer_stem ) * deriv( D_outer_stem )
    // Inner diameter variation
    deriv( D_inner_stem ) = deriv( D_outer_stem ) - 2.0 * deriv( d_S_stem )
```

```
// for the head section (peduncle stem segment)

    // Volume of the storage compartment
    V_head = pi() * d_S_head * D_inner_head * l_head
    // Change in pressure potential
    deriv( psi_s_head_p ) = deriv( W_head ) * Epsilon_0_head * psi_s_head_p *
                                    D_outer_head / ( Rho_w * V_head )
    // Check for growth
    if ( psi_s_head_p > Gamma )
    // Stem diameter variation due to elastic changes and growth
    {
     deriv( D_outer_head ) = f_diameter * 2.0 * d_S_head * deriv( psi_s_head_p )
                            / ( Epsilon_0_stem * psi_s_head_p * D_outer_head )
                            + ( d_S_head * Phi * ( psi_s_head_p - Gamma )
                            / ( b * ( a - d_S_head ) ) )
    }
    // Stem diameter variation due to elastic changes only
    else
    {
      deriv( D_outer_head ) = f_diameter * 2.0 * d_S_head * deriv( psi_s_head_p )
                            / ( Epsilon_0_head * psi_s_head_p * D_outer_head )
    }
    // Bulk elastic modulus
    Epsilon_head = Epsilon_0_head * psi_s_head_p * D_outer_head
    // Osmotic water potential component
    psi_s_head_o = psi_s_head_p - psi_s_head
    // Thickness change of the storage compartment
    deriv( d_S_head ) = a * b * exp( -b * D_outer_head ) * deriv( D_outer_head )
    // Inner diameter variation
    deriv( D_inner_head ) = deriv( D_outer_head ) - 2.0 * deriv( d_S_head )

// Diameter in mm
D_outer_stem_mm = D_outer_stem/m_mm
D_outer_head_mm = D_outer_head/m_mm
```

B Extra figures
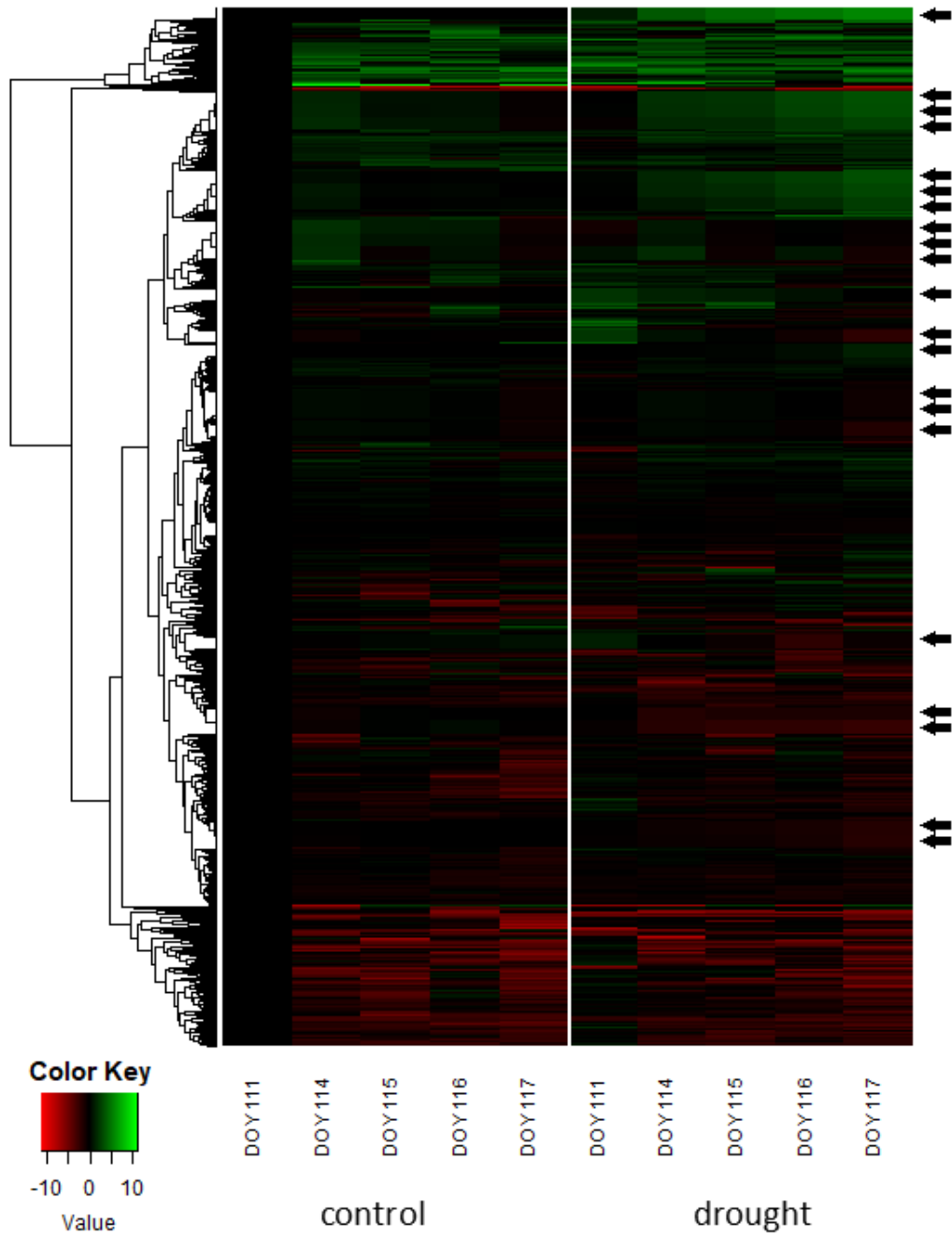
Figure B.1: Heat map of the model variables together with the phosphorylation of proteins. To visualise the model variables, their values were duplicated 20 times. The variables are also emphasized with black arrows